SIMULTANEOUS HEAT AND MASS TRANSFER IN A

DIFFUSION-CONTROLLED CHEMICAL REACTION

by

HYMAN RESNICK

B.S., Northeastern University

(1947)

M.S., Massachusetts Institute of Technology

(1949)

SUBMITTED IN PARTIAL FULFILLMENT OF THE

REQUIREMENTS FOR THE DEGREE OF

DOCTOR OF SCIENCE

at the

MASSACHUSETTS INSTITUTE OF TECHNOLOGY

(1952)

Signature of Author_____
Dept. of Chem. Eng., May 8, 1952

Certified by_____
Thesis Supervisor

_____
Chairman, Departmental Committee on Graduate Students

SIMULTANEOUS HEAT AND MASS TRANSFER IN A
DIFFUSION-CONTROLLED CHEMICAL REACTION

Hyman Resnick

Submitted to the Department of Chemical Engineering
on May 9, 1952, in partial fulfillment of the
requirements for the degree of Doctor of Science

Abstract

The rate of gas-solid reactions may be limited by either
the rate of mass transport of the reacting gases to the sur-
face or by the rate of surface processes, or by a combination
of both. Although most gas-solid systems of engineering
interest are of the second type, there are a few systems in
which observations indicate that the rate of mass transport
limits the overall observed rate of reaction. It has also
been observed that if the rate of transport is an important
factor in an exothermic reaction, the surface attains a tem-
perature higher than that of the main body of the fluid. The
purpose of this thesis was to make a quantitative study of
the simultaneous heat and mass transfer characteristics of
such an exothermic, transport-rate controlled, gas-solid
reaction.

The vapor phase decomposition of hydrogen peroxide vapor
on the surface of an active catalyst was chosen for the study
since it met such requirements as (1) highly irreversible
reaction, (2) no side-reactions, (3) all reaction occurs at
surface, (4) simple mechanism, and (5) transport-rate control.
Two different geometrical systems were studied:

   a. Flow of hydrogen peroxide vapor through a cylindri-
      cal tube fabricated from a metal which is an active
      decomposition catalyst. A theoretical analysis
      could be carried out for the flow conditions of
      this system and an integrated equation was obtained
      for the overall rate of diffusion in the system.

   b. Flow of hydrogen peroxide vapor through a bed
      packed with spheres of the same catalytic material.
      The calculations in this system were carried out
      entirely on an empirical basis.

The range of variables investigated was:

Catalyst Tube

Tube Length	18 and 24 inches
Hydrogen Peroxide Concentration	3-32 wt. %
Surface Temperature	400-1000°F.
Reynolds Number	3,200-10,000

Catalyst Bed

Sphere Diameter	0.200 inches
Bed Diameter	4.7, 4.8 and 7.5 cm.
Hydrogen Peroxide Concentration	5-24 wt. %
Surface Temperature	400-900°F.
Reynolds Number (based on superficial area and sphere diameter)	15-161

The major results and conclusions were as follows:

a. The effect of flow rates and surface temperatures on the mass transfer rate was such as to prove the system to be diffusion-controlled.

b. The magnitude of the temperature difference between the solid and fluid stream can be predicted by a consideration of the heat and mass transfer characteristics and heat losses of the system.

c. A simultaneous temperature gradient did not significantly affect the rate of mass transfer. The influence of varying physical properties along the diffusion path was included in the correlations by the use of an averaged film temperature.

d. The correlations obtained for heat and mass transfer and the average per cent deviations of the data from the correlations were as follows:

Catalyst Tube

$$j_D = 0.021(Re_f)^{-0.2} \qquad (\pm 9.5\%)$$
$$j_H = 0.023(Re_f)^{-0.2} \qquad (\pm 14.8\%)$$
$$j_H/j_D = 1.09 \qquad (\pm 13.7\%)$$

Packed Bed

$$j_D = 0.667(Re_f)^{-0.34} \qquad (\pm 5.8\%)$$
$$j_H = 0.922(Re_f)^{-0.34} \qquad (\pm 6.4\%)$$
$$j_H/j_D = 1.37 \qquad (\pm 5.5\%)$$

Heat transfer coefficients could not be accurately calculated in the packed bed on the basis of overall heat transfer rates and the log mean of the entrance and exit temperature differences, because of the heat flow characteristics in the bed. However, an accurate determination of values of j_H could be made by use of the point values existing at the center sphere of the bottom catalyst layer.

Thesis Supervisor: Charles N. Satterfield
Title: Assistant Professor of Chemical Engineering

Massachusetts Institute of Technology
Cambridge 39, Massachusetts

May 8, 1952

Professor Joseph S. Newell
Secretary of the Faculty
Massachusetts Institute of Technology
Cambridge 39, Massachusetts

Dear Sir:

This thesis entitled "Simultaneous Heat and Mass
Transfer in a Diffusion-Controlled Chemical Reaction"
is hereby submitted in partial fulfillment of the
requirements for the degree of Doctor of Science in
Chemical Engineering.

Respectfully submitted,

Hyman Resnick

ACKNOWLEDGMENT

The author wishes to express his sincere thanks and appreciation to Professor C. N. Satterfield for his continued interest and guidance throughout the work and to Mr. R. L. Wentworth for his many timely suggestions and criticisms and especially for his initial development of the theoretical analysis of the catalyst tube system.

In addition, the author is deeply indebted to co-workers P. Ceccotti, R. Rome, S. Meeken and A. Winters for their aid in carrying out the program of study and to the other members of the Hydrogen Peroxide Laboratories (DIC Project 6552) for their occasional assistance in carrying out experimental measurements.

TABLE OF CONTENTS

INDEX TO FIGURES

INDEX TO TABLES

I.   SUMMARY

Purpose and Scope

The overall rate of gas-solid reactions--a type of reaction met very frequently in chemical engineering--may be limited by either the rate of mass transport of the reacting gases between the gas stream and the solid (transport-rate control) or by the rate at which processes occur on the surface, such as adsorption, desorption, or chemical reaction (surface-rate control) or by a combination of the two. The major distinguishing features of the two extremes are that rates of transport are strong functions of the bulk flow rate and weak functions of temperature, while the surface processes are pronounced functions of temperature but are independent of flow rate. Although many of the gas-solid systems of chemical engineering interest are surface-rate controlled, there are a few systems (e.g., combustion of carbon) in which observations indicate that the rate of mass transport becomes an important factor and eventually, at high temperatures, limits the overall observed rate of reaction. It has also been observed that if the rate of transport is an important limiting factor in an exothermic reaction, the surface attains a temperature higher than that of the main body of the fluid. The purpose of this thesis was

to make a quantitative study of the simultaneous heat and mass transfer characteristics of such an exothermic, transport-rate controlled, gas-solid reaction.

Although some studies have been reported previously of mass transfer in chemically reacting, gas-solid systems, the results of the previous work have been difficult to interpret quantitatively because of uncertainties or complexities in the chemical reaction mechanism or because of difficulties in separating the effects of mass transport from those of surface reaction. For quantitative study of a transport-rate controlled system, it is desirable that the chemical reaction exhibit the following characteristics:

1. Highly irreversible

2. Have no side-reactions

3. All reaction occurs at the surface (i.e., completely heterogeneous)

4. Simple chemical-reaction mechanism

5. Surface reaction is rapid relative to transport rate.

The vapor-phase decomposition of hydrogen peroxide on an active catalyst surface was chosen for this study because it adequately fulfills the above requirements. The aims of the study were two-fold; (1) to compare the mass transfer rates occurring under high temperature gradients and involving chemical reaction with those reported in the literature for

mass transfer alone under little or no temperature differences, and (2) to analyze and develop a method for predicting temperatures which the surface may acquire in a transport-rate controlled chemical reaction.

Experimental Procedure

Two different geometrical systems were studied:

1. Flow of hydrogen peroxide vapor through a cylindrical tube fabricated from a metal which is an active decomposition catalyst

2. Flow of hydrogen peroxide vapor through a bed packed with spheres of the same catalytic metal.

The experimental procedure consisted basically of boiling a hydrogen peroxide-water solution in a vaporization system which produced superheated vapor at a constant rate and of constant composition. The vapor was then passed through one of the decomposition systems. The temperature and composition of the entering and leaving gas streams were obtained and the catalyst surface temperatures were measured at several points on the surfaces. The range of variables which could be and was investigated with the equipment was:

Catalyst Tube

Tube Length	18 and 24 inches
Hydrogen Peroxide Concentration	3-32 wt. %
Surface Temperature	400-1000°F.
Reynolds Number	3,200-10,000

Catalyst Bed

Sphere Diameter	0.200 inches
Bed Diameter	4.7, 4.8, and 7.5 cm.
Hydrogen Peroxide Concentration	5-24 wt. %
Surface Temperature	400-900°F.
Reynolds Number (based on superficial area and sphere diameter)	15-161

Method of Calculation

The flow pattern through a cylindrical tube is reasonably well understood. Therefore, the basic differential equation for diffusion could be integrated for the changing conditions along the length of the tube. The final integrated equation included the effect of the nonequimolecular counterdiffusion in the system but neglected the effect of thermal diffusion, which was found negligible for the conditions investigated. Substitution of the experimental data into the integrated equation gave effective film thicknesses which were then converted to mass transfer factors for comparison with the data in the literature.

In the packed beds, however, the complex geometry made it necessary to employ empirical methods of calculation. Use of the measured decomposition rates and compositions made it

possible to determine mass transfer coefficients and mass transfer factors.

The heat transfer calculations in both systems were carried out in terms of heat transfer coefficients calculated from measured heat flow rates and temperature gradients.

Results and Conclusions

General

1. The decomposition of hydrogen peroxide vapor, under the conditions studied, was shown to be controlled by the rate of mass transport to the catalyst surface. This conclusion was based on two observations:

   a. The dependence of the mass transfer factor, j_D, on the Reynolds number agreed with the dependence found in systems where diffusion without chemical reaction was being studied.

   b. A wide variation of wall temperature had no effect on the measured rate of reaction.

2. The temperature difference between the catalyst surface and stream results from the fact that the heat released by the reaction at the surface must return to the stream, thereby setting up a temperature gradient. The magnitude of the temperature gradient can be predicted by the following method: Mass transfer correlations are first employed to

obtain expected rates of mass transfer to the surface. From the heat of reaction and expected heat losses, the rate of heat transfer is then calculated and combined with a coefficient of heat transfer (obtained from heat transfer correlations) to give a predicted temperature gradient between the solid and gas stream. The precision of the method depends on the accuracy with which the heat and mass transfer characteristics can be predicted. The temperature differences from wall to stream found in the present work agree with those predicted by the proposed correlations with an average deviation of about 13% in the tube and 6% in the packed bed.

3. A simultaneous temperature gradient did not significantly affect the rate of mass transfer under conditions studied here. The influence of varying physical properties along the diffusion path was included in correlations by the use of an averaged film temperature.

Catalyst Tube

1. The mass transfer rates in the catalyst tube were correlated with an average deviation of 9.5% by the equation

$$j_D = 0.021 \ (Re_f)^{-0.2} \tag{62}$$

In the correlation, average values of physical properties, which varied with length in the system, were taken at a film temperature corresponding to the point in the tube at which

the partial pressure driving force equals numerically the
log mean of the driving forces at the entrance and exit of
the tube. Equation (62) is of the same form as that of
Chilton-Colburn (11), differing only in that the coefficient
is 0.021 instead of 0.023. In the range of Schmidt numbers
covered here, Equation (62) predicts values of J_D about 9.5%
below those predicted by von Karman (37) and Martinelli (50).

2. The heat transfer results were correlated with an
average deviation of 14.8% by

$$J_H = 0.023 \ (Re_f)^{-0.2} \tag{22}$$

This equation is identical to the Chilton-Colburn (11) and
McAdams (43) equations.

3. The J_H/J_D ratio was found to have an average devia-
tion of 13.7% from 1.09, a value which is in excellent
agreement with the usual assumption of unity.

Catalyst Bed

1. The mass transfer results had an average deviation
of 5.8% from the equation

$$J_D = 0.667 \ (Re_f)^{-0.34} \tag{63}$$

These results are somewhat lower than most of the previous
work; this is probably a result of the smoothness of the
spheres used as packing in the present work.

2. Accurate heat transfer coefficients could not be calculated on the basis of overall heat transfer rates and the log mean of the entrance and exit temperature differences because of the heat loss and regenerative heat flow characteristics of the packed bed. However, an accurate determination of J_H could be made by use of the point values existing at the center sphere of the bottom catalyst layer. These values gave an average deviation of 6.4% from the expression

$$J_H = 0.922 \ (Re_f)^{-0.34} \tag{66}$$

Equation (66) agrees very well with previous data.

3. The J_H/J_D ratios gave an average deviation of 5.5% from 1.37, a value in general agreement with the usually assumed value of 1.0.

4. The data on both heat and mass transfer agree reasonably well with the extension of the turbulent lines of the generalized Gamson correlation (21).

II.   INTRODUCTION

A.   Purpose and Scope of Work

Gas-solid reactions are met very frequently in chemical engineering, common examples being the catalytic cracking of petroleum, oxidation of sulfur dioxide, oxidation of ammonia, and combustion of carbon. The overall rate of such heterogeneous reactions may be limited by one or more of the following steps:

1. Transport of the reacting components from the bulk gas stream to the solid surface.

2. Adsorption of one or more of the components onto the surface.

3. Chemical reaction at the surface (solid may enter into the reaction either as a reactant or as a catalyst).

4. Desorption of the products from the surface.

5. Transport of the products from the surface to the stream.

The rates of transport, steps 1 and 5, are strong functions of the bulk flow rate but weak functions of temperature, as opposed to steps 2, 3, and 4, which involve surface effects and are pronounced functions of temperature but are independent of flow rate. Therefore, observation of the changes in the total reaction rate with flow rate and/or temperature

helps distinguish between a system whose rate is limited by steps 1 and 5 (transport-rate control) and a system limited by steps 2, 3, and 4 (surface-rate control). Steps 1 and 5 occur simultaneously in such a manner that an overall transport rate need only be considered. To distinguish between steps 2, 3, and 4 requires a large amount of additional investigation and therefore relatively few systems have been studied in sufficient detail to determine in each case which of these three steps was truly rate-controlling. If the rate of adsorption is an important rate-limiting factor in the overall series of steps, there will usually result a maximum in the observed rate with temperature (e.g., hydrogenation of olefins). If true chemical reaction between adsorbed molecules (or adsorbed molecules and colliding molecules) controls, then the rate will exhibit a steady, rapid increase with temperature. In addition, the presence of a reverse reaction may also complicate the relationship of the total reaction rate with temperature.

Although most of the systems which have been studied thoroughly are surface-rate controlled, there are a few systems in which observations indicate that the rate of mass transport becomes an important factor and eventually, at high temperatures, limits the overall observed rate of reaction. It has also been observed that if the rate of transport is an important factor in an exothermic reaction, the

surface will attain a temperature higher than the main body of the fluid and there will result a flow of heat from the surface to the fluid. The purpose of this thesis was to make a quantitative study of the simultaneous heat and mass transfer characteristics of such an exothermic, transport-rate controlled, gas-solid reaction. Although studies have been reported previously of mass transfer in chemically reacting, gas-solid systems, the results of all previous work have been difficult or impossible to interpret quantitatively because of uncertainties or complexities in the chemical reaction mechanism or because the rates of both mass transport and surface reaction have been important.

For quantitative study of a transport-rate controlled system, it is desirable that the chemical reaction exhibit the following properties:

1. Highly irreversible.

2. Have no side-reactions.

3. All reaction occurs at the surface (no homogeneous reaction).

4. Simple mechanism.

5. Surface reaction is rapid relative to the transport rate.

The vapor-phase decomposition of hydrogen peroxide on an active catalyst surface was chosen for this study because it adequately fulfills the above requirements. The aims of the

study were two-fold;   (1) to compare the mass transfer rates occurring under high temperature gradients and involving chemical reaction with those reported in the literature for mass transfer alone under little or no temperature differences, and (2) to analyze and develop a method for predicting temperatures which the surface may acquire in a transport-rate controlled system.   Two different geometrical systems were studied:

1. Flow of hydrogen peroxide vapor through a cylindrical tube fabricated from a metal which is an active decomposition catalyst.

2. Flow of hydrogen peroxide vapor through a bed packed with spheres of the same metal.

While developed specifically from a diffusion controlled reaction, the results of this study are of interest in any gas-solid reaction, in that an analysis based on the assumption of mass transport-control indicates the maximum rate of reaction that can result from the ultimate in surface activity, and the maximum temperature which the surface may attain. The results are also of interest in relation to the general knowledge of heat and mass transfer.

B. Discussion of Transport-Rate Controlled Reactions

The most important example of transport-rate controlled reactions is the high-temperature combustion of carbon.

Although the literature contains an abundance of data on carbon combustion, these data were acquired mainly to determine the fundamental reaction order and mechanism, and hence are confined to the low temperature range where resistance to surface reaction controls the overall reaction rate. Some research into the high-temperature combustion of carbon has been carried out (14, 56, 69, 74) in order to develop a combustion theory which would include both surface and diffusional resistances. However, these data showed that changes in carbon type led to differences in the observed reaction rates and the heat balances obtained. Since a diffusion-controlled combustion would not normally be affected by a change in chemical characteristics of the fuel, several possibilities were considered to account for the differences found. It was finally postulated that the variations in reaction rates for different carbon types under identical reaction conditions are attributable to the formation of carbon monoxide and carbon dioxide as primary products in varying ratios dependent on the carbon type and system temperatures. There is a large amount of conflicting evidence leading to various theories as to the primary combustion products, the latest theory favoring the formation of a C_xO_y complex which later breaks down to carbon monoxide and dioxide. Analyses of micro gas samples at the combustion surface were inconclusive due to difficulties in the sampling

techniques. Thus, due to the absence of knowledge as to the exact gas composition at the carbon surface, it is almost impossible to make a complete study of the rate of diffusion in carbon combustion.

The situation is further complicated by the presence of a large temperature gradient and of bulk flow through the diffusion film. There are apparently no data in the literature which correlate the diffusion resistance in systems where there simultaneously exists a large temperature difference between surface and stream. As is shown below, the best correlations available are those for essentially isothermal ($\Delta T < 10°C$.) mass transfer and those for heat transfer. The combustion mechanism equations of Smith (69) were derived assuming the diffusion resistance to be correlated by an equation of the form used by McAdams (43), and assuming carbon dioxide formation at the surface in order to eliminate the more complicated calculations for diffusion with a simultaneous bulk flow through the film. By the use of four arbitrary constants, this equation could be made to check the data for any one carbon type, but as a general correlation it left much to be desired. It is also possible that thermal diffusion may play a large enough role in this reaction to cause the discrepancies obtained for a particular type of carbon, but this conjecture cannot be checked until more data are available on the thermal diffusivities of the species present.

The oxidation of sulfur dioxide in packed catalytic beds has been studied in a recent investigation (55). Under conditions of high temperature and low flow rates, the resistance to mass transfer required approximately 25 per cent of the total partial pressure driving force and, thus, while not controlling, was very important in the total reaction mechanism. However, the data were not precise enough to allow accurate mass transfer calculations.

The decomposition of hydrogen peroxide vapor on the surface of the active catalyst, which was chosen for study here, is a transport-rate-controlled reaction similar to the high-temperature oxidation of carbon with the major, and most fortunate, difference being that the gas composition at the surface of the solid is known. This exothermic reaction proceeds according to the equation

$$2 \ H_2O_2 \ (g) \ \longrightarrow \ 2 \ H_2O \ (g) + O_2. \qquad (1)$$
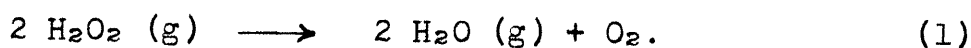
No other species are present except possibly very small concentrations of the free radicals (OH, HO_2) formed and consumed during the reaction (63). This fact allows an exact diffusion-controlled, reaction mechanism to be developed and, consequently, permits a method for predicting the rate of transport in such a gas-solid system to be obtained.

The physical picture presented in the development of a diffusion equation for this system is quite complex, involving

the nonequimolecular counterdiffusion of hydrogen peroxide, water and oxygen under a temperature gradient from the catalyst surface to the bulk stream. The total resistance to the mass transport of hydrogen peroxide is the combination of the resistance to bulk and molecular transfer through the eddy, buffer, and laminar regions of the gas stream, complicated by the presence of a bulk flow of gas from the wall to the stream due to an increase in the number of moles during the reaction. Although it has been demonstrated (68) that eddy diffusion plays an important role, it is customary to visualize the transport as occurring through a single laminar film, the thickness of such an "effective" or "fictitious" film being so chosen as to incorporate all resistance to diffusion.

By making this assumption (the validity of which will be discussed later), one obtains the following differential equation for the total diffusion in this system:

$$y_A y_B (u_A - u_B) = - D_{AB} \frac{dy}{dx} - \frac{D_T}{T} \frac{dT}{dx} \quad ^* \qquad (2)$$

y_A, y_B - Mol fractions of components A and B

u_A, u_B - Convection velocities of components A and B

T - Temperature

D_{AB} - Molecular diffusivity of A through B

D_T - Thermal diffusivity

x - Distance through film.

- -

*A complete Table of Nomenclature is given in the Appendix.

The first term on the right represents molecular transport under the influence of a concentration gradient while the second represents the transport under a temperature gradient (thermal diffusion). An integrated form of this equation can be applied to the studies in a catalyst tube, where the flow pattern is reasonably well understood. In packed beds, however, the complex geometry makes it necessary to use empirical methods of correlation.

It has already been noted that in an exothermic, diffusion-controlled reaction, the surface temperature is higher than the bulk stream temperature. This is because, under adiabatic conditions, all the heat released by the reaction at the surface must flow back to the bulk gas stream, thereby setting up a temperature gradient. This effect can be graphically demonstrated by suspending a silver wire in a stream of hydrogen peroxide vapor of relatively high concentration. The silver wire immediately melts even though its melting point is above the adiabatic decomposition temperature of the gas stream, the highest temperature which the bulk of the stream may attain in such a situation. The same effect has been observed in the operation of packed catalyst beds where the temperature of the solids in the beds has been found to be higher than that of the fluid passing through the bed. For example, Apelbaum and Temkin (1) measured gauze temperatures in the catalytic oxidation of ammonia and found

that the platinum surface was at a higher temperature than the gas passing the gauze. Although it has been assumed that the explanation of this anomaly may involve a regenerative heat flow in a catalyst bed, it can be demonstrated, by a heat balance across the "effective" film, that the temperature difference between the surface and stream is determined by the relative rates of mass transfer to, and heat transfer from the surface. Since high surface temperatures may have a marked effect on catalyst performance and deterioration (e.g., regeneration of petroleum cracking catalysts), it is important to be able to determine quantitatively the magnitude of the temperature difference and its dependence on the operating variables in such systems. Thus, this thesis is concerned not only with predicting the rates of mass transport in gas-solid systems but is also concerned with developing a method for predicting surface temperatures in such systems.

To accomplish this aim, the rate of heat transfer from solid to stream was calculated from (1) the observed rate of reaction, (2) the known heat of reaction, and (3) the experimentally determined heat loss from the surface to the surroundings. Combining the rate of heat transfer with the observed temperature differences gives a heat transfer coefficient which can then be compared with existing correlations.

C. Previous Investigations

Heat and Mass Transfer Inside Tubes

As one would expect from the engineering importance of
the transfer of heat and mass between fluids and tubes, a
very substantial amount of effort has been devoted to theo-
retical and experimental studies of these phenomena. Con-
sideration of the characteristics of turbulent flow in tubes
makes evident the intimate relationship of heat and mass
transfer to fluid friction (momentum transfer) and their
dependence on the motion of the fluid. If the path of each
element of fluid in its passage through a pipe were known,
it would be possible to calculate the rates of heat, mass,
and momentum transfer. It is the imperfect knowledge of
fluid dynamics that precludes any complete theoretical study
of the transport processes. However, there is available a
large amount of empirical data on momentum transfer and the
resulting fluid friction in turbulent flow through pipes.
By applying this information and the similarity between fluid
friction on the one hand and heat and mass transfer on the
other, semi-theoretical relationships for heat and mass
transfer can be formulated. This is accomplished, as will
be thoroughly described below, by setting up the basic differ-
ential equations for the transfer processes. A simultaneous
solution of these equations makes possible the use of the
data obtained for fluid friction to predict the heat and mass

transfer characteristics in the system. (All the equations
to be discussed below were originally obtained as analogies
between heat transfer and friction but they may be adapted
to mass transfer by a simple interchange of dimensionless
groups.)

It is well established that the turbulent flow of fluids
through pipes gives rise to a definite velocity distribution.
Adjacent to the wall there is a very narrow region of laminar
flow in which no flow or eddy mixing occurs in a direction
normal to the wall and in which the velocity is proportional
to distance from the wall. Whatever transfer may take place
in this laminar region is the result of molecular motion, a
mechanism about which much is known. Occupying most of the
pipe's cross section is the main stream of fully developed
turbulence, characterized by the continuous action of eddies
which carry small masses of fluid into regions of different
velocity. The mixing and transfer due to these eddies is
very rapid in comparison with that due to molecular motion
but, unfortunately, very little is known about the mechanism
of eddy transfer. In between the two flow regimes, there is
an intermediate region, called the "transition" or "buffer"
layer, in which both processes contribute substantially to
radial transfer. It is seen that the two means by which
properties can be transferred--molecular action and eddy
action--occur simultaneously and that any theory of an overall

transfer process from the stream to the pipe wall must allow
for the varying contributions of molecular and eddy action
across the diameter.

The basic equation which expresses the local rate of
momentum transfer due to the combined action of molecular
and eddy motion can be obtained from a detailed analysis of
the turbulent flow characteristics in pipes and tubes, and
is expressed as

$$\frac{\tau g_c}{\rho} = \left(\frac{\mu}{\rho} + \epsilon\right)\frac{dU}{dy} = (\nu + \epsilon)\frac{dU}{dy} \tag{3}$$

where ν (kinematic viscosity) expresses the contribution of
molecular transport and ϵ is a coefficient of eddy viscosity
such that the eddy stress is $+ \epsilon\rho\,(dU/dy)$. The analogous
equations for heat and mass transport are

$$\frac{q}{C_p\rho} = -\left(\frac{k}{C_p\rho} + E_H\right)\frac{dT}{dy} = -(\alpha_H + E_H)\frac{dT}{dy} \tag{4}$$

and

$$N_A = -(D + E_M)\frac{dc}{dy} \tag{5}$$

where α_H (the thermal diffusivity) and D (the diffusion
coefficient) represent molecular transport and E_H and E_M
(eddy diffusivities for heat and mass transfer) represent
eddy transport.

The first attempt to relate these mechanisms was made
in 1874 by Osborne Reynolds (61). From the similarity of

heat and momentum transport in a fluid, he concluded that there must exist in geometrically similar systems, a simple proportionality relationship between fluid friction and heat transfer and therefore made the basic assumption (the famous Reynolds analogy) that ϵ was equal to E_H. On making the further assumption that the variation of τ and q with y is similar to the extent that τ/q is constant (requiring similar velocity and temperature distribution curves), it follows from Equations (3) and (4) that direct proportionality between heat and mass transfer will result if

(a) ν and α_H are negligible compared to ϵ (or E_H)

(b) $\nu = \alpha_H$ or $\nu/\alpha_H = (\mu/\rho) \times (C_p\rho/k) = C_p\mu/k = Pr = 1$.

If either (a) or (b) is true, we obtain by combination of Equations (3) and (4) the equation

$$\frac{dU}{\tau g_c/\rho} = - \frac{dT}{q/C_p\rho} \tag{6}$$

which on integration from the average stream properties to the wall becomes

$$\frac{U_o}{\tau_w g_c/\rho} = \frac{T_w - T_o}{q_w/C_p\rho} \tag{7}$$

Upon inverting and dividing by U_o, we obtain

$$\frac{\tau_w}{U_o^2\rho/g_c} = \frac{q_w}{C_p U_o \rho(T_o - T_w)} \tag{8}$$

This is the mathematical expression for the usual statement of the Reynolds analogy: the head lost due to skin friction

divided by the momentum of the stream is equal to the ratio
of heat transferred to that which would be transferred if
the stream should reach thermal equilibrium with the wall.

The final simplification is obtained by noting that the
left side of Equation (8) is equal to $f/2$, where f is the
Fanning friction factor, and that $q_w/(T_o - T_w) = h$,
the heat transfer coefficient. Making these substitutions
gives the familiar Reynolds analogy equation

$$\frac{f}{2} = \frac{h}{C_p G} \tag{9}$$

Condition (a), the first of the two conditions given
above as a requirement for Equation (9) to apply, is met in
the turbulent section of flow where the molecular effect is
small compared to eddy mixing. However, close to the surface
in either laminar or transitional layers, molecular action
is important and the equation will not apply unless condition
(b) is found, i.e., unless $Pr = 1$. In flow through pipes,
most of the resistance to transfer occurs in the laminar and
buffer zones and it therefore follows that Equation (9) will
not apply for wall to fluid transfer unless condition (b) is
met.

(A similar treatment for mass transport results in the
equation

$$\frac{k_c}{U_o} = \frac{k_G RT}{U_o} = \frac{f}{2} \tag{10}$$

and the condition that $Sc = 1$.)

The Reynolds analogy has proven to be a satisfactory approximation for the common gases since the Prandtl modulus is not far from 1.0. However, it is in considerable error when $C_p\mu/k$ is far from unity, first because assumption (b) is violated and, secondly, because the radial distributions of velocity and temperature become increasingly dissimilar as the Prandtl number deviates from 1.0.

An attempt to improve the assumptions and to allow for the role of the laminar and buffer zones was made by Taylor (72) and Prandtl (57). They subdivided the flow into two regions:

1. A turbulent region in which molecular effects are negligible and, therefore, in which the basic Reynolds analogy can be applied.

2. A laminar region in which eddy transfer is neglected and in which the transfer is entirely molecular.

If the thickness of their laminar layer is δ , it follows from Equations (3) and (4) that

$$U_\delta = \frac{T_w g_c}{\rho} \int_0^\delta \frac{dy}{\nu} \quad , \tag{11}$$

$$T_\delta - T_w = - \frac{q_w}{C_p\rho} \int_0^\delta \frac{dy}{\alpha_H} = - \frac{q_w}{C_p\rho} \int_0^\delta (Pr) \frac{dy}{\nu} \tag{12}$$

and, therefore,

$$Pr(\frac{\rho U_\delta}{T_w g_c}) = - C_p\rho(T_\delta - T_w)/q_w \quad . \tag{13}$$

The Reynolds analogy applied to the turbulent region gives

$$\rho(U_0 - U_f)/\tau_w g_c = - C_p \rho(T_0 - T_f)/q_w \qquad (14)$$

where U_0 and T_0 are the mean values of the velocity and temperature taken over the cross section of the pipe.

Solving Equations (13) and (14) simultaneously by eliminating T_f, and rearranging as above gives the final equation

$$\frac{h}{C_p G} = \frac{f}{2[1+r(Pr-1)]} \qquad (15)$$

where r is the ratio of the fluid velocity at the boundary of the laminar film to the average velocity of the main stream.

For mass transfer, Colburn (12) showed the analogous equation to be

$$\frac{k_c P_{BM}}{U_0 P} = \frac{f}{2[1+r(Sc-1)]} \qquad . \qquad (16)$$

Experimental evidence indicates that Equation (15) holds for relatively small values of (Pr - 1), but as Pr increases beyond 5 there is an increasing discrepancy between the experimental results and the equation. The reason for this, as Prandtl himself is known to have realized, is that the concept of a completely laminar film at the phase boundary and a wholly turbulent main stream is an oversimplification of the actual situation. Velocity traverses near the

phase boundary show that there is a gradual transition between the two types of flow and, therefore, that any successful theory must be based on a reasonable guess or knowledge of the conditions in the boundary region.

Murphree (53) attempted to solve this problem by postulating that the eddy viscosity was constant in the main turbulent area but that in the region close to the wall it was proportional to the third power of the distance from the wall. From this "reasonable guess" and experimental measurements of fluid friction, he obtained tables of constants which were very cumbersome in use but which gave much better results than the simple Prandtl relation.

von Karman (37) extended the theory by employing the generalized velocity distribution curve shown in Figure 1 as a basis for the calculation of eddy diffusivities in the region of the phase boundary. The distribution shown was based on the experimental measurements of Nikuradse (54) plotted in the manner suggested by Bakhmeteff (3). Although the data points reported by Nikuradse were later shown by Miller (52) to have included a constant empirically added to the measured values, the more recent work of Reichart (58) and Deissler (15) agree with Nikuradse's reported curves very closely.

According to Figure 1,

$$u^+ = U \sqrt{\rho / \tau_w g_c} = f(y^+) \ . \tag{17}$$

LAMINAR SUBLAYER

BUFFER LAYER

TURBULENT CORE

$$u^+ = U \sqrt{\rho / \tau_w \, g_c}$$

$$= \frac{U}{U_0} \sqrt{2/f}$$

$$u^+ = 5.5 + 2.5 \ln y^+$$

$$u^+ = -3.05 + 5.00 \ln y^+$$

$$u^+ = y^+$$

$$y^+ = \frac{y}{\nu} \sqrt{\tau_w \, g_c / \rho} = \frac{y U_0}{\nu} \sqrt{f/2}$$
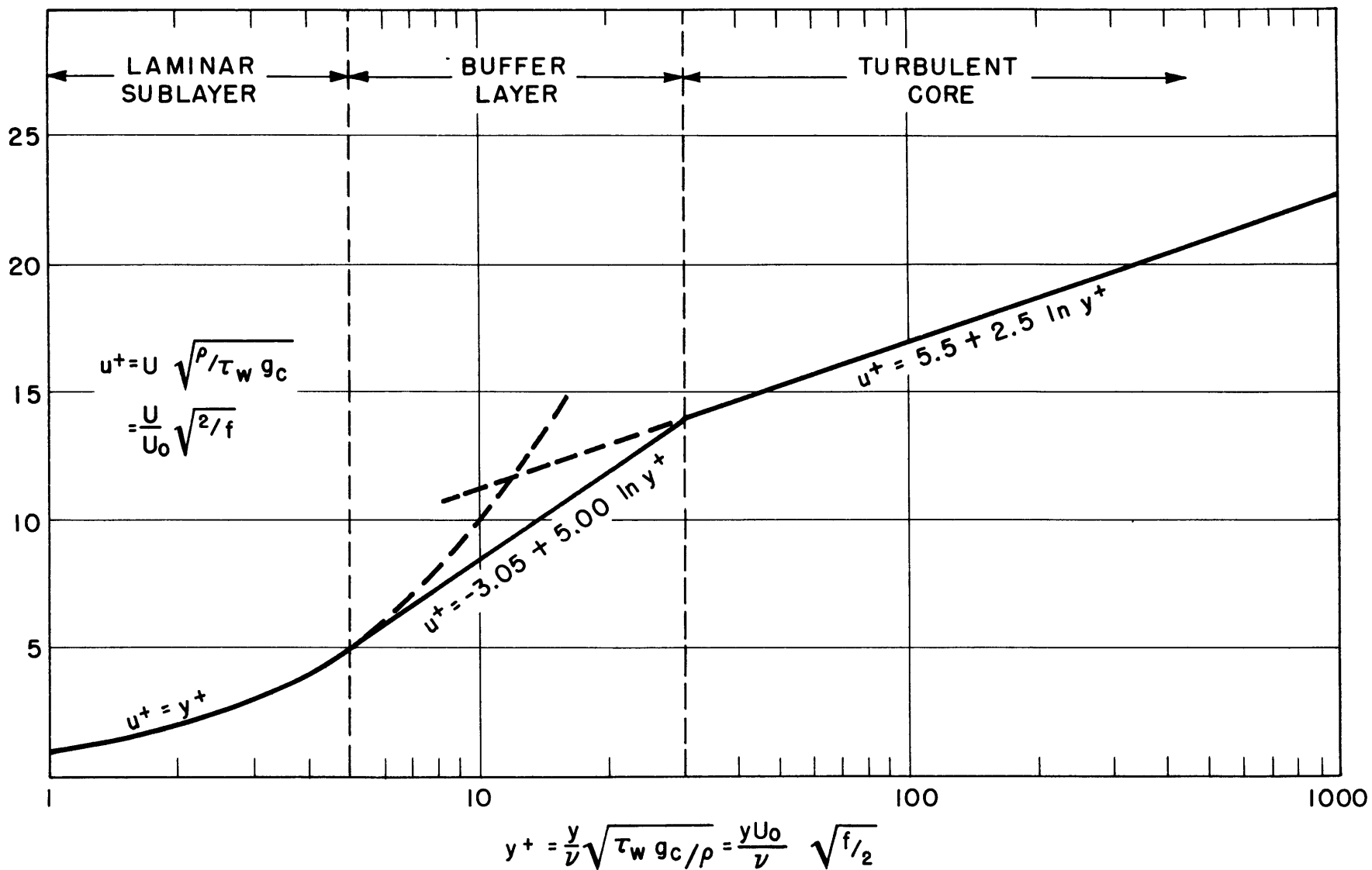
FIG. I   GENERALIZED VELOCITY DISTRIBUTION FOR TURBULENT FLOW IN PIPES

27

Therefore

$$\frac{dU}{dy} = (\sqrt{\frac{\tau_w g_c}{\rho}})(f'(y^+)) \frac{dy^+}{dy} \tag{18}$$

$$= (\sqrt{\frac{\tau_w g_c}{\rho}})(f'(y^+))(\sqrt{\frac{\tau_w g_c}{\rho}})(\frac{1}{\nu}) = \frac{\tau_w g_c}{\rho \nu} f'(y^+)$$

and

$$\frac{\tau_w g_c}{\rho dU/dy} = \frac{\nu}{f'(y^+)} = \nu + \epsilon \qquad . \tag{19}$$

Since the value of $f'(y^+)$ can be obtained from Figure 1,
Equation (19) can be employed to give values of ϵ. Von Karman
combined these values of ϵ over the laminar and buffer
layers with the Reynolds equation for the turbulent region
to give

$$\frac{h}{C_p G} = \frac{f/2}{1+5\sqrt{f/2} \ (Pr-1+ \ln \frac{1+5Pr}{6})} \qquad . \tag{20}$$

Boelter et al (8) and Martinelli (50) extended the
method of Von Karman by considering the turbulent and
molecular transfer from center line to the edge of the
buffer layer and obtained the final result

$$\frac{h}{C_p G} = \frac{f/2}{5R_T \sqrt{f/2} \left[Pr+ \ln(1+5Pr)+ \frac{1}{2} N_{RR}\ln \frac{Re}{60} \sqrt{f/2}\right]} \tag{21}$$

where R_T is the ratio of the mean temperature difference to
the maximum temperature difference, wall to center line, and
N_{RR} is a complex factor which allows for molecular transfer

in the turbulent region at very low Prandtl numbers. In the
bracket of the denominator, the terms are proportional to
the relative thermal resistances of the laminar sublayer,
the buffer layer and the turbulent core respectively.
Reichart (58) and Deissler (15) have obtained similar equa-
tions on the basis of slightly different velocity distribu-
tions but they give results which agree within the wide
spread of experimental data. (The above relationships can
be obtained in their analogous mass transfer form by substi-
tution of the proper dimensionless groups.)

There are two principal objections to the analogies
described above. The first is the basic Reynolds assumption
that the turbulent Prandtl and Schmidt groups, ϵ/E_H and
ϵ/E_M, are always 1.0. This value agrees with the results of
the Prandtl theory of momentum transport (26) but differs
from the predictions of Taylor's vorticity theory (26, 73)
which is satisfied by values ranging from 0.5 - 1.0. Experi-
mental studies of the ratios are not numerous but they mostly
give values of 0.6 to 0.8 and the analogies have been modi-
fied (50, 67) to include this effect. However, comparisons
of heat-transfer data show that a ratio of 1.0 is in good
agreement with experimental results, while mass transfer
data are as yet inconclusive. More data are required before
any definite conclusions as to this point can be drawn.

The second objection, which applies principally to heat transfer, is that the properties of the fluid are assumed constant across the tube. This assumption is fairly well satisfied by gases but deviates markedly in liquids, giving rise to uncertainty as to which values of the physical properties are to be used. Boelter (8) considered nonisothermal flow and altered his equation to take into consideration the different velocity distribution resulting from temperature gradients across the tube. However, the usual procedure is to assume the properties to be constant at some average temperature and use these values in checking the theories. Deissler (15) shows by a theoretical study that, for Prandtl numbers of 1.0, the effect of variable fluid properties can be predicted by evaluating the fluid properties at a film temperature which is the average of the bulk stream and wall temperatures.

For practical purposes, all the theories mentioned above reduce to the original analogy modified by a factor which is a function of the Prandtl group and, very slightly, of the Reynolds number. Colburn (13) after examining extensive experimental data on heat transfer suggested that the correct expression should be

$$J_H = (\frac{h}{C_pG})(Pr_f)^{2/3} = \frac{f}{2} = 0.023(Re_f)^{-0.2} \tag{22}$$

an equation which is identical to the empirical heat transfer equation of McAdams (43)

$$\frac{hd}{k} = \frac{d}{x_H} = 0.023(Re_f)^{0.8}(Pr_f)^{1/3} \quad . \tag{23}$$

Chilton and Colburn (11) later developed the analogous mass transfer equation

$$j_D = \frac{k_c p_{BM}}{U_o P}(Sc_f)^{2/3} = \frac{k_G p_{BM} M_M}{G}(Sc_f)^{2/3} = \frac{f}{2} = 0.023(Re_f)^{-0.2} \tag{24}$$

Equations (20) and (22) appear to be a simple and most effective means for correlating data on heat and mass transfer and will be used in this thesis. Other investigators of heat transfer properties have empirically obtained similar equations but with coefficients varying from 0.020 to 0.027 (44) and have used various temperatures to evaluate the physical properties of the fluid. This deviation of $\pm$ 25 per cent about the mean value is a good example of how the data from various investigators is expected to differ even in such a geometrically simple system as flow through a tube.

The few mass transfer data available show the same degree of variation. The wetted-wall data of Gilliland (25) give a correlation

$$\frac{d}{x_D} = 0.023(Re_f)^{0.83}(Sc_f)^{0.44} \tag{25}$$

which, for the small range of Schmidt numbers employed, is

25 per cent above Equation (22) expressed in the analogous manner

$$\frac{d}{x_D} = .023 \ (Re_f)^{0.8} \ (Sc_f)^{1/3} \ . \tag{26}$$

As mentioned earlier, no data are available for mass transfer under large temperature gradients.

It can be noticed from Figure 2 that the theoretical equations and the j-factor equations give very close agreement at Prandtl and Schmidt numbers near 1.0. In the present investigation, the Prandtl number is 1.0 while the Schmidt number varies from 0.7 to 0.9. Therefore the data to be obtained will have the same agreement with all equations and cannot be used to differentiate between them. In regions where there exists a large difference between the various equations, the recent work of Linton (41) shows that at Schmidt numbers of 1000-3000, the best correlation of the data was obtained using the j-factor relationship.

Heat and Mass Transfer in Packed Beds

Until 1940, there were essentially no published experimental data on heat and mass transfer between solids in packed beds and the fluids passing through the beds. However, the importance of such diverse operations as the reaction of fluids in the presence of solid catalysts, the reaction between a granular solid and a fluid, adsorption, extraction, drying and ion exchange has emphasized the desirability for quantitative methods of predicting these transport rates for
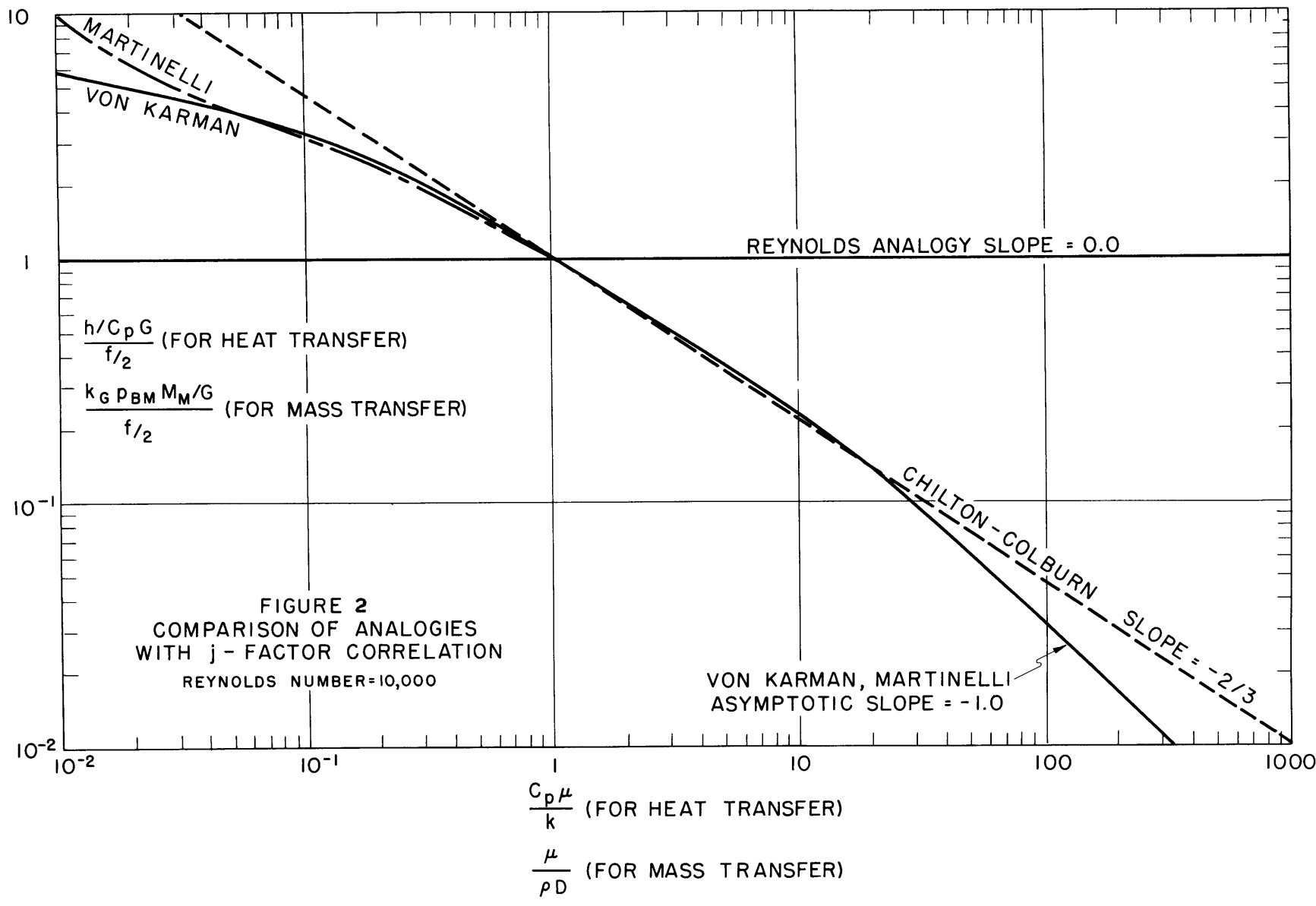
FIGURE 2
COMPARISON OF ANALOGIES
WITH j – FACTOR CORRELATION
REYNOLDS NUMBER=10,000

$\dfrac{h/C_p G}{f/2}$ (FOR HEAT TRANSFER)

$\dfrac{k_G P_{BM} M_M/G}{f/2}$ (FOR MASS TRANSFER)

REYNOLDS ANALOGY SLOPE = 0.0

CHILTON-COLBURN SLOPE = -2/3

VON KARMAN, MARTINELLI
ASYMPTOTIC SLOPE = -1.0

MARTINELLI

VON KARMAN

$\dfrac{C_p \mu}{k}$ (FOR HEAT TRANSFER)

$\dfrac{\mu}{\rho D}$ (FOR MASS TRANSFER)

use in the rational design of reactors and equipment. As a consequence, the last decade has witnessed the appearance of a considerable number of experimental studies of these phenomena.

The flow of fluids through packed beds of granular solids does not lend itself to mathematical analysis as readily as flow through conduits. Therefore, the investigators have empirically expressed their heat and mass transfer rates in terms of the heat and mass transfer factors, j_H and j_D, developed, as shown above, by Chilton and Colburn ($\underline{11}$, $\underline{13}$). These dimensionless factors, which take into account system characteristics and their variation with temperature, are found to be a more general and appropriate form of expressing the results than the dimensional heat and mass transfer coefficients, h and k_G. The j-factors in packed beds have no relationship to the total pressure drop through the bed since here the total friction is made up of not only slip friction but also of the form drag caused by blunt objects in flowing streams.

The previous experimental data on mass transfer in packed beds in the range of Reynolds numbers considered here have been obtained with four different physical systems, none of which involved high temperature gradients between solid and fluid or chemical reaction:

1. Evaporation of volatile liquids from porous
   particles into gases ($\underline{22}$, $\underline{28}$, $\underline{71}$, $\underline{79}$)

2. Sublimation of solids into gases ($\underline{32}$, $\underline{60}$)

3. Solution of liquids from porous particles into
   liquids ($\underline{27}$)

4. Solution of solids into liquids ($\underline{17}$, $\underline{20}$, $\underline{45}$).

As is to be expected in this type of work, values of j_D
at a given Reynolds number, as determined by different inves-
tigators, differed from one another by as much as 100 per
cent, while significant differences were found between the
results of the various workers as to the effect of the
Schmidt number, the Reynolds number (based on particle
diameter and superficial mass flow rates), particle diameter
and the transition from turbulent to laminar flow. On the
whole, however, the agreement between the systems is remark-
ably good and has given rise to several generalized correla-
tions. Gamson ($\underline{21}$) has proposed a general correlation of the
data from several systems of solution and evaporation in
fixed and fluidized beds of spherical particles. The systems
considered were

1. Evaporation of water into air from porous packing ($\underline{22}$)

2. Solution of methyl-ethyl ketone and iso-butyl
   alcohol into water from porous packing ($\underline{27}$)

3. Solution of β-naphthol into water from fixed and
   fluidized beds ($\underline{45}$).

The extensive range of variables covered by these systems were the use of fixed and fluidized beds, particle diameters of 0.09 to 0.63 inches, void volumes of 35 - 94 per cent, either gas or liquid systems, Schmidt numbers of 0.6 - 2000 and modified Reynolds numbers (defined below) of 7 - 7000. Gamson consolidated these data by plotting $j_D/(1-\epsilon)^{0.2}$, where ϵ is the fraction of voids in the bed, against a modified Reynolds number, $D_pG/\mu(1-\epsilon)$ (see Figures 14 and 15). Although the data fall on a smooth continuous curve, Gamson represents the correlation by two lines and an intermediate region (analogous to the laminar, transition, and turbulent regions in flow through conduits):

$$j_D/(1-\epsilon)^{0.2} = 17(Re_M)^{-1} \qquad 10 > Re_M \qquad (27)$$

$$j_D/(1-\epsilon)^{0.2} = 1.46(Re_M)^{-0.41} \qquad Re_M > 100 \qquad (28)$$

The transition region is not characterized mathematically but gives a smooth connecting curve for which the co-ordinates are listed in tabular form.

The agreement of these diverse data is excellent, the average deviation being approximately 10 per cent with a maximum deviation of about 60 per cent. The scatter of the data is quite large in the transitional region with the data of McCune (45) tending to follow the turbulent curve down to Re_M of 20, well into the transitional region. This variation

in the point at which molecular diffusivity begins to become important agrees with the work of Bernard and Wilhelm (6) who found that the transition zone started at Re_M values between 10 and 1000 depending on the characteristics of the system under observation.

Gamson also demonstrates that the use of a shape factor to compensate for the portions of the particle surface not available for mass transfer allows his correlation to include the data obtained by several investigators (22, 45, 71, 79) with cylinders, flakes, partition rings and Raschig rings. The data on sublimation of naphthalene into gas streams (32, 60) are not included since they were not in agreement with each other and demonstrated an effect of particle size not found by any other workers.

The more recent data of Hobson and Thodos (28) and of Gaffney and Drew (20) also substantiate the Gamson correlation although the solid solution data of Gaffney and Drew have a variation of the Schmidt number not accounted for by the two-thirds power relationship of the j-factor. These authors correlated their data and that of McCune and Wilhelm (45) by the use of $(Sc)^{0.58}$ instead of $(Sc)^{2/3}$. However, use of their exponent causes a marked deviation between gas and liquid data and it is recommended that the two-thirds power be used until much more data on packed beds are accumulated and examined. It is quite possible that the results

will indicate that the exponent is in itself a function of
the Schmidt number.

The most recent work (17) investigates the solution of
spherical solids in water at low Reynolds numbers (10^{-2} to
10) and shows considerable deviation between the different
solid materials and also from the work of Hobson and Thodos
(27, 28) at similar Reynolds numbers. This discrepancy in
the laminar flow results has several possible explanations:

1. If the void spaces around the particles are con-
   sidered to be a number of small diameter tubes
   through which the fluid passes in laminar flow, it
   becomes necessary to consider an L/D ratio charac-
   teristic of the flow passages formed by each parti-
   cle configuration.

2. Free convection effects dependent both on the
   geometry of the system and on the temperature and
   concentration gradients set up during transfer will
   cause differences which probably have to be con-
   sidered by means of a Grashof number.

3. The effect of the extended transition range
   described above.

From these reasons, it can be seen that it is unlikely that
a single line should represent all mass transfer data in the
laminar region when plotting j-factors versus the Reynolds
number, a correlation originally devised for turbulent
regions.

A second generalized correlation has been introduced by various authors to combine the data on single spheres with packed beds. This method employs for the velocity term the average interstitial condition within the bed, giving as the co-ordinates $j\epsilon$ and Re/ϵ. The correlation, however, results in no better general agreement than does Gamson's method.

It should be emphasized that, for randomly packed beds of spheres, with which system the present investigation is concerned, both general correlations and simple j_D vs. Re plots give approximately the same degree of agreement of the data, since the void fractions of the systems employed by the various investigators are nearly identical. The mass transfer data obtained in the present work are correlated and compared with previous work on the basis of j_D vs. Reynolds number plots and are also compared with the generalized Gamson correlation.

Reliable data on heat transfer are confined to the work of Gamson, Thodos and Hougen (22) who related heat and mass transfer factors for the evaporation of water into air by the expression

$$j_H/j_D = 1.076. \qquad (29)$$

However, it can be shown (66) that this value results from the assumption of wet-bulb temperature at the surface of the

porous spheres and that the value 1.076 can be obtained independently of the rate data from the slope of the adiabatic saturation line and the physical characteristics of air. Inasmuch as this assumption was shown to be not entirely correct ($\underline{28}$), the ratio is probably **low**, since their values of j_H should be higher and j_D should be lower. However, any error introduced by assuming the surface to be at the wet-bulb temperature can be shown to affect j_D much more than j_H, so it may be assumed that their values of j_H are more reliable than those of j_D. Therefore, their equation for j_H will be used as a basis of comparison for the heat transfer data to be obtained in this work.

Work With Hydrogen Peroxide

Hydrogen peroxide is an essentially stable but very reactive substance which has been long used in dilute solutions in such applications as a bleach in the textile and paper industries, as a disinfectant, and as a reagent in oxidations. However, in the past ten years, the techniques of manufacture have attained a state such that a ninety weight per cent aqueous solution can be safely produced and handled, making possible the use of hydrogen peroxide solutions as a source of power. The decomposition of concentrated hydrogen peroxide in a suitable apparatus according to the equation

$$H_2O_2(\ell) \longrightarrow H_2O(\ell) + 1/2\ O_2(g)\ (+23,470\ cal/g.mol)$$

$$(30)$$
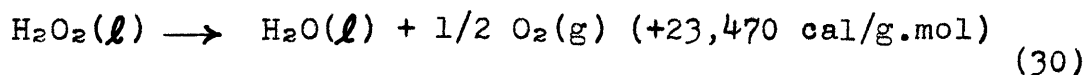
provides a supply of high-pressure, high-temperature steam and oxygen, which can be an important source of energy in power units where fuel cost is secondary and high power performance per unit weight is the principal consideration.

Practical exploitation of the use of hydrogen peroxide in high-power propulsion units was first realized by the Germans in World War II (4, 7). Hydrogen peroxide power systems were applied to submarine power plants, rocket-powered interceptor aircraft, rocket launching units and fuel pumps in V-2 rockets. The decomposition of the peroxide solution was accomplished in several ways: Calcium permanganate solution in V-2 rocket propulsion pumps and solid catalysts impregnated with manganese, chromium and lead salts in submarine propulsion units. In order to obtain still more energy, rockets used fuels which ignited spontaneously with the hydrogen peroxide.

Since World War II, extensive research and development on power plants employing hydrogen peroxide has been carried on. However, it was quickly realized that the design of decomposition chambers required basic knowledge of the characteristics of the reaction itself. The first design studies were carried out by Isbin (33, 34, 35) who investigated the decomposition of fifty and eighty-three weight per cent

hydrogen peroxide using catalyst beds of his own design.
His procedure was to measure the overall decomposition of a
stream of liquid hydrogen peroxide in an adiabatic catalyst
chamber. The heat of decomposition liberated by the initial
reaction of the concentrated solution was sufficient to
vaporize the stream, so that much of the decomposition sub-
sequently occurred in the vapor phase.

In considering the decomposition in these beds, Isbin
noticed the following characteristics which indicate that
diffusion of vapor-phase hydrogen peroxide to the catalyst
surface is the controlling factor:

1. There is little difference in activity at high
   temperature between solid catalysts which show
   considerable variation in catalytic activity at
   lower temperatures.

2. A number of runs made with hydrogen peroxide con-
   taining chemicals which progressively deactivated
   the catalyst surface demonstrated a constant rate
   of reaction for the initial portion of the run
   followed by a steadily decreasing rate for the
   remainder of the run. This can be explained by the
   assumption that the potential reaction rate on the
   catalyst surface was initially much higher than the
   diffusion rate, but that poisoning eventually re-
   duced the catalyst activity to a level such that

the chemical rate and not the diffusion rate
became the controlling factor.

3. The rate of decomposition per unit area was pro-
portional to the six-tenths power of the flow rate,
the relationship which is expected in mass transfer
in packed beds.

4. The most successful attempt of Isbin to predict
results from theoretical considerations was based
on the assumption that the decomposition rate was
limited by the rate of diffusion of the vapor to
the surface.

These facts provided a reasonable basis for assuming
that vapor diffusion is the controlling feature of high-
temperature hydrogen peroxide decomposition. However, it
was not possible to compare the rate data obtained in Isbin's
work with the values predicted from a theoretical mass
transfer analysis of the operation because of large tempera-
ture and concentration variations in the two-phase flow
through the bed and because of the complexity of the geometry
of Isbin's packed beds.

Wentworth (75, 76) therefore undertook a study of the
decomposition of a vapor mixture of hydrogen peroxide,
oxygen and water while passing through a catalyst tube. A
theoretical rate of diffusion to the catalyst surface could
be derived from the nature of the flow in this system and it

was proposed to compare the actual decomposition obtained with that predicted from the diffusion rate expression. The vapor mixture of hydrogen peroxide and its decomposition products was obtained by a partial decomposition of the liquid in a catalyst bed. This mixture was then passed through the tube, samples being removed at points along the tube in order to determine the decomposition rate. However, considerable difficulty was encountered with entrainment, results of the study showing that the stream of vapor issuing from the catalyst bed was not in thermal equilibrium. Hydrogen peroxide existed in the liquid phase in downstream portions of the catalyst chamber where sufficient heat of decomposition had been evolved and the temperature was sufficiently high to completely vaporize the liquid under equilibrium conditions. Inasmuch as the sampling technique used in the investigation had been devised for a homogeneous stream, reliable results were not obtained in the sampling of the two-phase stream. However, it was concluded on a semi-quantitative basis that diffusion was controlling under the conditions of the experiment.

Meeken (51) continued the work of Wentworth, using a newly developed boiler (64) to produce a steady supply of vapor with a low rate of decomposition and small danger of explosion. The object of his investigation, like that of Wentworth, was to study the diffusion-controlled reaction

and to obtain data on the decomposition rate for comparison
with values predicted from mass transfer theory. The initial
hydrogen peroxide vapor concentrations ranged from five to
thirty per cent by weight. Operation was at a total pressure
of one atmosphere with flow rates corresponding to Reynolds
numbers ranging from four thousand to five thousand in a
catalyst tube, one quarter inch inside diameter and twenty-
four inches long. The results indicated that the reaction
is diffusion-controlled under the conditions investigated
although a theoretical expression predicted lengths approxi-
mately thirty-five per cent below the actual tube length
employed. This deviation was ascribed in part to approxima-
tions made in the derivations and in part to the insufficient
capacity of the boiler which probably resulted in transi-
tional rather than turbulent flow. An improved version of
Meeken's apparatus was used in the present work.

III. THEORETICAL ANALYSIS OF THE CATALYST TUBE SYSTEM

A. Development of Mass Transfer Equations

As stated in the Introduction, the problem of deriving the reaction rate equation for the catalytic decomposition of hydrogen peroxide is resolved into determining the rate of diffusion of hydrogen peroxide vapor to the catalyst surface. The differential equation for the system was given as

$$y_A y_B(u_A - u_B) = - D_{AB}(dy/dx) - (D_T/T)(dT/dx) \qquad (2)$$

which represents the transport under a combination of concentration and temperature gradients.

Furry and Jones (19) discuss this equation in its application to a method for separation of isotopes and introduce the relationship

$$D_T = D_{AB} y_A y_B \alpha. \qquad (31)$$

The coefficient α is independent of pressure but is dependent on temperature and probably on the concentrations. In the present case, this dependence of α on temperature and concentration can be neglected because of the small magnitude of the thermal diffusion term relative to that for molecular diffusion; this is fortunate since no information is available on the nature of this dependency. Both Furry and Jones and Chapman and Cowling (10) present methods for estimating

the values of α for simple non-polar molecules. However,
for the polar system here—hydrogen peroxide-water-oxygen—
α is unknown and cannot be estimated by their equations since
the equations require the application of a correction factor,
related to inter-molecular forces, which is unknown for the
present system. In spite of this lack of knowledge, one is
justified, from the observation of other systems (77, 80),
in examining the effect of values of α ranging from 0.0 to
0.3.

Because the exact value of D_T for this system is unknown
but believed to be small, the first equations to be developed
in this analysis neglect the effect of thermal diffusion.
Then, by making various assumptions, an equation including
this effect is derived. At this point in the thesis, only a
summary of these derivations and a discussion of the necessary
assumptions are given. The details of the derivation and
methods of evaluating the various constants are given in the
Appendix.

If the effect of thermal diffusion is neglected, the
right-hand side of Equation (2) includes only the term for
molecular diffusion. The relationship of the molecular dif-
fusion coefficient, D_{AB}, to molecular properties has been
developed through the concepts of kinetic theory (36, 42)
and good correlations for the coefficients are available
(24, 65). By introducing the relations

$$u = NM/\rho \tag{32}$$

$$\rho = Mp/RT \tag{33}$$

$$p = yP, \tag{34}$$

Equation (2), neglecting thermal diffusion, is transformed to the more familiar

$$y_B N_A - y_A N_B = (-D_{AB}P/RT)(dy_A/dx). \tag{35}$$

(This equation may be developed for any number of diffusing components.)

The relationship $y_B = 1 - y_A$ allows the equation to be rearranged to give

$$N_A = (-D_{AB}P/RT)(dy_A/dx) + (N_A + N_B)y_A \tag{36}$$

When considering a chemical reaction in which there is a change in number of mols on reaction, mathematical development of Equation (36) is simplified if the algebraic sum of the transport rates, $(N_A + N_B)$, is expressed as N_t, and a ratio ϕ is defined for each component as

$$\phi_i = N_i/N_t. \tag{37}$$

This ratio was introduced by Wilke (78) and for component M in the equation below, has been shown by him to be equal to

$$\phi_M = m'/(m'+n'-r'-s') \tag{38}$$

where m', n', r', and s' are taken from the reaction equation

$$m'M + n'N \longrightarrow r'R + s'S, \tag{39}$$
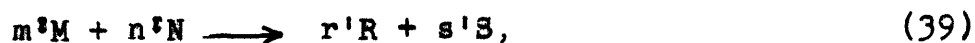
the reaction taking place at the surface to and from which
the reactants and products diffuse.

Equation (36) now becomes

$$N_A(\phi_A - y_A) = (-D_{AB}P\phi_A/RT)(dy_A/dx) \tag{40}$$

where D_{AB} represents the average diffusivity of component A
through the remaining components in the system. The methods
of obtaining this value are discussed fully in the Appendix.

Equation (40) can now be integrated over the diffusion
path, assuming the concept of an effective film thickness,
to give

$$N_A x_D = (D_{AB}P\phi_A/RT) \ln (\phi_A - y_{Aw})/(\phi_A - y_{As}). \tag{41}$$

Although slightly different in form, this equation is identi-
cal to the equation for non-equimolecular counterdiffusion
proposed by Hougen and Watson (30) and, for the present
system, gives values within 1 per cent of the results ob-
tained by use of the more rigorous solution developed by
Gilliland (65) in the form of two simultaneous equations.
Gilliland's equations differ in that he does not make the
simplifying assumption that, in a complex system of diffusing
gases, the diffusional gradient established for any component
A is equal to the sum of the gradients which would result
from the separate diffusion of A with each of the other com-
ponents in separate binary systems in which the concentrations

and rate are the same as the complex system. The difference between the results of the various equations becomes significant only when the ratio of molal rates of diffusion of two of the components becomes excessively large (greater than 10 to 1). This situation is not likely in most chemical reactions where the molal ratio of reactants to products (or the reciprocal) is seldom greater than about 3 to 1, e.g., here the ratio is 2 to 3.

For the integral reactor being used in this experimental work, Equation (41) must now be evaluated along the catalyst tube. In the past, most investigators have treated integral reactors by the use of the point-rate equation evaluated at some average condition within the tube. For the present work, it was felt advisable to obtain additional accuracy by integrating the point-rate equation for the changing conditions in the system. In order to make this integration possible, the following assumptions have been made and will be discussed more fully below:

1. Axial heat transfer is negligible.
2. Axial diffusion is negligible.
3. Entrance effects may be neglected.
4. The partial pressure of the hydrogen peroxide vapor at the catalyst surface is zero.
5. No homogeneous reaction occurs in the gas phase.
6. The diffusion coefficient may be found by

calculating the diffusivity of hydrogen peroxide through vapor of the proper proportions of water and oxygen by use of Gilliland's equation (24).

7. A constant average value of the effective film thickness may be employed along the tube.

8. The integration requires a method of representing the diffusivity and temperature of the gas within the film as a function of length. At any point in the tube, it is assumed that the average diffusivity across the film is that at a film temperature calculated as the arithmetic mean of the stream and wall temperatures. To obtain an expression for the film temperature along the tube, either one of the two following assumptions is made:

(a) A constant average film temperature over the length of the tube is used. Its value is determined as the arithmetic average of the entrance and exit film temperatures, each of these having been obtained by averaging the bulk gas temperature at that point with the average wall temperature along the tube. This last value is taken as the arithmetic average of the five wall-temperature measurements.

(b) A varying film temperature is calculated by assuming the bulk stream temperature to be a

linear function of the fraction of the enter-

ing hydrogen peroxide decomposed and averaging

this value with the average wall temperature.

By making these assumptions, for which justification is

given below, Equation (41) for the point rate of diffusion

is integrated along the tube, assuming a constant average

film temperature T_a, to give

$$\frac{y_{A2}-y_{A1}}{(y_{A2}-\phi_A)(y_{A1}-\phi_A)} + \frac{2}{\phi_A} \ln \frac{y_{A2}(y_{A1}-\phi_A)}{y_{A1}(y_{A2}-\phi_A)}$$

$$= \frac{D_{AB}P}{RT_a x_D n_o} \cdot \frac{2h'}{h'-\phi_A} \cdot \pi(dia.)L \tag{42}$$

In order to use a temperature function varying with

length, as described in assumption 8(b), the symbol f (frac-

tion decomposed) is introduced and defined as

$$f = (n_o-n)/n_o \tag{43}$$

where n is the rate of flow of hydrogen peroxide in an axial

direction at any point in the tube in mols per unit time and

n_o is the value with no decomposition. The stream tempera-

ture, T_s, at any point along the tube now becomes

$$T_s = c'f + d'. \tag{44}$$

Combining this with the average wall temperature provides

the relationship for film temperature,

$$T_f = cf + d.$$ (45)

By now using Gilliland's equation which reduces to

$$D_{AB} = aT^{3/2}$$ (46)

Equation (41) is integrated along the tube to give the final equation for diffusion to the catalyst wall

$$2n_0(\phi_A - h') \left| \frac{2}{\sqrt{c+d}} \tanh^{-1} \sqrt{1 - \frac{c(1-f)}{c+d}} \right|_{f_1}^{f_2}$$

$$+ h' \left| \frac{2n_0\sqrt{c+d}}{c} \sqrt{1 - \frac{c(1-f)}{c+d}} \right|_{f_1}^{f_2} = \left(\frac{2aP\phi_A h'}{Rx_D} \right) \pi(dia.)L$$ (47)

The development of Equation (2), which includes the effect of thermal diffusion, requires knowledge of dT/dx. The three possible mechanisms for heat transfer from wall to stream are radiation, conduction, and that transfer due to the sensible heat carried by the diffusing components. An analysis in the Appendix shows that only heat transfer by conduction need be considered and that an energy balance across the film gives

$$N_A \Delta H = k(dT/dx)$$ (48)

Equation (2) may now be restated in the form

$$N_A = -\frac{D_{AB}\phi_A P}{RT(\phi_A - y_A)} \frac{dy_A}{dx} - \frac{D_{AB}\phi_A P}{RT^2} \cdot \frac{y_A(1-y_A)\alpha}{\phi_A - y_A} \cdot \frac{N_A \Delta H}{k} \quad (49)$$

which is integrated to give

$$N_A x_D = l' \left| \frac{-2}{\sqrt{4n'\phi_A m' + (n'-m')^2}} \tanh^{-1} \frac{2m'y_A + (n'-m')}{\sqrt{4n'\phi_A m' + (n'-m')^2}} \right|_{y_{As}}^{y_{Aw}}$$

$$(50)$$

This point-rate equation can be compared with Equation (41) to indicate the effect of thermal diffusion in this system.

The accuracy of these equations will depend on the validity of the assumptions made in the derivations. These assumptions, as listed above, may be justified as follows:

1. Axial Heat Transfer is Negligible: By employing a catalyst tube of sufficiently small wall thickness, the heat transfer by conduction from one point on the wall to an adjacent point may be reduced to negligible proportions. It can be shown (Appendix) that with a wall thickness of 0.01 inches and the steepest temperature gradient which was found to exist along the wall in this work, the heat flow along the tube is less than 0.1 per cent of the increase in sensible heat of the vapor stream passing through the tube.

2. Axial Diffusion Is Negligible: Axial diffusion of hydrogen peroxide along the tube, under the concentration gradient established by decomposition, may be shown to be negligible at the flow rates employed in this study.

3. **No Entrance Effects:** A fifty-diameter calming section
is employed to give fully developed turbulent flow at the
tube entrance. At the inlet portion of the catalyst tube,
temperature and concentration gradients are being estab-
lished between the stream and the surface, but this effect
is probably negligible on the overall observed rates, as is
indicated by Linton (41) who found no effect at length-to-
diameter ratios greater than six.

4. **Zero Partial Pressure of Hydrogen Peroxide at Surface:**
This assumption is equivalent to stating that the chemical
reaction rate is many times greater than the diffusion rate
and the partial pressure of hydrogen peroxide on the surface
of the catalyst is consequently very small, approaching zero
as a limit. This can be checked by considering the effect
of concentration and flow rate on the experimental results.

5. **No Homogeneous Reaction in the Gas Phase:** Homogeneous
reaction is believed to be negligible under the conditions
existing in the catalyst tube (33, 34, 63). In addition, if
a homogeneous reaction were occurring to a significant
extent, the calculated mass transfer coefficient would in-
crease as the concentration increases. The experimental
results show no such increase and, therefore, indicate that
the assumption is justified.

6. **Calculation of Diffusion Coefficient:** The diffusivity
of the hydrogen peroxide vapor is calculated from Gilliland's

empirical equation

$$D_{AB} = \frac{0.0069\ T^{3/2}}{P(V_A^{1/3} + V_B^{1/3})^2}\ \sqrt{\frac{1}{M_A} + \frac{1}{M_B}} \qquad (51)$$

using molecular volumes available in Sherwood (65), as the diffusivity of hydrogen peroxide through an effective second component whose properties are obtained from a weighted average of the properties of the oxygen and water present in the system. The value obtained by this method does not differ substantially from the weighted average of the binary diffusivities recommended by Hougen and Watson (30) or the more elegant harmonic mean recommended by Wilke (78) (Appendix). In order to check the validity of the basic assumption of the applicability of Equation (51) to a hydrogen peroxide system, the diffusion coefficient for a hydrogen peroxide-air system was calculated by the method described and found to agree within 1 per cent with that measured experimentally by McMurtrie and Keyes (48).

7. Film Thickness: The use of an effective film thickness is probably the weakest link in the entire analysis. The concept of a single laminar film, the thickness of which is so chosen as to incorporate all the resistance, both eddy and molecular, assumes that the variables affecting molecular diffusion exert the same effect on eddy transport. This concept can truly represent the facts only when (1) all the

resistance is actually laminar in nature, or since a signifi-
cant part of the resistance to mass transport may occur in
the bulk stream, when (2) the ratio of molecular resistance
to total resistance remains constant. Even thought it may
appear that this method is of questionable merit, it has
been used with considerable success in correlating heat
transfer data and mass transfer in wetted-wall towers. Be-
cause of its adequacy in these cases, it is reasonable to
use the same concept in the development of the mass transfer
equation in this work.

An examination of Equation (41) shows that by applying
the relationship

$$k_G = \frac{D_{AB}P}{RTp_B x_D} \tag{52}$$

a final integrated equation for diffusion in the system can
be developed in terms of the mass transfer coefficient, k_G,
and thus require no assumption concerning an effective film
thickness. However, use of Equation (52) leads to an expres-
sion which does not include a term for diffusivity or tempera-
ture. Therefore, Equation (47) was left in terms of x_D in
order that the effect of the varying temperature along the
tube might be included.

The second assumption in the use of an effective film
thickness is that a constant average value can be employed
over the entire length of the tube. Actually, the variation

in film thickness, due to temperature changes along the tube, should, in principle, have been included in the integrations, but all efforts to this end resulted in equations which could not be analytically integrated. However, as discussed below, comparison of correlations on the basis of various temperatures within the system shows very little effect of the temperature variation within the tube, i.e., correlation on the basis of stream temperature instead of film temperature changes the average deviation from the correlation from 9.5% to 9.6%.

8. Film Temperature Function: The two possibilities for evaluation of the film temperature along the tube are (a) use of a constant value equal to the average of the average stream temperature and wall temperature or (b) a value varying with length equal to an average of the wall temperature and the stream temperature, and expressed as a linear function of the fraction of peroxide decomposed. By consideration of the adiabatic case, it can be demonstrated that the stream temperature in the tube is indeed a linear function of the fraction decomposed inasmuch as the heat loss through the insulation per unit length of the catalyst tube was essentially constant. The results obtained from Equations (42) and (47) agreed within 1%, showing very little effect of the choice of temperature function. However, the value given by Equation (47) was chosen as more accurate since it

considered the effect of a varying film temperature along the tube.

In considering this analysis, it must be emphasized that the entire diffusional resistance is replaced by an effective film thickness and the validity of the theoretical Equation (47) depends on how well this empirical value represents the actual resistance.

B. Development of Heat Transfer Equation

The method for predicting heat transfer rates is based on a heat balance across the film which forms the resistance to heat transfer from the surface to the stream. If no heat is lost from the system, all the heat liberated at the catalyst surface under steady-state operation must be transferred back to the stream. Therefore, the magnitude of the temperature difference is governed by the relative rates of diffusion to the surface and heat transfer from the surface.

The heat liberated at the surface may be expressed as $N_A \Delta H$ where N_A is the rate of diffusion of the hydrogen peroxide to the surface per unit area and ΔH is the heat liberated by the decomposition at the temperature of the surface. This quantity less any heat loss from the system must be equal to the heat transferred from the surface to the stream. The heat can be transferred from the wall to the stream by

conduction, radiation, and by the bulk flow of the diffusing gases. An analysis in the Appendix shows that, for the range of variables encountered in this work, the temperature within the film is a linear function of the distance through the film and that only heat transfer by conduction need be considered. This result is also in accord with the theoretical analyses of Squyres (70), who shows that with the rates of mass transport and the specific heats encountered in this work, the simultaneous mass transfer through the film has an effect of less than 1% on the heat transfer coefficient. Thus, a heat balance across the film gives

$$N_A \Delta H = kdT/dx = k\Delta T/x_H = h\Delta T \tag{53}$$

This equation is the theoretical equation for heat transport from the wall to the stream, assuming the concept of an effective film thickness.

The method of applying the theoretical equations developed in this section are outlined in the Procedure and described in detail in the Appendix.

IV. PROCEDURE

A. Catalyst Tube

Construction of Apparatus. The apparatus employed to
investigate decomposition in a catalyst tube consisted
basically of a 1/4-inch inside diameter catalyst tube
through which hydrogen peroxide vapor flowed. The catalyst
was a metal of high thermal conductivity; the inside tube
surface was smooth and was not affected chemically by the
decomposition reaction. The vapor was produced by boiling a
hydrogen peroxide-water solution in a pressurized vaporiza-
tion system and was passed through a superheater and calming
section before entering the tube. The temperature and con-
centrations of the entering and leaving gas streams were
obtained and the tube wall temperatures were measured at
several points along the tube.

Figures 3 and 4 show the two principal parts of the
equipment--the vaporization section and the decomposition
section. As pictured in Figure 3, the boiler was constructed
of an 18-inch section of 4-inch standard Pyrex pipe closed
at one end and fitted with a standard flange at the other
end. The flange was gasketed to an aluminum plate which
carried a 2-inch diameter heating finger. Steam at a pres-
sure of 50 psig. passed through a throttling valve and con-
densed on the inside of the finger which extended 5 inches
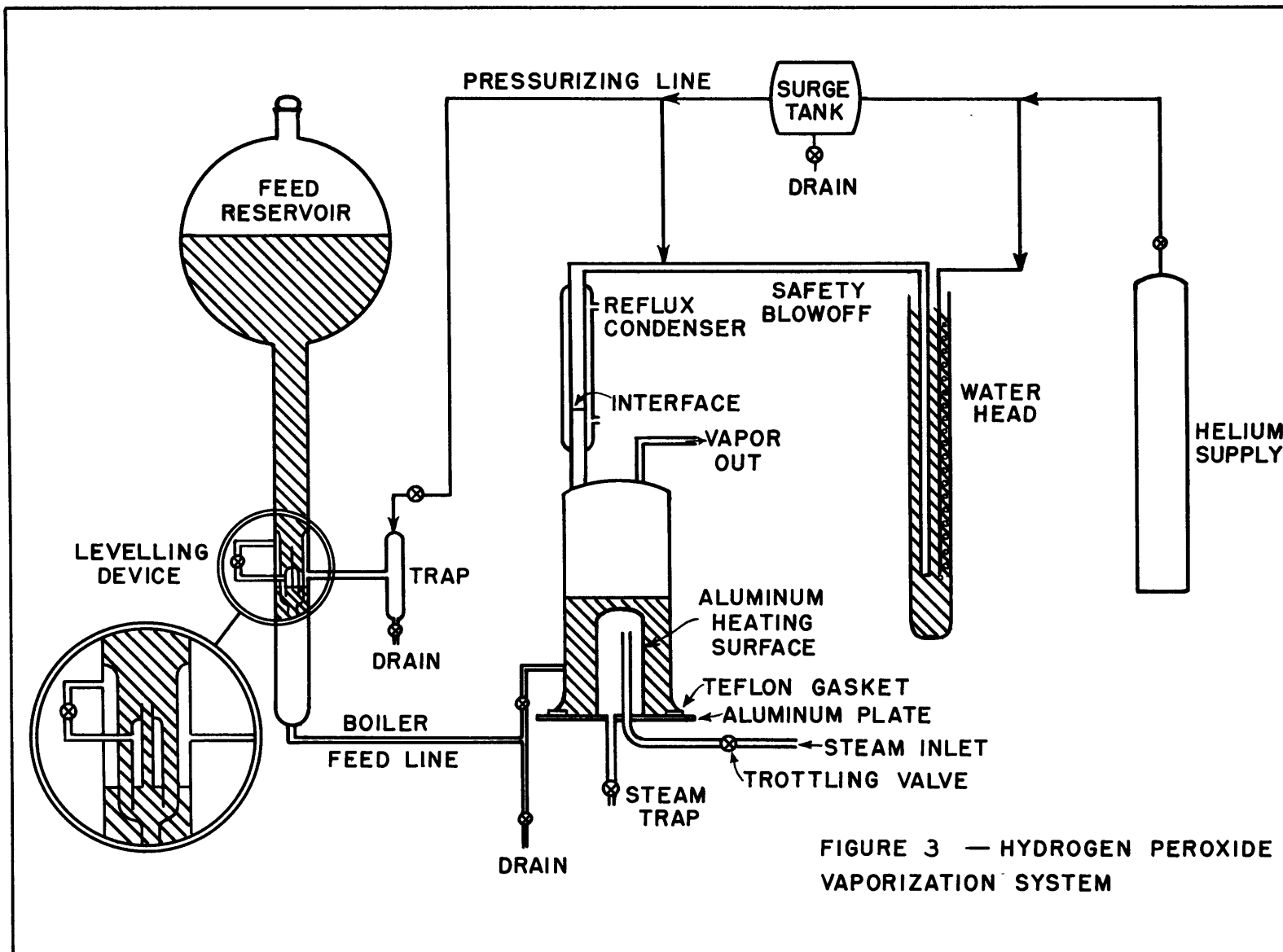
FIGURE 3 — HYDROGEN PEROXIDE VAPORIZATION SYSTEM

FIGURE 4
CATALYST TUBE
DECOMPOSITION APPARATUS

(SHOWN WITHOUT INSULATION)
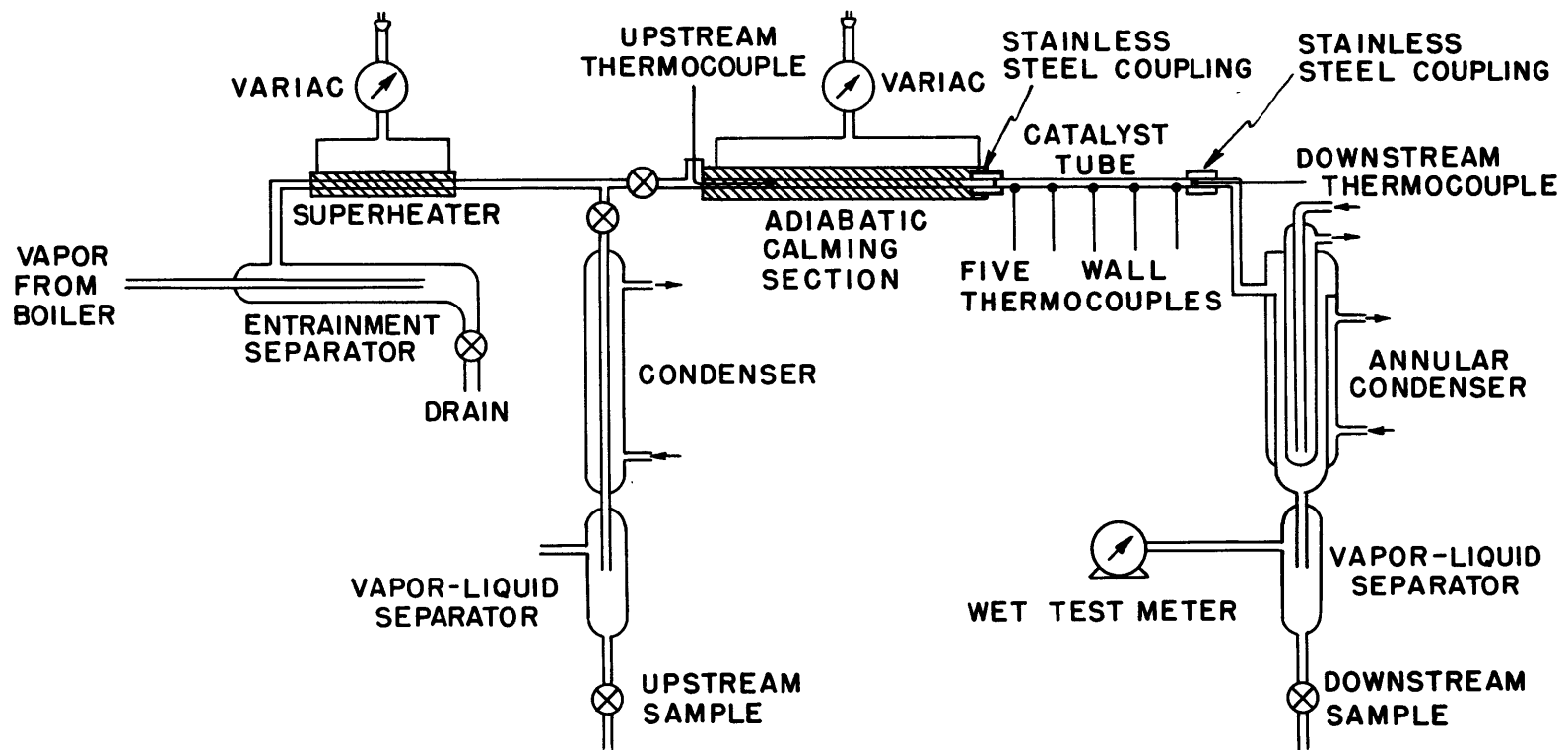
into the pool of hydrogen peroxide in the boiler. Liquid depth was maintained at 6 inches, the free space above the liquid serving as a settling chamber for droplets.

Feed was introduced from a 12-liter feed reservoir through a constant-level feed system which was necessarily complicated by the system requirements of a steady flow of constant-concentration vapor at a pressure somewhat above atmospheric, in order to overcome the pressure drop encountered in the flow system. It was also necessary to eliminate the sensitivity of the feed system to the changes in the pressure drop which were encountered in the manipulation of the stopcocks in the sampling devices. Several modifications of levelling devices were found to be unsatisfactory since slight changes in the pressure drop unbalanced the feed devices and altered the boiler level, either backing concentrated boiler liquid into the feed line or introducing a large amount of cold feed into the boiler. Either of these eventualities resulted in immediate changes in the composition and quantity of vapor produced. This problem of a satisfactory levelling device was finally solved by maintaining the device and the boiler at the same pressure and by employing a levelling device (shown in insert in Figure 3) which introduced the feed in small amounts at short intervals. This device is described fully by Holmes (29). Since the boiler vapors were condensable, the boiler and levelling

device had to be connected through an intermediate non-condensable gas. Helium, chosen because it is inert and lighter than the vapors, was connected from the boiler through a reflux condenser to the free space above the levelling device. A water head maintained the helium at a pressure up to 32 inches of water in order to give the flow rates desired in the system. The helium was prevented from entering the vapor stream by keeping the visible interface between the condensable vapors and the helium above the boiler. In operation, this arrangement allowed for the variation in pressure drop through changes in the amount of reflux flowing back to the boiler, and the vapors were delivered at a very steady concentration and rate of flow.

A large duct was attached from the boiler through the reflux condenser to a water head slightly greater than that of the helium and provided a blow-off for the vapors in case of rapid decomposition in the boiler. In addition, the entire vaporization assembly was placed behind a steel-plate shield to offer protection to personnel.

The vapor left the top of the boiler and passed through an entrainment separator and a superheater (Figure 4) which ensured complete vaporization. After leaving the super-heater, part of the vapor stream was withdrawn, condensed, and subsequently analyzed while the remainder flowed through a 1/4-inch inside diameter precision-ground Pyrex calming

section into the 1/4-inch inside diameter catalyst tube. Although it was necessary to know the temperature at the entrance of the catalyst tube, it could not be measured directly at that point without disturbing the flow pattern. Therefore the temperature was measured at the entrance to the calming section and the calming section was made adiabatic, in this way permitting an accurate determination of the entering gas temperature without disturbing its flow characteristics. Adiabaticity was obtained by winding a heating coil on the insulation around the approach section and adjusting the heat input through the coil so that no temperature difference occurred between the glass tube and the insulation, thus insuring zero heat flow. Temperatures within the adiabatic calming section were indicated by six thermocouples mounted on the glass calming section and in the insulation. Preliminary runs demonstrated that the adiabatic approach section could easily be brought to an equilibrium state such that the stream temperature measured by a temporary thermocouple at the junction of the approach section and the catalyst tube was within one degree of the stream temperature measured at the entrance to the approach section.

The connection between the glass calming section and the catalyst tube was obtained by means of the stainless steel coupling and Teflon gasket discussed more fully in the

Appendix. This joint was a major difficulty in the operation of the equipment and caused several shut-downs due to the Teflon gasket expanding and either forcing its way between the glass and catalyst tubes or breaking the glass tube. However, when operating correctly, the arrangement gave a smooth connection between the two sections. After leaving the catalyst tube, the vapor stream flowed through a condenser, the condensate was removed in the separator and the oxygen rate was determined by a wet-test meter.

The adiabatic calming section and the catalyst tube were supported in blocks of "foam-glass" insulation while the remainder of the apparatus from the boiler to the condensers was insulated with Pyrex glass wool and wrapped with aluminum foil. Except for the catalyst tube and aluminum heating finger and plate, construction was entirely of Pyrex glass, ground glass ball joints being used to connect units.

Copper-constantan thermocouples were silver-soldered to the catalyst tube wall at five positions: 1, 3, 10, 16, and 22 inches from the upstream end in the 24-inch tube and 1, 3, 9, 15, and 17 inches from the upstream end in the 18-inch tube. Two thermocouple probes, inserted in glass wells, measured stream temperatures at the entrance to the adiabatic section and at the exit of the catalyst tube. In addition, six other thermocouples were placed in the insulation of the adiabatic calming section in order to insure its correct operation. A switching arrangement allowed successive thermocouple circuits to be read on an accurate potentiometer.

Operation of Apparatus. Before starting a run, the
boiler was drained and flushed in order to remove any
impurities which would tend to concentrate in the liquid
remaining in the boiler and cause excessive decomposition
on boiling. The feed reservoir and levelling device were
then charged with a feed made by diluting unstabilized, 90
per cent Becco hydrogen peroxide with enough distilled water
to give ten or twelve liters of solution of the desired con-
centration. The boiler was filled through the reflux con-
denser with a more concentrated solution in order to permit
more rapid attainment of steady-state conditions. Boiling
was commenced and operation continued until an equilibrium
state had been reached, the steam pressure, helium pressure,
and superheater and adiabatic heater voltages being varied
as necessary in order to give the desired operation.
Approximately two hours were required for establishment of
steady-state conditions, as evidenced by constancy of thermo-
couple readings and condensate volumes and concentrations.

The actual data run required three observers. One
observer collected liquid samples at the downstream sampling
station and called out the proper sampling time to the
second observer at the upstream station. Liquid samples
were collected at each condenser every minute for ten con-
secutive minutes, the liquid collecting in the separator for
55 seconds and draining into the sample beakers for 5 seconds.

The downstream observer also read the wet-test meter during the interval when the separators were closed. The third observer read as rapidly as possible the voltages of the catalyst tube and gas thermocouples, three complete sets usually being taken.

At the conclusion of a run, the apparatus was shut down and drained. The liquid samples were immediately analyzed for peroxide content by titration with standardized potassium permanganate (see Appendix).

This procedure was followed until Run 72, at which time it was discovered that the glass tube at the end of the catalyst tube had acquired a very small amount of the catalyst, causing erroneous results for the preceding three runs. The metal could not be detected by eye but was discovered in the process of glass-blowing when the glass turned to a color characteristic of the catalyst diffused in glass. The presence of the catalyst was finally explained by a consideration of the condensation of vapor which may occur in the system at the end of a run and definitely does occur at the beginning of a run. The catalytic decomposition of this liquid-phase hydrogen peroxide on almost any metal surface is known to result in the solution of tiny amounts of metal. When this liquid containing the dissolved catalyst flowed out of the catalyst tube and into the glass tubing, some of the catalyst may have been adsorbed onto the

glass surface. Therefore, the operating procedure was
altered after Run 72 so that, at the start of a run, hot
helium was blown through the system to preheat it above the
condensation temperature of the vapor, while at the end of a
run, helium was again blown through the hot system until all
condensable vapors had been eliminated.

The independent variables investigated were the flow
rate, feed concentration, and, to a slight extent, the
entering gas temperatures. Runs 52 through 105 were made
with a 24-inch long catalyst tube while Runs 106 through 114
were made with the 18-inch tube. The flow rates used gave
Reynolds numbers from 3200 to 10,000, the upper limit being
fixed by boiler capacity and the lower limit by the desire
to stay within the turbulent flow region. Feed concentra-
tions ranged from 3 to 32 per cent, 3 per cent feed being
the lowest compatible with accurate downstream analyses,
while 32 per cent gave exit-vapor temperatures approaching
910°F., the maximum working temperature of Pyrex. The tem-
peratures within the system were largely dependent on the
other variables but could be varied somewhat by the degree
of superheat.

Calculation of Data. The data obtained for each run
included volumes and peroxide concentrations of upstream and
downstream liquid samples, the volume of oxygen leaving the

downstream condenser, and temperatures of the catalyst tube
and of the inlet and exit gas streams. From these experi-
mental data could be calculated the exact concentration of
the gases entering and leaving the tube, y_1 and y_2 respec-
tively, and the amount of decomposition resulting from pas-
sage through the tube, called w. These values were then
substituted into the theoretically derived Equations (42)
and (47) in order to obtain values of x_D — the effective
film thickness for mass transfer. The results of the two
equations agreed within one per cent, the value given by
Equation (47) being preferred since it considered a varying
film temperature along the tube. Use of Equation (52) then
allowed conversion of the effective film thickness to k_G —
the coefficient of mass transfer--which could be correlated
on the basis of j-factor expressions. Average conditions
within the tube were taken to be the point in the catalyst
tube at which the log mean partial pressure driving force
occurred. This point was chosen since use of the point rate
Equation (41) showed that the value of x_D calculated at this
point agreed within two per cent with the values determined
from the integrated Equations (42) and (47). However,
examination of the final results showed that the choice of
average conditions within the tube was unimportant in deter-
mining a final correlation because the change in physical
properties over the range of temperatures studied was such

that various choices of average conditions affected the
correlation very slightly (average deviation changed less
than one per cent). Values of the heat transfer coefficient
were calculated by means of Equation (53), the heat transfer
term being corrected for the amount of heat loss to the sur-
roundings which was experimentally determined by comparing
the actual exit gas temperature with that calculated for an
adiabatic system. This heat loss ranged from 2 to 40 per
cent, averaging about 15 to 20 per cent for most of the runs.
As described in the Discussion of Results, values were ob-
tained both on an overall and point basis, the latter values
being the more accurate. These coefficients were then cor-
related as j_H factors. The method of calculation, while not
complex, was lengthy and is described fully in the Appendix.

A material balance between the known concentration fed
to the boiler, called C, and the total stream composition
leaving the catalyst tube usually showed an increase in the
hydrogen-oxygen ratio, the increase usually being equivalent
to the loss of from one to ten per cent of the peroxide-
oxygen present in the reservoir feed. It is believed that
this was due to escape of oxygen from the boiler through the
reflux condenser, although non-equilibrium boiling may also
have accounted for some of the change. For this reason, it
was convenient in the calculations to employ an "adjusted-
feed" concentration, C*, defined as that concentration of a

liquid hydrogen peroxide-water mixture which, on vaporization and decomposition, would give the experimentally found composition of the vapor leaving the catalyst tube. Thus, C^* differed from the actual reservoir feed because of the peculiar construction of the boiling apparatus which allowed the loss of one component--oxygen--while prohibiting the loss of hydrogen peroxide as such or water. The use of the "adjusted-feed" concentration therefore removed the peculiarities of the boiler operation from the analysis of the decomposition data. The value of C^*/C--the ratio of the "adjusted-feed" concentration to the true boiler feed concentration--is listed in the Tables of Results and indicates the fraction of the peroxide-oxygen in the reservoir feed that enters the decomposition apparatus either as oxygen or peroxide. The relationship between C^* and the actual concentrations entering and leaving the catalyst tube, y_1 and y_2, is given by Equations (A-70) and (A-17) in the Appendix.

Reproducibility of Data. An error analysis given in the Appendix indicates a 4 per cent error possible in the experimental data with a maximum error of less than 2 per cent in the final calculated values of j_D. Although the thermocouple readings were accurate to within 3°F., there existed the possibility of errors as large as 15 per cent in j_H in some of the runs with very small temperature differences.

However, in most of the runs the maximum possible error was of the order of 5 per cent.

In addition to these errors in physical measurements, other errors and causes of non-reproducibility may have been introduced by the apparatus and techniques employed. The possible sources of errors of this type are enumerated and discussed below:

1. Regulation of vapor flow rate and concentration:

    Measurements of vapor rates and concentrations showed that the constant-level device operated successfully. Vapor production was steady enough so that over the ten minutes employed for taking data, the variation in measured values was less than 2 per cent and an average value of the experimental data was employed for calculations.

2. Effect of helium buffer system:

    Since the boiler was pressurized with helium through a reflux condenser, the possibility existed that helium might be present in the bulk stream and be measured by the wet-test meter as oxygen. However, this error was considered negligible since (1) the interface was well up in the reflux condenser, (2) the direction of flow of vapor in the condenser was against any flow of helium, (3) helium was considerably lighter than the vapor, and (4) the direction of the errors in the

material balance was opposed to this possibility. In
fact, as stated above, it was more probable that the
helium buffer system, rather than acting as a source of
helium, permitted oxygen to escape from the system.

3. Boiler decomposition:

Any decomposition occurring in the boiler probably
occurred on the boiling surface and furnished heat for
further vaporization. The amount of this decomposition
was kept to a minimum, but could not be completely con-
trolled and therefore led to different vapor composi-
tions with the same feed concentration. However, the
amount of decomposition during any one run was constant,
giving steady vapor concentrations at the entrance of
the catalyst tube.

4. Decomposition of hydrogen peroxide on glass surfaces:

Any decomposition on the glass between the sampling
points and the actual entrance or exit to the catalyst
tube would have led to analyses which were not repre-
sentative of the actual inlet and exit concentrations.
To prevent this, all glassware in the equipment as well
as that used in preparing the feed and carrying out
analyses were cleaned by a special procedure described
in the Appendix, and kept free of dust, dirt, and other
contamination. Preliminary runs made without the cata-
lyst present showed negligible decomposition on the

glass surfaces between the upstream and downstream
sampling stations.

5. Reliability of thermocouple readings:

The thermocouple readings were believed accurate to
within at least 3°F., considerable attention having
been given to the construction of the thermocouple
installation. The 0.01-inch thickness of the walls
resulted in negligible axial heat flow and the thermo-
couple temperatures therefore represented point condi-
tions on the surface. The gas thermocouple wells
extended into the gas stream for considerable distances,
thereby insuring that the thermocouple was actually at
stream temperature.

From this discussion, it can be seen that the physical
measurements made were truly representative of desired con-
centrations and temperatures, and that the equipment employed
did not contribute markedly to non-reproducibility of the
results.

B. Catalyst Bed

Construction of Apparatus. The packed bed employed the
same vaporization unit, entrainment separator and super-
heater as the catalyst tube, a tee being placed in the line
after the sampler so that either the tube or bed could be
used. As shown in Figure 5, the vapors, after leaving the

FIGURE 5
PACKED BED
DECOMPOSITION APPARATUS

(SHOWN WITHOUT INSULATION)

VARIAC

PACKED
BED

CONDENSER

SUPERHEATER

VAPOR
FROM
BOILER

SEPARATOR

DRAIN

DRAIN

CONDENSER

WET TEST METER

SEPARATOR

SEPARATOR

DOWNSTREAM SAMPLE

UPSTREAM SAMPLE

GLASS SHIELDED
THERMOCOUPLE

FLOW

BALL
JOINT

BALL
JOINT

CATALYST
THERMOCOUPLE
UNIT ENTRANCES
(ARRANGED 120° APART)

GLASS SPHERES

CATALYST SPHERES

CATALYST
THERMOCOUPLE UNIT

BED SUPPORT

GLASS SPHERES

BALL
JOINT

FLOW

GLASS SHIELDED
THERMOCOUPLE

FIGURE 6   DETAILS OF FIXED BED REACTOR FOR THE
STUDY OF HYDROGEN PEROXIDE VAPOR
DECOMPOSITION

tee, passed up through the bed and thence through a downstream sampling station which, as in the case of the catalyst tube, afforded a complete analysis of the gas stream leaving the bed.

Three different beds with inside diameters of 4.7, 4.8, and 7.5 cm. were used in obtaining the data, a detailed diagram of the 4.7-cm. bed being shown in Figure 6. It consisted of a 4.7-cm. glass column packed with five layers (total height 2.35 cm.) of 0.200-inch diameter catalyst spheres. Two layers of inert Kimble Resistant Glass spheres below and one layer above the catalyst spheres helped to reduce entrance and exit effects. The ratio of bed diameter to particle diameter was large enough (approximately 10 to 1) to minimize wall effects. The bed was supported by a grid of glass rods fused together and resting on an indentation around the column. A 3-inch ball joint at the top of the column provided access to the bed for construction and maintenance.

The temperatures of the entrance and exit gas streams and the temperature of one catalyst sphere in each of the first, third, and fifth catalyst layers proceeding from bottom to top were measured. The thermocouples indicating gas temperatures were mounted in glass wells and could therefore be copper-constantan or iron-constantan couples. The catalyst thermocouples, however, were threaded through holes

drilled in the catalyst spheres and therefore had to be platinum--10 per cent rhodium, platinum couples in order to withstand the corrosive action of peroxide vapor. The decomposition occurring on the short lengths of exposed thermocouple wire surface could be neglected in comparison with the total decomposition in the bed. As indicated in the insert in Figure 6, the catalyst couples were constructed by leading the two wires in through two glass tubes blown onto a ball joint and connecting the wires by a lap weld which was then pulled into the catalyst sphere. The hole in the catalyst sphere was made twice as large as the diameter of the wire to accommodate the weld. The butt weld attempted at first was found to be unsuccessful since it tended to be larger than the lap weld due to the formation of a bead at the junction and, in addition, proved to be much weaker. The entire unit was then inserted into the bed, the position of the sphere being dictated by the necessity for the thermo-couple wires to be in contact only with the sphere whose temperature they were measuring. Therefore, the sphere con-taining the bottom-layer couple was placed in the center of the layer with the wires being brought down through the glass packing, the middle-layer couple was placed at the edge of the bed and the top-layer couple was positioned in the center of the layer, its wires being brought out through the glass spheres.

The 7.5 cm. bed was of the same general design but had
only four layers of catalyst spheres. At the lower mass
flow rates encountered with the larger bed, five layers of
spheres would have resulted in enough decomposition to make
the downstream concentration too low for accurate titration.
The catalyst spheres measuring bed temperature were placed
in the first, third and fourth layers, their positions in
the layers being the same as described above.

In operation, the bed was insulated with several inches
of glass wool and covered with aluminum foil. Although
adiabatic operation would have been desirable, the irregular
shape of the decomposition chamber made unfeasible the use
of external heating to minimize heat losses from the bed. A
thermocouple placed in the insulation opposite the middle of
the bed provided a qualitative check on heat losses.

Data on the dimensions and packing of the three beds
used are given in Table I.

Operation of Apparatus. Operation of the packed bed
equipment was basically the same as that of the catalyst
tube, the major difference being that it was necessary to
preheat the bed before passing vapors through it. Other-
wise, the condensate formed during the heating of the bed
caused two-phase flow and slugging, fluidizing the bed and
rearranging the spheres. Before boiling commenced, the bed

TABLE I

Dimensions of Packed Beds

Runs: Nos. 1 through 10

Bed Diameter	4.70 cm.
Bed Height	2.35 cm.
Packing*	358 catalyst spheres (0.200-inch dia.)
Number of Layers of Spheres	5
Packed Fraction	0.604

Runs: Nos. 11 through 24

Bed Diameter	4.80 cm.
Bed Height	2.35 cm.
Packing*	355 catalyst spheres (0.200-inch dia.)
Number of Layers of Spheres	5
Packed Fraction	0.573

Runs: Nos. 24 through 33

Bed Diameter	7.50 cm.
Bed Height	1.80 cm.
Packing*	650 catalyst spheres (0.200-inch dia.)
Number of Layers of Spheres	4
Packed Fraction	0.562

* Includes the three spheres containing the bed thermocouples

was therefore heated to a temperature 50°F. above the condensation temperature of the vapor by blowing helium through the superheater and thence through the bed.

The boiler was initially filled with feed solution rather than with the equilibrium concentration in order that the bed might reach the high operating temperatures gradually and thus permit thermal expansion to occur slowly. Approximately two and one-half hours were required to attain boiling equilibrium as determined by analyses of upstream samples. This time interval was sufficient for the establishment of temperature equilibrium throughout the bed and bed insulation.

At equilibrium, three observers carried out the same procedure as with the tube, obtaining thermocouple voltages, condensate samples and oxygen rates. In the case of the lower flow rates, it was necessary to take two-minute samples in order to procure a sufficient quantity for accurate analysis and measurement.

After the data had been obtained, boiling was stopped and superheated helium was passed through the bed in order to sweep out any peroxide or water vapor. This method of operation prevented condensation and the possibility of two-phase flow at the start of a subsequent run.

At Runs 10 and 15, the entrance gas temperature became unreasonably high when compared to the temperature determined

by the superheater setting. This effect could be attributed
to two phenomena: (1) decomposition in the bulk stream
between the superheater and the bed, thus raising the
entrance temperature, or (2) localized decomposition of the
stream on the upstream thermocouple well, causing the
thermocouple to read too high a temperature. The first
explanation seemed the more probable since replacing the
thermocouple well did not obviate the difficulty and, fur-
thermore, since the total decomposition in the system was
higher than would be expected. The cause of the suddenly
developed decomposition on the glass surfaces was probably
some active material deposited on the glass either from the
helium or from the "Flurolube" stopcock grease. After Run 15,
specially purified helium was employed and the operating
procedure was slightly changed so as to make unnecessary the
turning of the stopcocks above the bed. These two altera-
tions proved effective in eliminating this difficulty. In
addition, a thermocouple was installed immediately after the
superheater and comparison of the temperature at that point
and the inlet temperature served as a definite check on
possible decomposition before the bed.

The principal variables investigated were flow rate and
feed concentration. Concentrations ranged from 5 through 24
per cent, the values again being fixed by the desire for
experimental accuracy at the lower limit and maximum working

temperature of the materials of construction at the upper
limit. In the 4.7- and 4.8-cm. beds, the flow rates used
resulted in particle Reynolds numbers, D_pG/μ, of from 22 to
161 while those with the 7.5-cm. bed ranged from 15 to 60.
The upper limit in each case was fixed by boiler capacity
and the lower limit by the necessity to obtain sufficient
flow rates for accuracy of measurement and analysis.

Calculation of Data. The method of calculation was
very similar to that for the tube except that no theoretical
relationships were available. The final values of composi-
tion, flow rate, and temperature were used to obtain decom-
position rates and concentration and temperature driving
forces. These, in turn, gave empirical heat and mass trans-
fer coefficients which were correlated by means of j-factor
expressions. The film properties necessary in calculating
the factors were based on the logarithmic mean of the values
at entrance and exit film temperatures. An arithmetic mean
of the gas and catalyst temperatures was employed for the
film temperature. The mass transfer coefficients were based
upon the logarithmic mean of the entrance and exit partial
pressure differences, catalyst surface to the fluid. Due to
the heat flow characteristics in the bed, it was necessary
to calculate point values of the heat transfer coefficients
at the center of the bottom layer of the bed. A complete

discussion of the calculation procedure is found in the
Appendix.

Reproducibility of Data. The factors affecting the
accuracy and reproducibility of the data in the packed bed
were the same as those discussed in the corresponding sec-
tion on the catalyst tube. However, an additional problem
specific to packed beds is that of the reproducibility of
the packing. Martin et al. (49) investigated the pressure
drops obtained in flow through beds of spheres arranged in
six geometric patterns with void fractions of from 0.2595 to
0.476. They showed that there was a definite variation in
pressure drop for different patterns, even in the case of
two different patterns having the same void fraction. In
order to pack a bed in a specified geometrical pattern, as
done by Martin, it is necessary to employ sections of
spheres next to the wall. With the ratio of sphere-to-bed
diameter used here, it was felt unncessary to use the more
elegant technique and, consequently, a "random packing" was
employed with as many spheres as possible placed in each
layer, this procedure being usual in packed beds. Although
it might appear that such a method would lead to marked
variation between different packed beds of spheres, past
experience indicates that different randomly packed beds
give approximately the same results in heat and mass trans-
fer work.

V.   RESULTS AND DISCUSSION OF RESULTS

A. Catalyst Tube

Results. Table II presents a summary of the experimental data and results. All 62 calculated runs are listed in this table although five runs were not employed in drawing graphs or in determining the final correlations. Runs 60 and 61 were eliminated because of blockage of the catalyst tube by Teflon from the coupling and Runs 70, 71, and 72 were not included because of decomposition in the section of glass tubing joining the catalyst tube to the downstream-condenser. In the other runs, the maximum possible error due to experimental measurements was 2% in the values of J_D and could have been as high as 15% for values of J_H in runs with small temperature gradients from wall to stream. However, in most runs, the possible error in J_H was approximately 5%.

Figure 7 depicts a typical temperature profile of the tube and gas stream. This figure shows the relative constancy of the wall temperature in comparison to the large increase in the stream temperature. The initial sharp rise in wall temperature reflects the relatively large heat loss to the surroundings at the entrance to the tube.

Figures 8 and 9 are plots of the mass and heat transfer factors, J_D and J_H, vs. the film Reynolds number, Re_f. Also

TABLE II
SUMMARY OF DATA AND RESULTS — CATALYST TUBE

24 Inch Tube, Runs 52 - 105
18 Inch Tube, Runs 106 - 114

C^* — Adjusted feed concentration, wt.% hydrogen peroxide.

C^*/C — Ratio of adjusted to boiler feed concentration.

w — Rate of decomposition, lb.mols/hr.

F — Fraction of hydrogen peroxide in adjusted feed not decomposed; F_1, entering tube; F_2, leaving tube.

T — Gas temperature, °F.; T_1, entering tube; T_2, leaving tube.

T_W — Wall temperature, °F.; T_{W_A}, average; T_{W_M}, maximum.

y — Mol fraction hydrogen peroxide in vapor stream; y_1, entering tube; y_2, leaving tube.

Δy_{1m} — Log mean mol fraction driving force across film.

G — Total mass flow rate, lb./(sec.)(ft.)².

Re_f — Reynolds number at film temperature, $(dG/\mu)_f$.

x_D — Effective film thickness for mass transfer, ft.

Sc_f — Schmidt number at film temperature, $(\mu/\rho D)_f$.

J_D — Mass transfer factor

L — % of heat generated by reaction lost from system.

ΔT_{1m} — Log mean temperature difference across film, °F.

$J_{H_{1m}}$ — Heat transfer factor on basis of ΔT_{1m}.

ΔT_p — Temperature difference across film at point at which the driving force equals Δy_{1m}, °F.

h_p — Heat transfer coefficient based on ΔT_p, Btu./(hr.)(°F)(ft.)².

J_{H_p} — Heat transfer factor on basis of ΔT_p.

RUN	C^*	C^*/C	$w \times 10^2$	F_1	F_2	T_1	T_2	T_{W_A}	T_{W_M}	y_1	y_2	Δy_{1m}	G	Re_f	$x_D \times 10^4$	Sc_f	$J_D \times 10^3$	L	ΔT_{1m}	$J_{H_{1m}} \times 10^3$	ΔT_p	h_p	$J_{H_p} \times 10^3$	J_{H_p}/J_D	RUN
52	19.48	0.949	1.468	0.5949	0.1292	315	570	584	601	0.0657	0.01597	0.0334	4.49	7320	9.11	0.778	3.40	1.1	149	4.24	125	38.7	5.05	1.48	52
53	20.55	1.013	2.01	0.745	0.0916	313	652	669	687	0.0885	0.01047	0.0366	4.15	6260	7.45	0.808	4.79	10.0	111	7.61	145	38.0	5.32	1.11	53
54	9.93	0.964	0.833	0.6697	0.1345	285	417	424	434	0.0367	0.00725	0.01815	4.34	8230	8.12	0.742	3.44	10.4	44.1	7.58	54	46.4	6.30	1.83	54
56	2.74	0.819	0.174	0.594	0.190	272	289	294	298	0.00871	0.00278	0.00520	4.36	9510	10.55	0.704	2.34	10.7	4.34	10	33.4	4.48	1.92	56
57	14.51	1.002	1.446	0.9035	0.2174	317	548	617	630	0.0743	0.01744	0.0392	3.95	6360	10.8	0.787	3.27	18.2	157	3.69	168	23.8	3.52	1.08	57
58	25.31	0.985	2.78	0.8187	0.1476	329	745	817	852	0.1220	0.02108	0.05746	3.07	4190	13.3	0.831	4.00	14.5	217	6.79	214	25.1	4.66	1.16	58
59	20.50	0.990	1.718	0.9341	0.1577	326	686	755	786	0.1096	0.01768	0.0503	2.98	4290	12.14	0.825	4.26	18.9	197	4.57	209	22.7	4.37	1.03	59
60	16.52	0.938	1.455	0.857	0.0837	243	530	580	601	0.0812	0.00764	0.0313	3.16	5210	8.44	0.780	5.12	20.6	146	4.93	152	25.7	4.77	0.93	60
61	17.61	0.952	1.85	0.8976	0.1107	327	638	694	709	0.0909	0.01078	0.0376	3.69	5500	8.38	0.819	4.83	20.9	165	4.64	173	45.9	7.18	1.49	61
62	19.38	0.969	2.425	0.8984	0.1170	306	568	660	683	0.1009	0.01259	0.0424	4.36	6830	7.20	0.794	4.59	39.0	194	3.39	204	24.0	3.21	0.70	62
63	19.84	0.955	2.265	0.8667	0.1082	323	666	732	753	0.0998	0.01192	0.0413	4.16	6060	7.61	0.819	4.81	21.0	188	4.40	201	30.2	4.17	0.87	63
64	10.83	0.998	1.183	0.809	0.1172	288	444	484	495	0.0486	0.00690	0.0214	4.37	7830	6.82	0.760	4.25	24.2	98.1	4.12	109	27.9	3.76	0.89	64
65	4.67	0.862	0.434	0.7315	0.1540	287	346	359	367	0.1845	0.00385	0.00933	4.50	9100	7.74	0.725	3.30	20.5	34.5	4.48	38	30.6	4.00	1.21	65
66	14.30	0.957	1.635	0.831	0.0980	312	566	593	610	0.0670	0.00767	0.0274	4.32	7010	6.69	0.792	4.78	14.9	108.5	5.81	146	32.0	4.34	0.91	66
67	5.83	0.901	0.485	0.631	0.1125	288	349	362	369	0.01996	0.00352	0.00956	4.53	9160	7.25	0.726	3.49	28.4	35.0	4.38	38	30.2	3.94	1.13	67
68	7.72	0.930	0.715	0.673	0.1038	297	408	415	422	0.0283	0.00432	0.01277	4.50	8590	6.61	0.740	4.04	13.8	39.3	6.85	52	40.0	5.23	1.21	68
69	2.91	0.997	0.279	0.716	0.1264	285	314	317	322	0.01113	0.00196	0.00529	4.50	9550	6.77	0.711	3.61	35.8	12.2	6.67	15	39.6	5.18	1.43	69
70	19.35	1.018	2.02	0.784	0.0930	326	608	672	691	0.0876	0.0100	0.0358	4.20	6390	7.20	0.806	4.86	26.1	167	4.11	198	25.8	3.57	0.74	70
71	20.20	0.976	2.29	0.813	0.0894	328	664	697	709	0.0948	0.0100	0.0377	4.32	6390	6.76	0.818	5.15	18.9	139	5.96	156	40.7	5.44	1.06	71
72	19.89	0.964	2.18	0.783	0.0799	332	655	670	690	0.0896	0.00879	0.0348	4.33	6490	6.62	0.811	5.22	18.4	103.5	7.79	159	37.7	5.09	0.97	72
73	19.62	0.963	1.995	0.784	0.1302	336	607	670	688	0.0889	0.01423	0.0408	4.30	6610	8.34	0.802	4.06	26.2	162	4.07	188	26.4	3.57	0.88	73
74	19.75	0.957	1.785	0.717	0.1022	332	637	647	663	0.0812	0.01122	0.0353	4.06	6210	8.11	0.804	4.45	13.1	88.5	8.36	134	38.9	5.56	1.25	74
75	19.20	0.955	1.472	0.669	0.0878	320	592	609	623	0.0733	0.00931	0.0309	4.15	6790	7.95	0.790	3.97	14.4	95.8	7.02	116	39.2	5.84	1.27	75
76	17.15	0.853	1.472	0.679	0.1178	331	584	592	600	0.0660	0.01115	0.0308	4.23	6790	8.36	0.788	3.97	7.6	72.4	8.61	103	44.6	6.17	1.55	76
77	20.10	0.991	2.24	0.914	0.1790	338	704	732	749	0.1068	0.0201	0.0531	4.20	6080	9.81	0.818	3.74	11.9	139	6.47	181	37.2	5.10	1.36	77
78	12.88	0.879	1.249	0.819	0.182	311	494	544	550	0.0591	0.01287	0.0304	4.21	6170	9.53	0.770	3.32	21.0	119	3.89	127	26.0	3.62	1.09	78
79	13.40	0.903	1.470	0.898	0.224	320	541	587	598	0.0677	0.0165	0.0363	4.50	7370	9.80	0.789	3.13	13.3	126	4.38	145	29.6	3.85	1.23	79
80	14.30	0.970	1.44	0.852	0.206	318	544	595	607	0.069	0.0162	0.0364	4.31	7050	10.02	0.785	3.21	13.3	133	4.26	150	28.1	3.82	1.19	80
81	19.55	0.964	1.862	0.869	0.173	346	660	721	739	0.0982	0.01885	0.0481	3.78	5550	10.78	0.815	3.76	18.6	172	4.49	198	25.8	3.93	1.05	81
82	9.80	0.975	0.875	0.846	0.219	304	454	477	485	0.0457	0.01165	0.0248	3.94	7080	10.90	0.762	2.97	13.5	74.2	5.15	89	28.2	4.22	1.42	82

TABLE II (CONT'D)

| RUN	C*	C*/C	w x10²	F₁	F₂	T₁	T₂	T_{W_A}	T_{W_M}	y₁	y₂	Δy_{lm}	G	Re_f	x_D x10⁴	Sc_f	J_Dx10³	L	ΔT_{lm}	$J_{H_{1m}}$x10³	ΔT_p	h_p	J_{H_p}x10³	J_{H_p}/J_D	RUN
83	9.76	0.943	0.981	0.832	0.215	310	448	486	491	0.0449	0.01140	0.0244	4.51	8120	9.46	0.754	3.00	18.2	89.6	3.95	97	28.0	3.65	1.22	83
84	9.81	0.945	1.025	0.845	0.204	301	450	479	486	0.0456	0.0109	0.0243	4.51	8160	9.01	0.752	3.13	15.1	81.8	4.70	91	32.2	4.19	1.34	84
85	20.10	0.970	1.93	0.835	0.166	335	653	716	733	0.0975	0.01862	0.0476	3.98	5890	10.11	0.814	3.75	15.5	177	4.45	197	28.2	4.10	1.09	85
86	22.40	0.960	2.10	0.825	0.154	339	714	759	780	0.1079	0.0193	0.0514	3.86	5510	10.32	0.819	3.93	12.4	168	5.49	206	30.1	4.47	1.14	86
87	22.20	0.957	2.19	0.901	0.175	334	699	774	796	0.1172	0.0217	0.0566	3.76	5340	10.90	0.822	3.84	20.4	206	4.33	235	25.1	3.93	1.02	87
88	22.30	0.960	2.07	0.882	0.178	351	707	787	807	0.1147	0.0222	0.0563	3.65	5140	11.52	0.825	3.76	20.0	210	4.13	235	23.8	3.73	0.99	88
89	21.70	0.934	1.53	0.855	0.168	342	664	735	755	0.1085	0.0204	0.0525	2.83	4130	14.29	0.811	3.79	24.4	188	4.16	212	18.4	3.74	0.99	89
90	24.65	0.951	1.62	0.790	0.160	394	744	823	848	0.1152	0.0222	0.0564	2.88	3900	14.91	0.840	3.81	21.1	207	4.08	235	18.4	3.64	0.96	90
91	25.00	0.960	1.915	0.851	0.160	372	754	840	864	0.1262	0.0225	0.0601	3.08	4140	13.56	0.837	3.92	19.9	224	4.22	252	20.6	3.81	0.97	91
92	24.70	0.947	1.963	0.855	0.1576	383	762	848	873	0.1252	0.0220	0.0595	3.15	4210	13.05	0.845	4.05	23.4	224	4.05	252	20.3	3.67	0.91	92
93	24.55	0.942	1.695	0.865	0.1648	343	718	803	827	0.1259	0.0228	0.0602	2.72	3780	15.02	0.828	3.91	23.3	188	4.84	248	17.8	3.75	0.96	93
94	27.22	0.924	1.65	0.788	0.1557	399	787	876	903	0.1282	0.0240	0.0621	2.65	3470	16.37	0.844	3.90	20.6	231	4.05	259	17.2	3.67	0.94	94
95	18.75	0.917	1.32	0.893	0.172	363	639	702	721	0.0966	0.0179	0.0466	2.70	4010	14.67	0.809	3.82	27.4	164	4.19	185	17.4	3.73	0.98	95
96	9.58	0.952	0.979	0.864	0.224	305	440	479	485	0.0457	0.01165	0.0248	4.42	8010	9.65	0.754	2.96	22.9	90	3.80	97	26.3	3.50	1.18	96
97	9.75	0.929	0.537	0.838	0.177	298	416	448	456	0.0432	0.00896	0.0218	2.41	4500	15.20	0.748	3.38	31.7	76.1	3.98	83	14.9	3.64	1.08	97
98	10.22	0.980	0.885	0.880	0.195	306	452	492	499	0.0498	0.01083	0.0255	3.49	6250	11.09	0.761	3.34	24.5	94.6	4.02	101	22.1	3.75	1.12	98
99	25.30	0.950	2.69	0.928	0.187	357	771	878	901	0.140	0.0268	0.0684	3.97	5280	11.1	0.840	3.78	22.6	262	3.80	286	24.5	3.50	0.93	99
100	24.80	0.930	1.71	0.910	0.181	354	729	822	849	0.134	0.0252	0.0652	2.62	3600	16.4	0.832	3.78	27.3	232	3.91	264	15.8	3.45	0.91	100
101	29.00	0.941	2.44	0.888	0.1715	398	875	963	993	0.1565	0.0284	0.0748	3.25	4020	13.75	0.866	4.00	19.1	256	4.47	297	22.6	3.88	0.97	101
102	28.30	0.961	2.25	0.884	0.175	376	838	927	956	0.1515	0.0283	0.0734	3.10	3940	14.68	0.854	3.84	18.7	254	4.38	294	20.7	3.77	0.98	102
103	27.80	0.944	2.01	0.900	0.1508	352	812	885	912	0.1510	0.0237	0.0688	2.67	3480	15.05	0.850	4.28	29.0	231	4.34	270	17.8	3.77	0.88	103
104	30.20	0.943	2.09	0.884	0.198	404	876	968	999	0.1625	0.0342	0.0822	2.79	3440	17.7	0.858	3.62	19.7	261	4.33	306	18.5	3.71	1.03	104
105	29.70	0.941	1.94	0.918	0.194	355	823	919	948	0.1680	0.0333	0.0831	2.50	3220	18.5	0.842	3.72	24.1	264	4.22	306	16.6	3.79	1.02	105
106	4.81	0.884	0.509	0.882	0.296	313	365	388	399	0.0230	0.00768	0.0140	4.98	9820	7.63	0.739	3.12	31.8	44.1	3.10	55	27.9	3.30	1.06	106
107	4.95	0.948	0.246	0.735	0.215	330	368	377	387	0.0197	0.00572	0.0113	2.65	5220	12.63	0.738	3.51	45.2	23.0	4.33	35	17.3	3.85	1.10	107
108	9.65	0.942	0.852	0.732	0.237	320	422	468	482	0.0391	0.0125	0.0233	4.93	9020	7.86	0.751	3.24	24.2	87	3.01	102	28.2	3.37	1.04	108
109	9.17	0.890	0.392	0.599	0.174	326	396	421	432	0.0302	0.00865	0.01725	2.78	5270	12.28	0.742	3.57	36.2	52.3	3.43	62	18.1	3.84	1.08	109
110	14.33	0.965	0.986	0.708	0.203	345	502	555	575	0.0569	0.0160	0.0322	3.77	6330	9.65	0.775	3.72	23.4	114	3.43	133	25.5	3.97	1.07	110
111	14.18	0.955	0.528	0.589	0.154	351	468	498	515	0.0467	0.0120	0.0256	2.37	4160	14.10	0.764	3.90	32.0	73.5	4.11	90	17.9	4.45	1.14	111
112	19.55	0.954	1.801	0.838	0.218	338	612	695	725	0.0949	0.02385	0.0516	4.11	6250	8.83	0.802	4.07	21.4	188	3.53	218	29.2	4.12	1.01	112
113	19.25	0.939	1.022	0.736	0.166	345	570	621	650	0.0814	0.0178	0.0419	2.58	4080	12.35	0.785	4.46	28.0	133	4.17	165	20.1	4.55	1.02	113
114	9.57	0.928	0.650	0.765	0.251	325	427	474	487	0.0402	0.01252	0.0237	3.65	6670	10.66	0.750	3.23	24.4	88.2	3.02	99	21.8	3.51	1.09	114
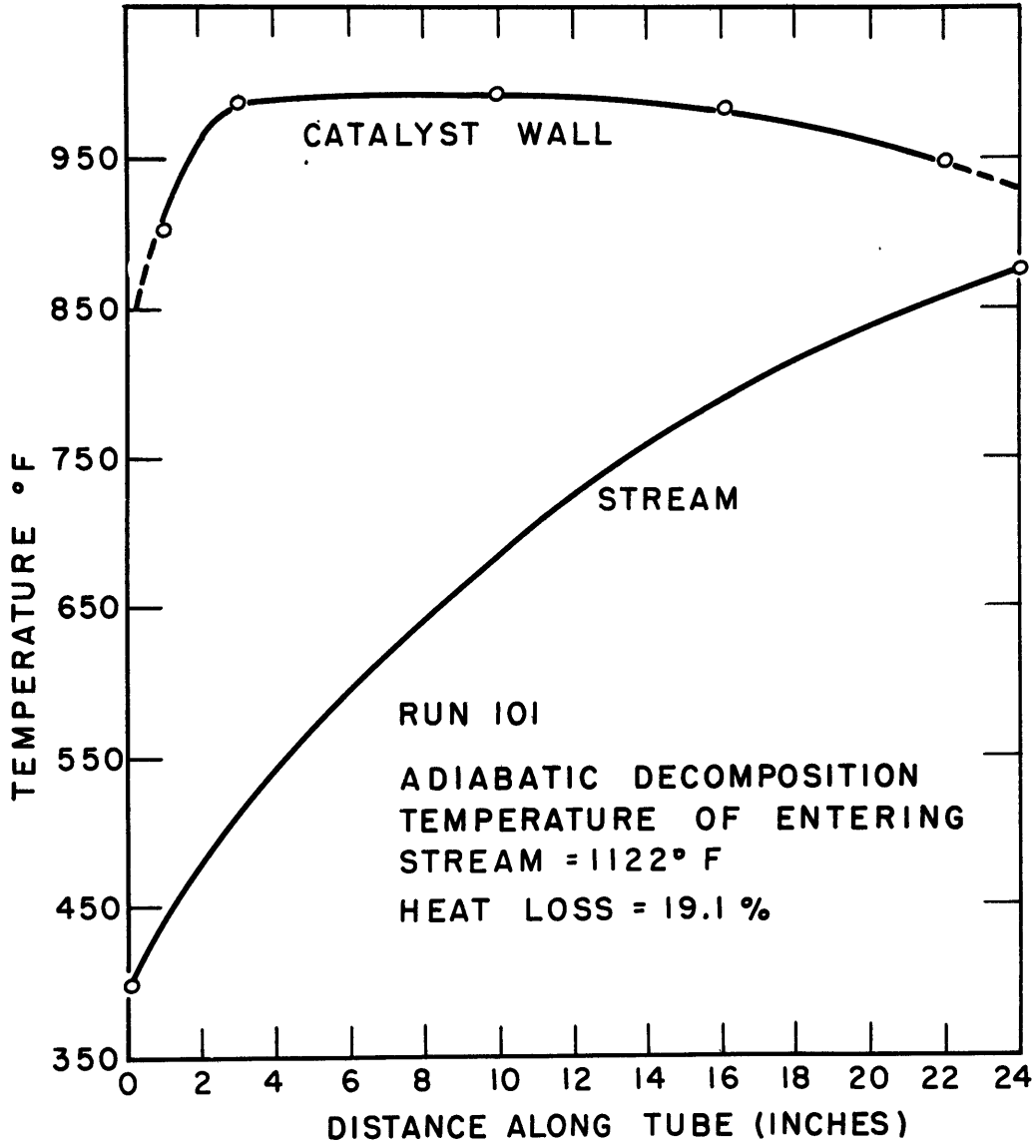
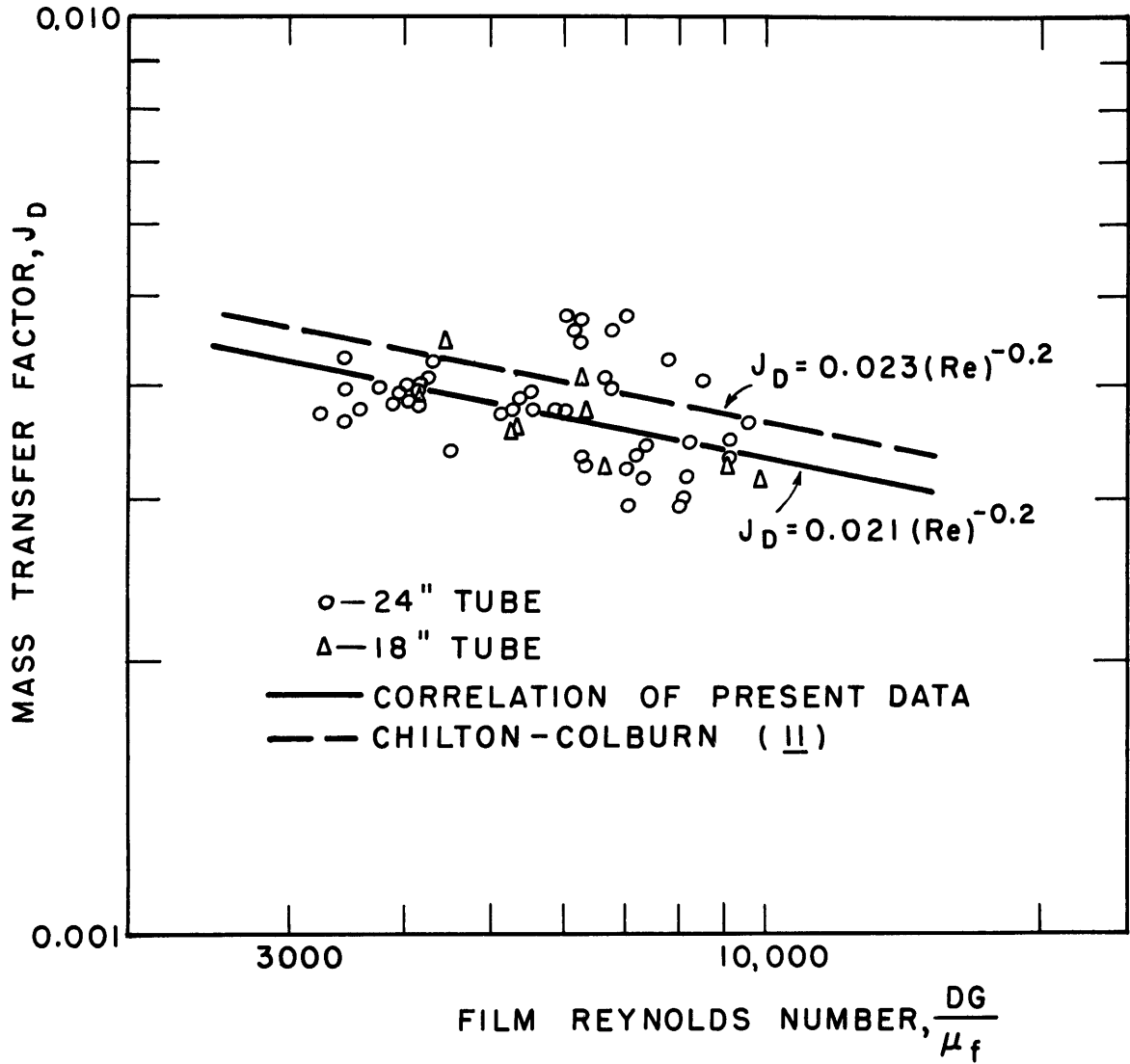FIGURE 7 — TYPICAL TEMPERATURE DISTRIBUTION IN CATALYST TUBE

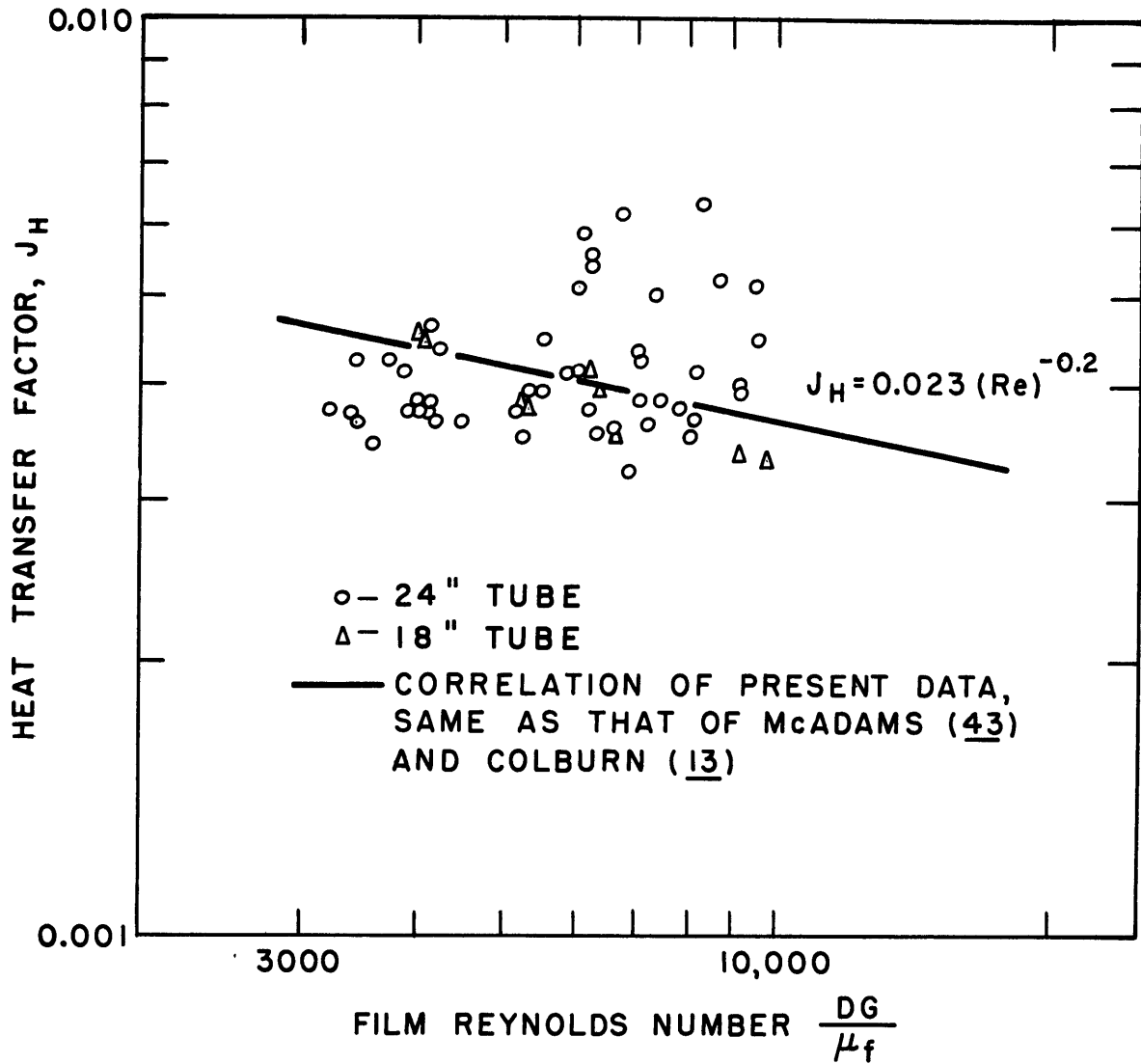FIGURE 8 – VARIATION OF J_D WITH REYNOLDS
NUMBER IN FLOW THROUGH TUBES

FIGURE 9   VARIATION OF J_H WITH REYNOLDS
NUMBER IN FLOW THROUGH TUBES

included in these figures is the line representing the
Chilton-Colburn correlations. In Figure 9, the above corre-
lation coincides with the best line through the data while
in Figure 8 it is 9.5% above the best line determined from
the data.

Proof of Diffusion-Controlled Reaction. As discussed in the
Introduction, previous work has proved almost conclusively
that the reaction being studied is diffusion-controlled.
However, the importance of this assumption in this thesis
makes it desirable to consider the results and to show how
they support this assumption. As shown in Figure 8, the
experimental values of j_D give a slope of -0.2 on a plot of
the j-factor vs. the Reynolds number. (It is unfortunate
that the tube data exhibit the average deviation of 9.5%
since even this relatively small spread over the short range
of Reynolds numbers available might cast some doubt on the
discussion to follow. However, it may be pointed out that
the packed-bed data exhibit a much smaller spread and con-
sideration of those data leads to the same conclusions as
drawn in this section.) This value of -0.2 is the value of
the slope that has been found elsewhere as representing the
dependence of the j-factor on the Reynolds number in systems
of pure diffusion, i.e., in situations where the total availa-
ble driving force is used in overcoming resistance to mass

transfer. If, in contrast, we now consider a system which is actually surface-rate controlled, we find that j-factors (calculated on the assumption of diffusion control) would give a -1.0 slope when plotted against Reynolds number. Systems which are in the transition region between surface-rate control and transport-rate control would exhibit a slope of between -0.2 and -1.0 in a plot of j_D (calculated on the basis of transport-rate control) vs. Reynolds number, the slope being closer to -0.2 as the system became more diffusion-controlled. Therefore, the present slope of -0.2 indicates complete diffusion control.

In addition, the data plotted in Figure 8 are obtained with a wide range of wall temperatures, 400°F. to 1000°F. Such a range would almost certainly have affected the surface reaction rate and if the resistance to surface reaction had been a significant part of the total resistance, the effect of the wide variation in temperature should have been evident in the results. No such trend was found, thus indicating again that the reaction is diffusion-controlled.

The two methods of reasoning given above can also be expressed in mathematical terms, both arguments being based on point-rate equations. The conditions at the points are chosen so as to present the conditions enumerated in the above discussion. The method followed is to show that, since the values of the j-factor and, therefore, of k_G found in the

present system have the same relationship to flow rates and
physical conditions that they do in pure diffusion systems,
it follows that the partial pressure of the hydrogen peroxide
at the surface is zero or negligible. (For comparison with
the actual runs, point conditions could be taken at the point
in the tube at which the log mean partial pressure driving
force occurs. As stated in the Procedure, use of the point-
rate Equation (41) at this point gave values of the mass
transfer factors which agreed within 2% with the values given
by Equations (42) and (47), the integrated expressions.)
First, let us consider two point conditions (Figure 10)
which exhibit the same wall temperature and gas concentra-
tion but have different flow rates. (Although no two experi-
mental runs have the exact equalities desired, many pairs
are reasonably close, i.e., 54 and 109, 67 and 107, 96 and
98, and 77 and 89.) Assume that the two flow rates and the
physical characteristics are such that the correlations
indicate that the coefficients have the relationship k_{G_I} =
2 $k_{G_{II}}$. The general discussion above shows that in such a
situation the experimentally measured reaction rates would
have the same relationships as the mass transfer coefficients,
i.e., $N_I = 2 N_{II}$.
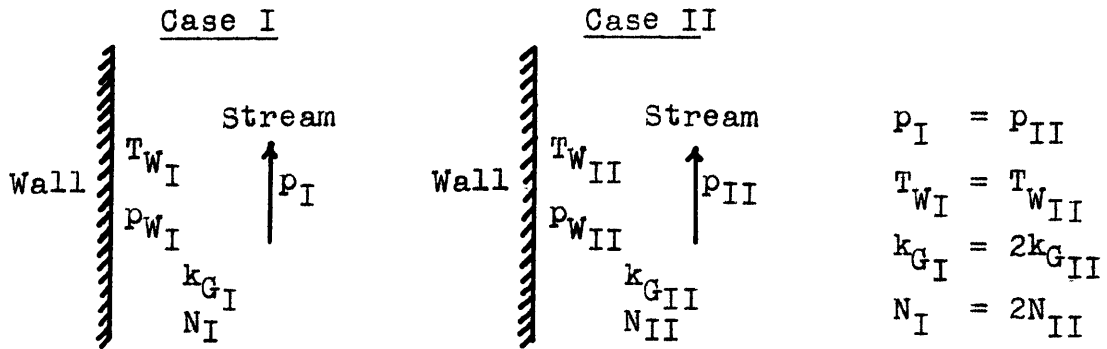
Figure 10. Sketch Demonstrating Proof of Diffusion-Control

The two conditions give the basic equations

$$N_I = k_{G_I} (p_I - p_{W_I})$$ (54)

$$N_{II} = k_{G_{II}} (p_{II} - p_{W_{II}})$$ (55)

Equation (54) combined with the conditions of Figure 10 gives

$$2N_{II} = 2k_{G_{II}} (p_{II} - p_{W_I}).$$ (56)

Now from Equations (55) and (56),

$$p_{W_I} = p_{W_{II}}$$ (57)

However, to obtain an increased reaction rate at the same surface temperature, the partial pressure must increase and assuming a first-order surface reaction, we get

$$p_{W_I} = 2p_{W_{II}} \quad .$$ (58)

The only manner in which Equations (57) and (58) can be reconciled is to state that both partial pressures are zero or at least so small as to be negligible in Equations (54) and (55).

The second proof is based on a consideration of two point conditions having flow rates and physical conditions such that they exhibit equal values of k_G but with one situation having a higher stream partial pressure and higher wall temperature than the second. The fact that the data presented in Figure 8 indicate no effect of surface temperature shows that the experimentally found rates of mass transfer in such a situation would be directly proportional to the partial pressures in the stream. A mathematical analysis similar to that given above shows two explanations for such a relationship:

1. Zero or negligible partial pressure at the wall

2. A surface reaction having a zero temperature coefficient.

The second explanation would seem wrong when compared to other gas-solid systems and in addition does not agree with the results of several investigators (2, 23, 46, 47) who found an increase in the surface reaction rate constant with temperature at lower temperatures and partial pressures.

Thus, both methods of reasoning lead to definite mathematical proofs that diffusion controls.

Heat Flow Characteristics of the System. It would have been desirable for the system to be completely adiabatic so that all the heat released at the wall would have been transferred back to the stream. The rates of heat transfer would then have been easily calculable by multiplying the rate of decomposition by the heat of reaction. However, the apparatus used, although heavily insulated, allowed heat losses to the surroundings and therefore, the simple method above could not be used unless it was corrected for heat losses. Consideration was given to making the system adiabatic by winding heating wire around the insulation on the catalyst tube and maintaining a current so that no temperature gradients were set up through the insulation. This idea was finally abandoned since it would have resulted in heat addition to some parts of the system.

The actual amount of heat transferred to the stream as it flows through the tube can be obtained from the increase in its sensible enthalpy from the entrance to the exit of the tube. This is calculated from the measured inlet and exit temperatures and the known heat capacities of the species present. The increase in kinetic energy was found to be negligible (less than 1% of increase in sensible enthalpy). To obtain the per cent heat loss, the actual sensible enthalpy gain is compared with the increase in enthalpy that would have resulted from the known amount of

decomposition if the system had been adiabatic. Point rates of heat transfer are then calculated by obtaining the point rate of mass transfer by Equation (41), multiplying this by the heat of reaction and correcting the value for the percentage heat loss determined above.

Temperature Distribution. The typical temperature profile of Figure 7 demonstrates the relative constancy of the catalyst wall temperature even though the gas temperature increases substantially during flow through the tube. This is explained as follows: At the entrance to the tube, the gas is cool but concentrated in hydrogen peroxide, leading to a high rate of mass transfer to the wall and heat release at the wall. This in turn requires a large temperature gradient to transport the heat back to the bulk stream. At the end of the tube, the gas is hotter but its lower concentration results in a lower rate of heat release and therefore, a lower gradient from wall to stream. The sum total of these effects is a relatively constant temperature profile.

The exact temperature gradient, and, therefore, the wall temperature at any point is a function of (1) gas concentration, (2) heat and mass transfer coefficients, (3) heat losses, and (4) physical properties of the gas at that point while the entire profile represents the sum total of these physical characteristics. For instance, as is shown below,

in an adiabatic, diffusion-controlled system with $J_H = J_D$ and $Pr = Sc$, the wall temperature will be constant at the adiabatic reaction temperature of the system. The basic equation which states the magnitude of the temperature difference established between the wall and the stream at a point in an adiabatic system has been shown in the Theoretical Analysis to be

$$N_A \Delta H = h \Delta T \quad .\tag{53}$$

From the definition of the mass transfer coefficient k_c, we obtain

$$k_c c \Delta H = h \Delta T \quad .\tag{59}$$

The concentration of the stream, c, represents the entire gradient since the wall concentration is zero. If $J_H = J_D$, and $Pr = Sc$, we obtain the expression

$$\frac{h}{C_p G} = \frac{k_c P_{BM}}{U \ P} = \frac{\rho k_c P_{BM}}{G \ P}\tag{60}$$

If the concentration of the diffusing component is small, P_{BM}/P is approximately unity and substitution of Equation (60) into (59) gives

$$\frac{c \Delta H}{C_p \rho} = \Delta T \quad .\tag{61}$$

The numerator, $c \Delta H$, is the heat released by the reaction of a cubic foot of the gas and the denominator is the volumetric

specific heat of that gas, the left-hand side of the equation representing the temperature gained in an adiabatic reaction. Therefore, the temperature gradient at any point in the tube is sufficient to raise the wall temperature to the adiabatic reaction temperature of the gas passing that point. Under the simplifying conditions assumed, the adiabatic reaction temperature of the gas at any point remains constant, and thus the entire wall surface will be at the adiabatic reaction temperature of the entering gas stream.

From the above discussion, it can be seen that the surface temperature for an adiabatic system can be either above or below the adiabatic reaction temperature depending on the J_H/J_D ratio, the concentration of the reacting gas(es), and the values of the Prandtl and Schmidt numbers. Any variation from the assumption of adiabaticity will, of course, also affect the surface temperature.

The exact shape of the profile of Figure 7 can now be explained from a consideration of the effect of the heat losses from the tube. From the tables of data, it is seen that here the J_H/J_D ratio is approximately unity and that the Schmidt and Prandtl numbers are almost the same, the deviations, in fact, tending to cancel. Therefore, one would expect the wall temperature to be constant at a value close to the adiabatic decomposition temperature. Instead, Figure 7 shows a sharp dip at the entrance, a flat plateau

over the first half and a slightly but steadily decreasing
value over the last half of the tube, the average value being
somewhat lower than the adiabatic decomposition temperature,
due primarily to the 19.1% heat loss in this run. The dip at
the entrance is caused by the excessive heat losses at this
point, the losses being due to the construction of the coup-
ling between the glass calming section and the catalyst tube.
As shown in detail in Figure A-2, the stainless steel coup-
ling acts as a high thermal conductivity path from the front
end of the tube to the cooler adiabatic calming section,
resulting in relatively large heat losses. The coupling at
the exit of the tube is insulated from any cool section and
therefore does not cause as large heat losses at that point.
A second possible cause of the dip at the entrance to the
tube may have been the process of establishing temperature
and concentration gradients. This process causes increased
rates of both heat and mass transfer over this region. The
effect of these increased rates on the temperature gradient
at the entrance of the tube is unknown but is probably very
small since both rates are increased simultaneously and
therefore tend to maintain the same temperature differences
between wall and stream. However, as discussed below, the
effect of this phenomenon on the overall operation of this
system is negligible at the length-to-diameter ratios used
in this work. The steady decline over the latter half of

the tube occurs because the heat losses along the tube de-
crease the adiabatic decomposition temperature of the gas as
it passes through the tube. Therefore, it may be concluded
that the wall temperatures in a gas-solid system can be
determined from its heat and mass transfer characteristics,
the precision depending on the accuracy to which the heat and
mass transfer characteristics can be predicted.

The method of carrying out such a prediction is to
employ mass transfer correlations to obtain expected rates
of mass transfer to the surface. From the heat of reaction,
the heat release is calculated and combined with a coeffi-
cient of heat transfer (obtained from heat transfer correla-
tions) to give a predicted temperature gradient between the
solid and gas stream. The above method gives a wall tempera-
ture for an adiabatic system although any expected heat
losses can be included in the calculations to give a more
accurate prediction. As an example of the accuracy of this
method, with the correlations obtained in this work and
knowledge of the heat losses, temperature differences from
wall to stream would have been predicted with an average
deviation of about 13%.

Mass Transfer Correlation. The mass transfer data plotted
on Figure 8 have an average deviation of 9.5% from the best
line which may be expressed by the equation

$$J_D = \frac{k_G M_M P_{BM}}{G}(Sc_f)^{2/3} = 0.021 \ (Re_f)^{-0.2} \tag{62}$$

Due to the spread of the data, and the small effect of even large temperature differences on the physical properties of the gas stream, the data can be correlated almost as well by using Re_g, the stream Reynolds number. The average deviation of 9.5% compares very favorably with the deviations of greater than 15% often displayed by other correlations of mass or heat transfer data.

The data indicate a straight line with Reynolds numbers as low as 3200, a value which is well within the transitional range. The absence of the dip which Chilton and Colburn (11) indicate in this region could be ascribed to turbulence generated by the simultaneous effect of heat transfer. However, examination of the isothermal mass transfer data of Gilliland (25) and the heat transfer data of many investigators shows the same straight line when dealing with gas streams. Therefore, it is probable that the "dips" are more evident with viscous fluids and the straight-line correlation to 3200 is normal.

The correlation proposed here is parallel to, but 9.5% below that recommended by Chilton and Colburn (11),

$$J_D = 0.023 \ (Re_f)^{-0.2} \ . \tag{24}$$

As shown in the Introduction, their coefficient was obtained

by equating J_D to the best value for J_H and is found to agree within 25% with mass transfer data in systems of solution and evaporation. The proposed coefficient of 0.021 is within the range of 0.020-0.027 found by other investigators.

There are several possible reasons for the present value of the coefficient being slightly lower than that given in Equation (24). First is the temperature gradient and simultaneous heat transfer. The average temperature differences investigated ranged from 10° to 306°F. with a maximum point value of 564°F. This extensive range had no detectable effect on the mass transfer, indicating, therefore, that a simultaneous temperature gradient has no significant effect on mass transfer by molecular diffusion. As pointed out in the Procedure, the effect of the varying physical properties with temperature is averaged.in the correlations by using the film temperature at the point in the tube at which the log mean partial pressure driving force occurs. While other choices of an average temperature have very little effect on the final correlation, this point was chosen because (1) it gives a slightly better correlation and (2) because it has been found to give the best results in systems with a large change in physical properties with temperature.

A second reason is the effect of the counterdiffusion and bulk flow through the film. The theoretical equation

developed took cognizance of this effect by exhibiting a
slightly different concentration gradient through the film.
As is shown in the Appendix from a comparison of equations
including and neglecting counterdiffusion, the change in the
value of x_D and, therefore, of J_D ranges up to 6%. It may be
argued that counterdiffusion, in addition to altering the
gradient may also change the influence of the Schmidt number
and the power to which it should be raised. This assumption
cannot be investigated in the present system and, in addi-
tion, will not have a profound effect on the correlation
since the Schmidt number values encountered are close to
unity.

A third possibility is thermal diffusion, a very diffi-
cult factor to consider because of the lack of knowledge of
the required physical constants. However, a search through
the literature indicated a maximum range of possible values
of α of 0.0 to 0.3. This gives a maximum possible effect on
the transfer of 2% although it should be realized that for
such a system it is possible for the effect to be in either
direction (5). Thermal diffusion, therefore, seems to be a
negligible factor in the total mass transfer.

A final possible source of the 9.5% difference between
the values of the coefficients may have been end effects.
However, the ratios of tube length to diameter employed in
the present work (96:1 and 72:1) are such that past experience

would indicate this effect to be negligible. This conclusion is borne out by the experimental work since the close agreement of the 18" and 24" tube runs indicates that the end effects are indeed negligible. It should also be pointed out that the excess turbulence caused by any end effects would have resulted in the determined value of the coefficient here being higher rather than lower.

Therefore, it may be concluded that Equation (62) may be used to correlate mass transfer data in tubes although not enough difference exists between the results and the Chilton-Colburn correlation to preclude use of the latter. The data average 27% below Gilliland's (25) proposed correlation, Equation (25), which cannot be recommended on the basis of the present work. The agreement of the data with the von Karman and Martinelli equations (discussed in the Introduction) is the same as the agreement with the Chilton-Colburn correlation.

Heat Transfer Correlation. The heat transfer rates used to obtain the heat transfer correlation were determined as described in the earlier section on "Heat Flow Characteristics in the System." The coefficients of heat transfer were calculated in two different manners:

1. Use of (a) the overall heat transfer rate calculated from the known amount of decomposition occurring and

adjusted for heat losses, and (b) the log mean of the temperature differences between the entrance and exit gas and the average wall_temperatures to give an overall heat transfer coefficient.

2. Use of the actual temperature difference and heat transfer rate at the point in the tube at which the log mean partial pressure driving force occurs to give a point value of the heat transfer coefficient.

Method (1) is the less accurate due to the assumption of constant wall temperature and is also subject to larger experimental errors because of inaccuracies in measuring the small temperature differences between the tube wall and the gas leaving the tube.

The results obtained by both methods give best lines identical to the Chilton-Colburn correlation (and also the McAdams equation):

$$j_H = \frac{h}{c_p G} (Pr_f)^{2/3} = 0.023 \ (Re_f)^{-0.2} \ . \tag{22}$$

The point value data plotted in Figure 9 have an average deviation of 14.8%, while the log mean values, considered less accurate and less reliable, give an average deviation of 22.4%. The degree of agreement is not as good as the mass transfer data. This was expected due to the inaccuracies in measuring temperature differences and heat losses. However, the deviation found is not excessive in

comparison with other investiagors, especially when one considers that the data mostly lie in the transitional region, where large deviations are usually encountered.

Relationships of Heat and Mass Transfer Factors. A principal advantage in the use of j_H and j_D has been the assumption of their equality in similar physical systems, thus allowing the use of heat transfer data to predict mass transfer and vice versa. This assumption follows from the development of the Reynolds Analogy as well as from dimensional analysis (40) and is supported by data which show values of the j_H/j_D ratio from 0.8 to 1.5.

The present work gives a ratio of 1.09 with an average deviation of 13.7%, a value which is in excellent agreement with the assumption of equality.

B. Catalyst Bed

Results. The results obtained from the work on the packed bed are given in Tables III and IV and Figures 11-15. Table III summarizes the experimental data and the results for mass and heat transfer calculated on an overall basis. Table IV contains the results recalculated for the temperatures and concentrations existing at the center sphere of the first layer of catalyst spheres. The reasons and methods

TABLE III
SUMMARY OF DATA AND OVERALL RESULTS — PACKED BED

4.7 cm. bed, Runs 1 - 10
4.8 cm. bed, Runs 11 - 24
7.5 cm. bed, Runs 25 - 33

C* - Adjusted feed concentration, wt.% hydrogen peroxide.

C*/C - Ratio of adjusted to boiler feed concentration.

w/A - Rate of decomposition, lb.mols/(hr.)(ft.)²

F - Fraction of hydrogen peroxide in adjusted feed not decomposed; F_1, entering bed; F_2, leaving bed.

T - Gas temperature, °F.; T_1, entering bed; T_2, leaving bed.

T_C - Catalyst temperature, °F.; T_{CB}, first catalyst layer; T_{CM}, third catalyst layer, T_{CT}, top catalyst layer.

y - Mol fraction hydrogen peroxide in vapor stream; y_1, entering bed; y_2, leaving bed.

Δy_{lm} - Log mean mol fraction driving force.

G - Total mass flow rate, lb./(sec.)(ft.² superficial area).

Re_f - Reynolds number at film temperature, $(D_p G/\mu)_f$.

Sc_f - Schmidt number at film temperature, $(\mu/\rho D)_f$.

k_G - Mass transfer coefficient, lb.mols/(hr.)(atm.)(ft.)²

J_D - Mass transfer factor.

L - % of heat generated by reaction lost from system.

ΔT_{lm} - Log mean temperature difference, °F.

J_{Hlm} - Heat transfer factor on basis of ΔT_{lm}.

RUN	C*	C*/C	w/A	F_1	F_2	T_1	T_2	T_{CB}	T_{CM}	T_{CT}	y_1	y_2	Δy_{lm}	G	Re_f	Sc_f	k_G	J_D	L	ΔT_{lm}	J_{Hlm}	J_{Hlm}/J_D	RUN
1	10.60	1.065	0.789	0.706	0.0744	293	469	476	482	489	0.0414	0.00429	0.0164	0.1119	161	0.766	2.88	0.112	4.8	73.5	0.152	1.35	1
2	9.71	0.929	0.881	0.896	0.0638	289	496	507	509	514	0.0483	0.00336	0.01798	0.1030	147	0.755	2.79	0.122	8.3	80.4	0.164	1.35	2
3	9.70	0.965	0.718	0.811	0.0754	282	462	471	478	487	0.0436	0.00396	0.0165	0.0949	138	0.750	2.60	0.115	10.2	81.4	0.141	1.23	3
4	8.95	0.902	0.394	0.763	0.0403	282	424	435	446	448	0.0347	0.00180	0.01114	0.0575	87.0	0.749	2.12	0.154	21.1	68.9	0.152	0.985	4
5	9.43	0.980	0.193	0.743	0.0116	298	385	442	444	442	0.0385	0.00059	0.00906	0.0265	40.4	0.755	1.298	0.208	54.1	94.4	0.122	0.588	5
6	10.26	0.947	0.615	0.774	0.0410	306	459	475	478	486	0.0436	0.00227	0.01395	0.0774	113	0.767	2.64	0.146	26.6	77.6	0.161	1.10	6
7	4.95	0.950	0.326	0.724	0.0670	288	360	369	369	369	0.0193	0.00178	0.00735	0.0949	153	0.736	2.65	0.115	19.9	32.8	0.165	1.42	7
8	5.01	0.944	0.193	0.598	0.0338	306	358	365	365	367	0.0161	0.00090	0.00528	0.0647	104	0.739	2.18	0.139	32.3	26.7	0.175	1.41	8
9	13.92	0.938	0.975	0.725	0.0433	336	523	532	536	543	0.0543	0.00316	0.0204	0.0969	132	0.779	2.84	0.127	29.8	76.7	0.208	1.62	9
10	13.82	0.917	0.786	0.785	0.0258	261	561	568	574	581	0.0609	0.00194	0.0171	0.0716	95.8	0.782	2.76	0.168	----	98.5	----	----	10
11	8.92	0.984	0.725	0.915	0.0753	302	493	500	508	509	0.0450	0.00363	0.01648	0.0914	129	0.772	2.76	0.129	8.0	73.0	0.176	1.36	11
12	8.53	0.954	0.374	0.885	0.0372	302	468	488	488	491	0.0414	0.00171	0.01246	0.0490	70.3	0.773	1.888	0.166	17.5	79.6	0.156	0.940	12
13	15.32	1.010	1.130	0.870	0.0391	330	648	665	672	677	0.0757	0.00328	0.02305	0.0838	103	0.817	3.08	0.166	12.3	124.7	0.169	1.01	13
14	14.60	0.937	0.432	0.802	0.0118	331	558	610	610	608	0.0660	0.00094	0.0153	0.0354	46.1	0.797	1.776	0.222	31.4	133.6	0.146	0.654	14
15	15.08	0.990	0.865	0.904	0.0189	378	655	688	690	690	0.0749	0.00157	0.0190	0.0619	74.5	0.830	2.86	0.211	28.4	126.4	----	----	15
16	8.50	0.948	0.689	0.938	0.0689	310	487	496	504	506	0.0436	0.00314	0.0154	0.0880	124	0.766	2.81	0.136	13.3	73.0	0.172	1.27	16
17	14.62	0.955	0.859	0.922	0.0461	325	635	656	640	674	0.0753	0.00364	0.0237	0.0633	78.6	0.813	2.27	0.161	15.0	134.4	0.157	0.975	17
18	14.77	0.963	0.239	0.748	0.0107	324	508	557	525	559	0.0561	0.00078	0.01293	0.0207	28.2	0.778	1.159	0.243	44.0	119.8	0.144	0.591	18
19	19.93	0.965	1.207	0.910	0.0576	365	751	794	779	808	0.1052	0.00635	0.0352	0.0671	74.5	0.840	2.16	0.149	21.8	185.4	0.151	1.01	19
20	22.58	0.994	1.371	0.958	0.0648	370	834	859	847	886	0.1248	0.00815	0.0427	0.0657	70.0	0.852	2.02	0.144	19.5	195.0	0.164	1.14	20
21	22.90	1.005	0.801	0.886	0.0277	411	777	849	811	856	0.1195	0.00354	0.0330	0.0390	42.0	0.858	1.532	0.186	38.0	210.1	0.149	0.802	21
22	19.65	0.933	1.324	0.943	0.0960	371	762	780	788	823	0.1075	0.01046	0.0416	0.0749	83.6	0.840	1.998	0.124	24.2	182.4	0.149	1.20	22
23	19.30	0.938	0.395	0.834	0.0209	397	667	747	702	752	0.0959	0.00223	0.0218	0.0238	27.6	0.830	1.138	0.219	43.0	186.5	0.138	0.626	23
24	11.78	0.775	0.135	0.683	0.0069	373	459	528	489	522	0.0445	0.00044	0.00959	0.0160	22.2	0.782	0.886	0.240	63.7	102.6	0.130	0.540	24
25	4.92	0.916	0.149	0.852	0.0935	290	381	380	396	398	0.0226	0.00246	0.00907	0.0379	59.9	0.749	1.382	0.152	11.4	43.2	0.196	1.29	25
26	9.83	0.961	0.252	0.744	0.0741	316	496	499	524	525	0.0403	0.00395	0.0156	0.0361	50.8	0.780	1.358	0.162	1.5	82.8	0.180	1.11	26
27	9.88	0.935	0.133	0.695	0.0329	340	471	494	509	509	0.0378	0.00175	0.0117	0.0192	27.2	0.779	0.955	0.215	28.3	83.0	0.177	0.825	27
28	14.90	0.988	0.406	0.833	0.0546	336	612	633	661	662	0.0699	0.00445	0.02375	0.0331	41.5	0.811	1.440	0.195	16.2	139.4	0.188	0.965	28
29	14.68	0.960	0.182	0.674	0.0249	333	543	570	574	572	0.0554	0.00199	0.01605	0.0181	24.1	0.790	0.951	0.232	22.5	99.1	0.216	0.931	29
30	19.80	0.984	0.497	0.837	0.0603	348	708	736	777	777	0.0960	0.00660	0.03336	0.0306	35.2	0.832	1.252	0.188	19.1	183.8	0.185	0.985	30
31	19.07	0.949	0.239	0.765	0.0235	351	628	671	702	696	0.0838	0.00247	0.0230	0.0158	19.4	0.813	0.865	0.249	32.8	163.0	0.195	0.783	31
32	23.80	0.988	0.575	0.848	0.0542	373	792	816	858	883	0.1189	0.00720	0.0398	0.0288	31.3	0.852	1.213	0.199	24.6	221.6	0.187	0.944	32
33	23.05	0.958	0.264	0.902	0.0202	385	709	748	797	797	0.1082	0.00259	0.0282	0.0138	15.8	0.832	0.795	0.263	48.0	194.3	0.206	0.782	33

TABLE IV
POINT CONDITION RESULTS—PACKED BED

This table presents results on the basis of point conditions at the center sphere of the first catalyst layer.

4.7 cm. bed — Runs 1 - 9
4.8 cm. bed — Runs 11 - 24
7.5 cm. bed — Runs 25 - 33

F_p — Fraction hydrogen peroxide in adjusted feed <u>not</u> decomposed.

y_p — Mol fraction hydrogen peroxide in stream.

ΔT_p — Temperature difference, °F.

h_p — Heat transfer coefficient, Btu./(hr.)(°F)(ft.)^2.

Re_{f_p} — Film Reynolds number, $(D_p G/\mu)_f$.

Sc_{f_p} — Film Schmidt number, $(\mu/\rho D)_f$.

J_{D_p} — Mass transfer factor.

J_{H_p} — Heat transfer factor.

| RUN	F_p	y_p	ΔT_p	h_p	Re_{f_p}	Sc_{f_p}	J_{D_p}	J_{H_p}	J_{H_p}/J_{D_p}	RUN
1	0.561	0.0328	142	28.8	167	0.749	0.108	0.152	1.40	1
2	0.688	0.0368	166	28.3	150	0.755	0.120	0.161	1.34	2
3	0.640	0.0341	148	26.1	142	0.745	0.115	0.162	1.41	3
4	0.570	0.0258	115	20.6	89.0	0.740	0.153	0.210	1.38	4
5	0.491	0.0253	113	12.54	40.6	0.745	0.205	0.278	1.36	5
6	0.582	0.0328	130	29.0	115	0.750	0.144	0.220	1.53	6
7	0.573	0.0153	65	27.2	154	0.726	0.114	0.169	1.47	7
8	0.449	0.0121	45	25.5	105	0.731	0.138	0.232	1.69	8
9	0.543	0.0404	146	34.2	135	0.768	0.126	0.207	1.63	9
11	0.713	0.0349	151	27.6	133	0.761	0.128	0.177	1.38	11
12	0.649	0.0302	139	17.85	72.1	0.761	0.163	0.215	1.31	12
13	0.641	0.0552	248	29.8	106	0.794	0.163	0.208	1.28	13
14	0.531	0.0432	202	16.52	47.0	0.783	0.219	0.272	1.24	14
16	0.721	0.0334	142	28.6	128	0.762	0.135	0.191	1.41	16
17	0.684	0.0554	246	22.2	81.8	0.792	0.158	0.204	1.29	17
18	0.490	0.0364	169	10.85	28.6	0.769	0.243	0.308	1.27	18
19	0.688	0.0785	329	22.3	78.8	0.815	0.146	0.191	1.31	19
20	0.718	0.0941	372	22.2	74.0	0.820	0.141	0.193	1.37	20
21	0.625	0.0830	327	16.82	43.7	0.830	0.182	0.247	1.35	21
22	0.752	0.0849	320	23.0	88.9	0.806	0.121	0.177	1.46	22
23	0.578	0.0634	265	11.80	28.3	0.818	0.216	0.286	1.32	23
24	0.434	0.0281	123	8.75	22.3	0.778	0.240	0.320	1.33	24
25	0.650	0.0172	65	15.70	60.9	0.739	0.151	0.244	1.62	25
26	0.562	0.0304	134	13.42	52.5	0.760	0.160	0.218	1.36	26
27	0.474	0.0256	111	9.51	27.6	0.769	0.213	0.291	1.37	27
28	0.597	0.0497	214	14.48	43.1	0.794	0.192	0.256	1.33	28
29	0.451	0.0368	165	9.20	24.6	0.780	0.230	0.298	1.29	29
30	0.602	0.0681	279	13.21	37.0	0.805	0.185	0.250	1.34	30
31	0.491	0.0529	218	9.15	19.9	0.795	0.245	0.336	1.37	31
32	0.602	0.0829	313	13.90	32.8	0.819	0.194	0.278	1.43	32
33	0.508	0.0671	243	9.39	16.4	0.815	0.259	0.392	1.51	33
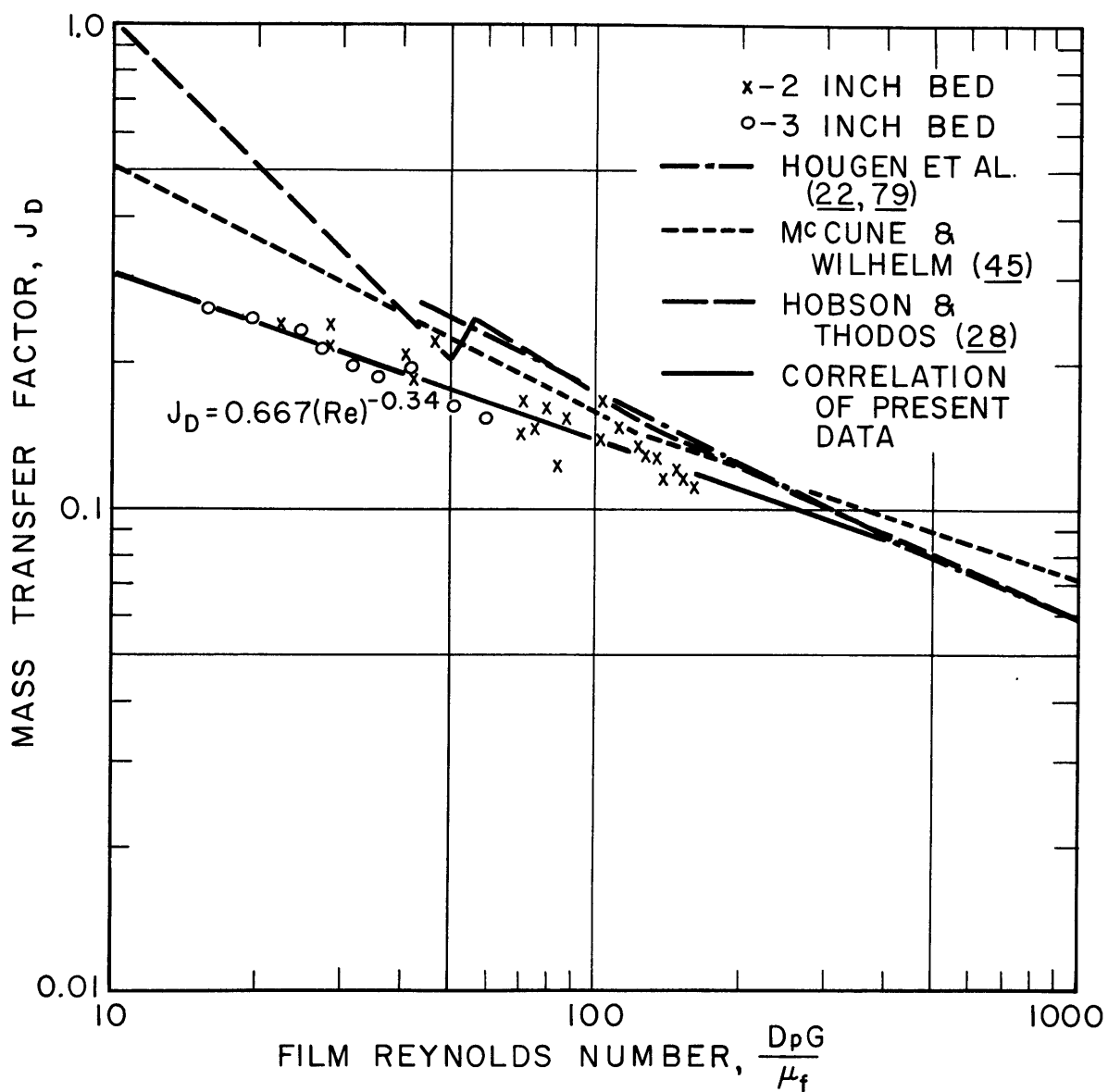
FIGURE II VARIATION OF MASS TRANSFER FACTOR WITH
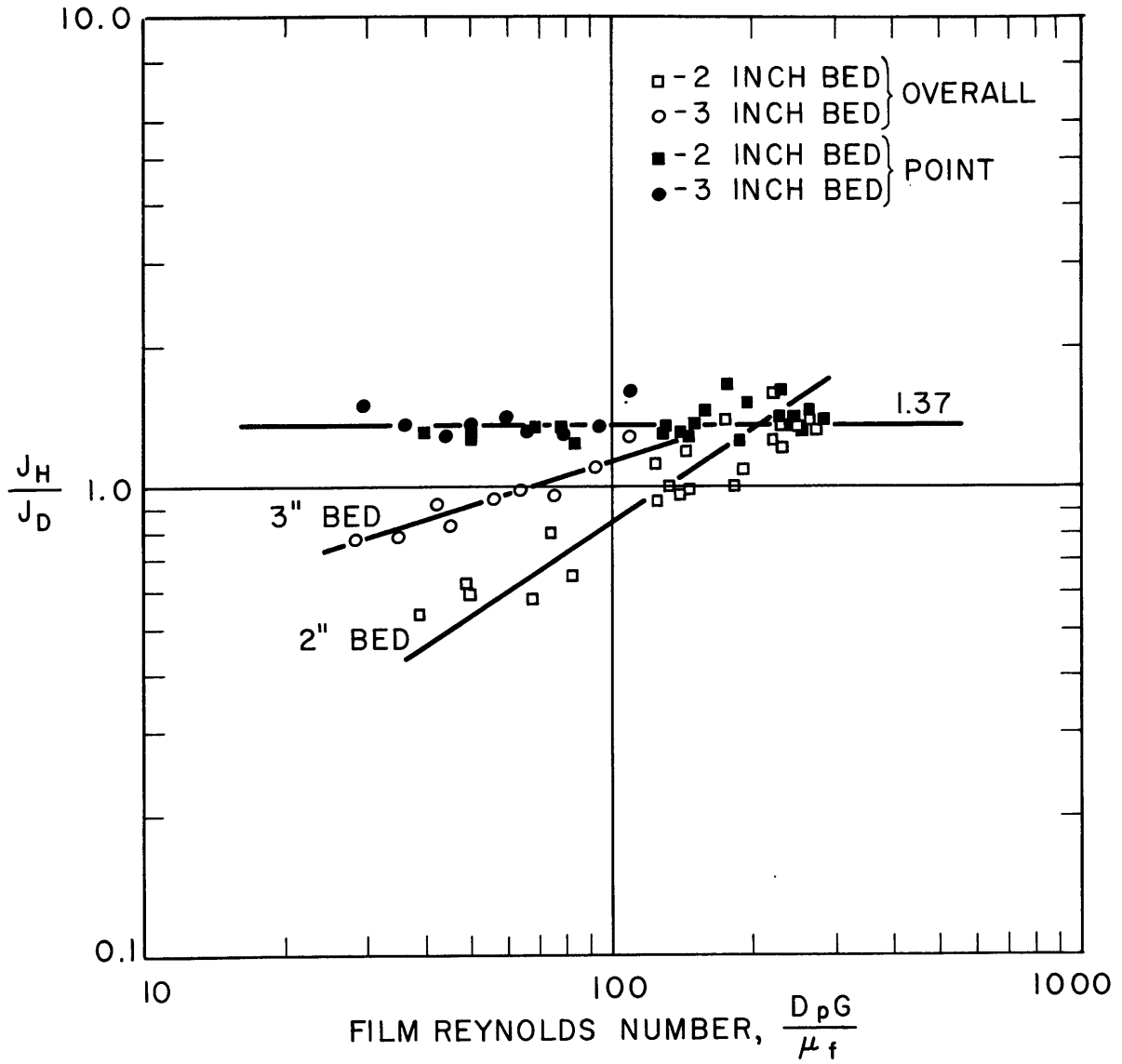REYNOLDS NUMBER IN PACKED BEDS

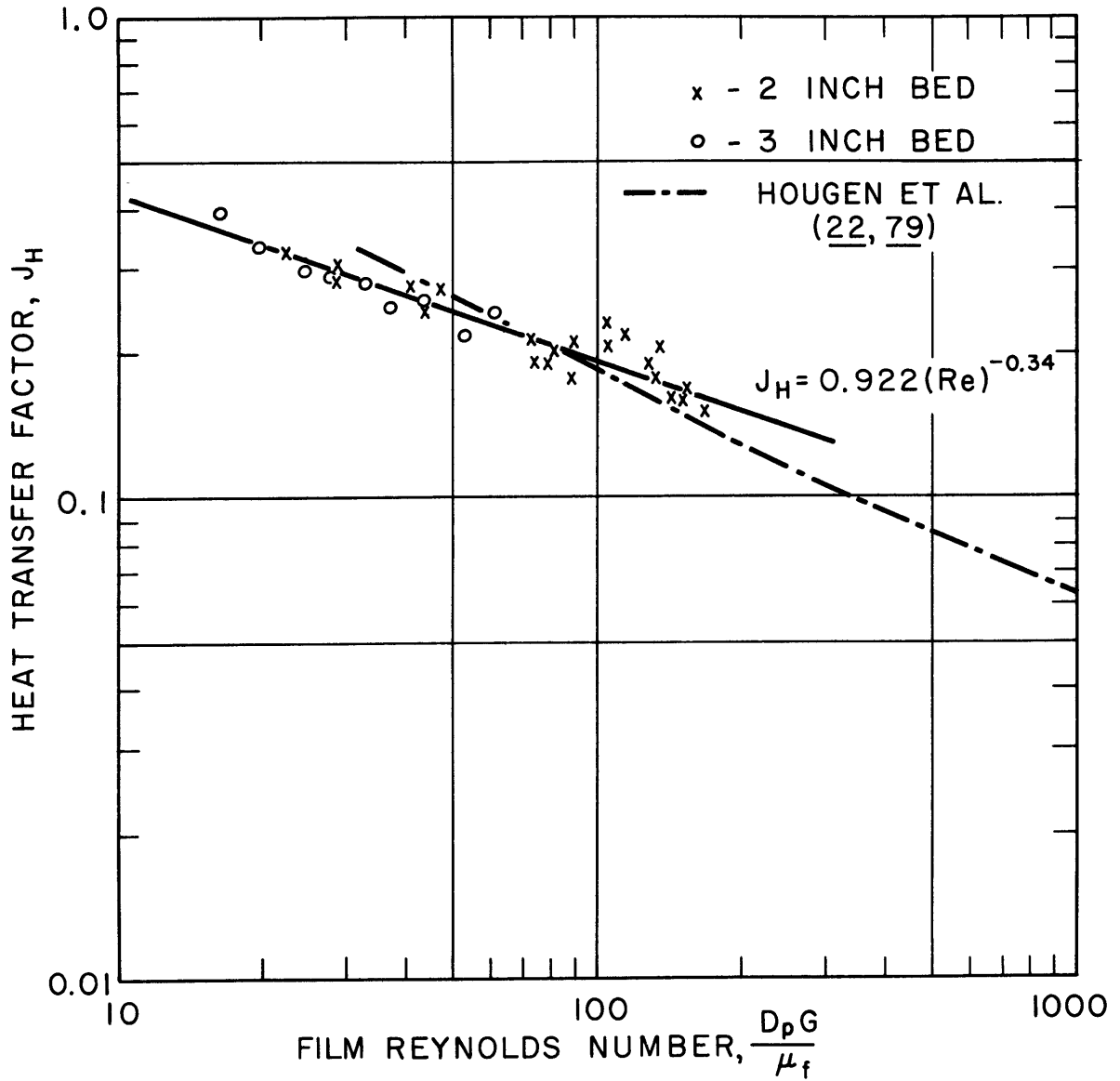FIGURE 12 RATIO OF TRANSFER FACTORS, J_H/J_D, FOR OVERALL AND POINT CONDITIONS

FIGURE 13 VARIATION OF HEAT TRANSFER FACTOR (ON A
POINT BASIS) WITH REYNOLDS NUMBER IN
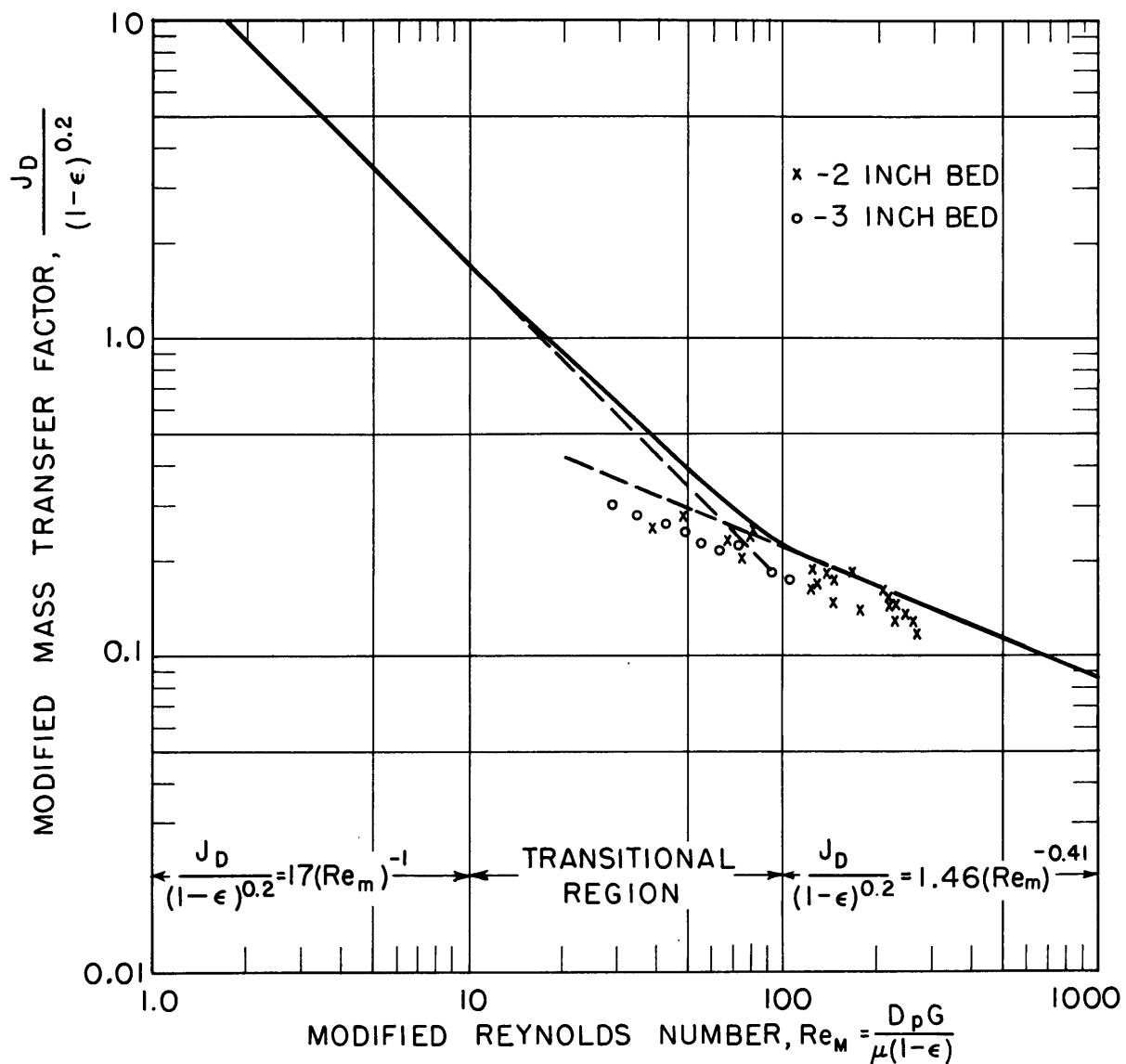PACKED BEDS

FIGURE 14   COMPARISON OF MASS TRANSFER IN THE
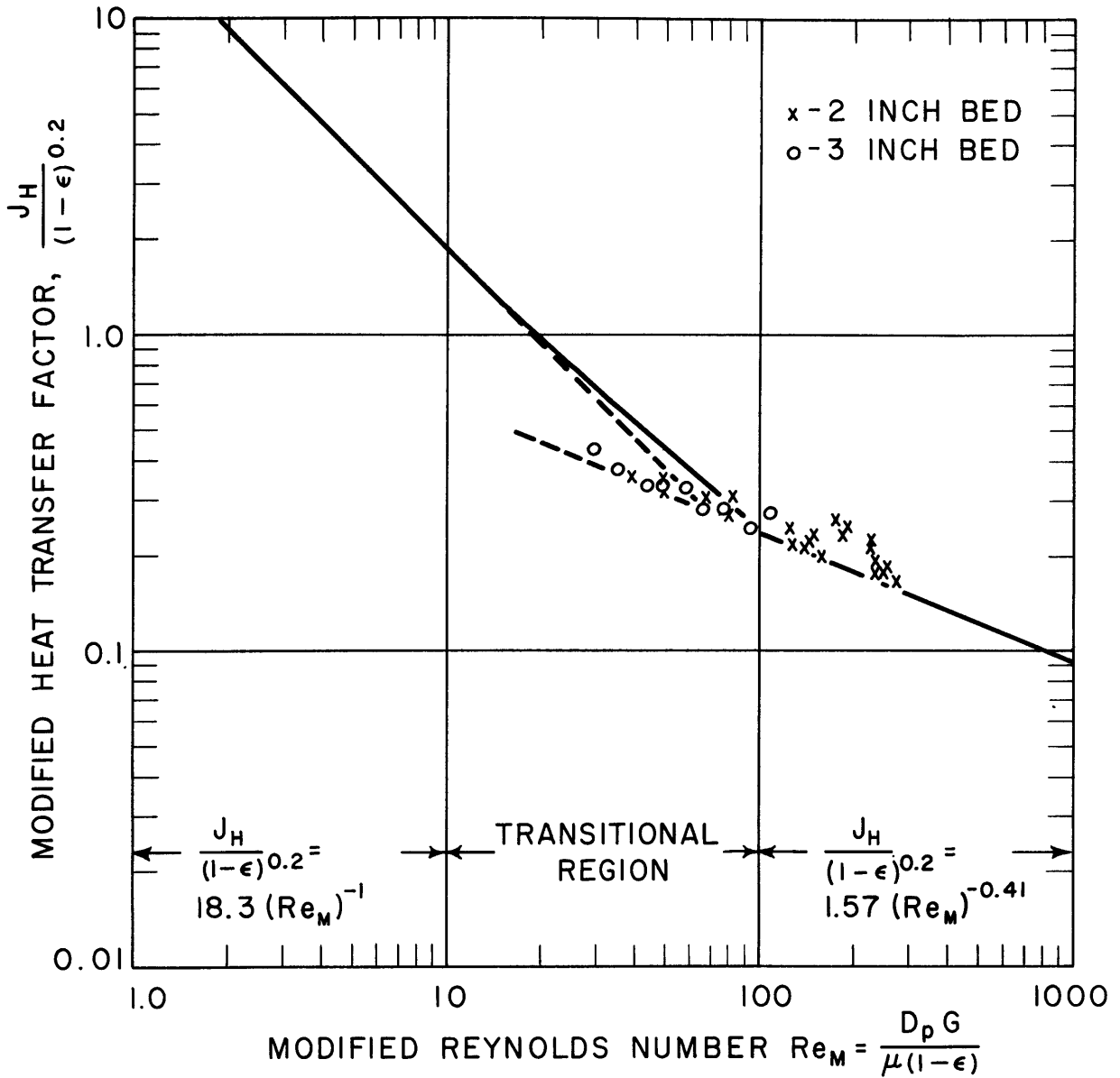HYDROGEN PEROXIDE SYSTEM WITH THE
GENERALIZED GAMSON CORRELATION

FIGURE 15   COMPARISON OF HEAT TRANSFER IN
THE HYDROGEN PEROXIDE SYSTEM
WITH THE GENERALIZED GAMSON
CORRELATION

for carrying out the point calculations are discussed below.
The values for Runs 10 and 15 are included in some of these
tables although they were omitted from the correlation and
plots because of decomposition on the glass surfaces. In
the remaining runs, the possible error due to experimental
measurements was 2% in the value of j_D and approximately 15%
in j_H in runs with small temperature gradients. In most
runs, however, the error in j_H was probably less than 5%.

Figure 11 is a plot of the mass transfer factor, j_D,
versus $D_p G/\mu_f$, the Reynolds number based on particle diameter
and film conditions. Also presented as a basis of comparison
are several correlations from the literature. Figure 12
presents the j_H/j_D ratio for both the overall values of Table
III and the point values of Table IV while Figure 13 is a
plot of the point values of the heat transfer factor, j_H,
versus the Reynolds number. Figures 14 and 15 compare the
results with the generalized Gamson correlations for mass
and heat transfer respectively.

Proof of Diffusion Control. The data from the work with the
packed beds lead to proofs of diffusion control in two man-
ners identical to those discussed for catalyst tubes, the
argument being even more convincing for two reasons. First,
the average deviation of 5.8% over the larger spread of
Reynolds numbers shown in Figure 11 makes the conclusion

more certain than in the case of the tube. Secondly, the best slope of -0.34 is shown in the figure to be less steep than the values given by other investigators for the same region of Reynolds numbers. The earlier workers indicate slopes of -0.40 to -0.50 for pure diffusion while, if surface reaction completely controlled, the slope should be -1.0. Therefore, the present slope is even slightly lower than the lowest slope that previous workers indicate would show diffusion control. The possible reason for this difference is discussed below.

Heat Flow Characteristics in the System. Although adiabatic operation would have been desirable, the complex shape of the reactor prohibited any attempts to wind the reactor and establish adiabatic flow conditions. Nevertheless, in the packed bed, the heat transfer rates from packing to flowing stream could always be calculated from the rates of decomposition without any consideration of heat losses from the system since all the heat released at the surface had to be transferred back to the stream. Therefore, the heat transfer rates, both on overall and point bases, were calculated by multiplying the known rate of decomposition by the heat of reaction at the surface temperature.

However, the heat losses and regenerative heat flow through the insulation did have a very pronounced effect on

the calculation of overall heat transfer coefficients. The gas temperatures were not measured exactly at the entrance and exit of the bed, the points at which the values were desired. Heat losses and regenerative heat flow occurring in the sections between the points of measurement and the catalyst bed caused an error which is discussed more fully in a later section. The effect was nullified by calculating the coefficients on a point rather than an overall basis.

Temperature Distribution. As shown in Table III, the catalyst temperature throughout the bed tended to be uniform, both laterally and transversely, exhibiting a slight rise in catalyst temperature in the direction of flow. This temperature profile agrees with the earlier analysis of a method for the prediction of surface temperatures. The J_H/J_D ratio in the bed is found to be 1.37, indicating that the surface temperature at any point should be less than the adiabatic reaction temperature, the difference between the two temperatures being larger at high reactant concentrations and therefore, higher temperature differences between surface and stream. This occurs at the entrance to the bed. The high ratio of J_H/J_D , calculated from data on the first layer of catalyst spheres, explains the increase in bed temperature with length which was found experimentally.

A deviation from this pattern is found in Runs 17-24 where the middle layer catalyst temperature is found experimentally to be somewhat lower than either of the other two. This deviation from the normal pattern is ascribed to changes made in the bed during the rebuilding of the apparatus after Run 15. In an attempt to keep the thermocouple wires from touching other spheres, the sphere containing the thermocouple was later found to have been placed a slight distance up into the catalyst-thermocouple-unit entrance so that its heat losses were much greater than those of other spheres in the bed.

The method described earlier for predicting surface temperatures can also be tested by the results obtained with the packed-bed system. Use of the heat and mass transfer correlations developed and the measured amounts of heat losses would have predicted the temperature gradient from the surface to the stream with an average deviation of about 6%, the increased accuracy as compared with the tube being due to the better agreement between the experimental data and the correlations.

The method of prediction also helps explain the presence of "hot-spots" or "cold-spots" which are so bothersome in packed-bed, gas-solid reactors, especially in cases where the fluid undergoes a change from liquid to gas during the reaction. "Hot-spots" can arise if the flow and heat transfer

patterns allow a portion of the fluid to become heated while retaining its initial composition. The eventual reaction of this fluid results in extremely high wall temperatures, much higher than the adiabatic reaction temperature of the entering material. "Cold-spots" are possible if portions of the surface become less catalytically active, so that diffusion is no longer controlling and the total rate of reaction at the surface becomes smaller. Since the coefficient of heat transfer is independent of this effect, it remains the same. Therefore a lower gradient is necessary between the deactivated portion of the surface and the stream than in the rest of the bed and a "cold-spot" results.

Mass Transfer Correlation. The mass transfer results are shown in Figure 11 as a plot of J_D vs. the Reynolds number. It is seen that the internal agreement of the values is excellent, giving an average deviation of 5.8% from the best line

$$J_D = \frac{k_G P_{BM} M_M}{G} = 0.667 \ (Re_f)^{-0.34} \ . \tag{63}$$

As shown by other investigators who have compared data obtained with different sphere diameters, the influence of particle diameter is accounted for by the use of a Reynolds number on a particle diameter basis. Therefore this correlation should apply to similar systems with different particle sizes.

Temperature differences between bed and stream of up to 500°F. appear to play a negligible role in determining the values of J_D. Any possible effect in the 2-inch bed runs is masked completely by the spread of the data while the internal agreement of the 3-inch values indicates definitely that no such effect exists. Physical properties are evaluated at the film temperature, although, as in the tube, the changes with temperature are such as to give almost as good a correlation on the basis of stream properties.

It is interesting to note that the data fall on a straight line and do not exhibit the break which other investigators(Figures 11 and 14) found in the range of Reynolds numbers examined. The straight line of the present work is lower in slope than the transitional and laminar region lines of earlier workers but represents a fairly good continuation of their turbulent region lines. This indicates that the flow pattern remains turbulent and does not transform into transitional or laminar patterns even at Reynolds numbers less than 20. Such behavior is in agreement with the findings of Bernard and Wilhelm (6) who demonstrated that the change from turbulent to laminar flow could occur at Reynolds numbers of from 10 to 1000 depending on the physical system involved. It seems entirely plausible, especially when one considers the additional effect of heat transfer through the film, that the system would remain turbulent throughout the entire range investigated.

Figure 11 also shows the results of this thesis to be somewhat lower than the majority of the data obtained by other investigators, although it is true that the wide spread of the earlier results covers the present work. Of the many possible causes for this difference, thermal diffusion, counterdiffusion and temperature gradients can be ruled out on the basis of arguments presented above. The most probable cause of the difference is the physical characteristics of the spheres used. In the present work, the spheres were made of polished metal, and although they lost their brilliant shine during use, examination showed that smooth surfaces remained even after ten runs, the largest number made with any one set of spheres. Other investigators employed either modified spheres made by pelletizing solid powders or porous spheres, both having rough surfaces. Such surfaces could contribute to the deviation between the two sets of values in two manners. First, the actual surface area of rough surfaces is greater than that calculated from the sphere diameter. A second and more probable effect is the increased turbulence and, therefore, increased mass transfer resulting from the roughness. The influence of added turbulence would tend to be more apparent at lower Reynolds numbers as is indicated by the larger deviation on Figure 11. Consideration of a smoothness factor would probably improve the agreement between the recommended correlation

and those of earlier workers. Therefore, it may be concluded that the mass transfer characteristics of the system are presented accurately by Equation (63).

Figure 14 compares the data with the generalized Gamson correlation. The internal agreement of the experimental values here is excellent although they average 14% below the values recommended by an extension of the turbulent line of Gamson. In this respect, they agree with the fixed-bed data of McCune and Wilhelm (45), which follow the extension of the turbulent line to modified Reynolds numbers of 23. Extreme precaution in the use of the generalized correlation is called for in the region of modified Reynolds numbers from 10 to 100 since large variations may occur depending on the exact conditions of the system being employed.

j_H/j_D Ratio. The values obtained for the j_H/j_D ratios, both factors being calculated on an overall basis, are seen in Figure 12 to be in very poor agreement both internally and with the value of about unity expected. The two- and three-inch beds give separate correlations, both exhibiting a positive slope in the plot of the ratio vs. the Reynolds number.

However, the slopes of the lines on Figure 12 and the discrepancy between the 2-inch and 3-inch data can be explained by consideration of the heat flow in the system. It

must first be realized that while the value of J_D is affected very slightly by a small error in the gas temperature measurement in the system, the value of J_H is a sensitive function of the measured temperature. As an example, if in a 15% hydrogen peroxide run, the average gas temperature is in error by being 18°F. too low, the calculated value of J_D is only 0.6% too low while J_H is 33% too low. Thus any possible errors in gas temperature measurement affect only J_H to any degree. If we now examine Figure 6, we see that the gas temperatures are not measured at the entrance and exit of the bed but rather at some distance from the bed. The exit gas temperature measured is definitely below that actually leaving the bed since heat losses occur in the system. These heat losses are relatively much greater at a low Reynolds number than at high Reynolds numbers, thus accounting for the positive slopes in Figure 12. A slight error in gas temperature measurement here is very important, the entire indicated temperature difference between gas and spheres at the bed exit being 20°F. in the run mentioned above. The actual temperature entering the bed can be either higher or lower than that measured by the thermocouple there, depending on the relative magnitude of heat loss from the stream and regenerative heat flow back down through the insulation to the entering stream. At a given concentration, the bed temperature is almost independent of flow rate and, as a

result, the temperature gradient and subsequent heat flow
from the bed through the insulation to the stream are also
independent of flow rate. Therefore, the regenerative heat
flow is relatively larger at low Reynolds numbers. A slight
error in gas temperature measurement at this point is proba-
bly not too important since the temperature difference is
large, being 190°F. in the run mentioned above. There is
also the fact that the stream thermocouples more nearly give
true stream temperatures at high Reynolds numbers although
this effect is probably negligible in the experimental appa-
ratus employed. Thus it is seen that there are several
simultaneous causes of lower apparent J_H's at low Reynolds
numbers. This explanation is supported by the difference
between the curves for the 2- and 3-inch beds in Figure 12.
In the 3-inch bed, heat loss and regenerative flow are rela-
tively less important than in the 2-inch bed, thus causing
the 3-inch data to be higher and at a smaller slope.

The above analysis of the cause of the poor agreement
shows, however, that the temperature difference measured at
the entrance of the bed is relatively accurate, first because
it is so large and secondly because the two mechanisms caus-
ing errors act in opposite directions and tend to cancel.
For this reason, point values of the J_H/J_D ratio were deter-
mined at the bottom layer of the bed. To obtain these point
values, average gas temperatures and concentrations over the

first layer of spheres are calculated by means of the relationship

$$\log F = KH \tag{64}$$

where F is fraction hydrogen peroxide not decomposed, H is bed depth and K is a constant. This expression was developed from the detailed analysis of the catalyst tube and can also be obtained roughly from the equation

$$\frac{dp}{dH} = K'p \tag{65}$$

which expresses the fact that, in diffusion-controlled systems, the change in partial pressure with height is almost directly proportional to the partial pressure. Integration of Equation (65) shows that the logarithm of the partial pressure, very nearly proportional to the fraction not decomposed, is linear in bed depth. Since F is known for inlet and exit conditions, a semi-logarithmic plot of F vs. height in the bed allows the calculation of the partial pressure and gas temperature at the center of the first layer of spheres, i.e., for the bed of five sphere layers deep, the average F for the first layer is taken at one-tenth of the distance through the bed.

From these calculated values and from the measured catalyst temperature, point values of J_D and J_H can be obtained.

The heat transfer rates are calculated by multiplying the
rate of reaction at the point by the heat of decomposition.
The heat transfer from the spheres in the bottom layer to
the glass spheres below was shown to be negligible, due
principally to the low emissivity of the metal surfaces.
The point values of J_D are nearly the same as the overall
values shown in Figure 11, all the points being slightly dis-
placed downward and to the right, parallel to the correla-
tion. However, as shown on Figure 12, the point values of
the J_H/J_D ratio now give an average deviation of 5.5% from
the value 1.37. The application of this point ratio to the
entire bed is supported by two observations:

1. This value would result in the increase in solid
   temperature which was usually found as the gas
   passed through the bed.

2. Values of the overall ratio are shown in Figure 12
   to agree with 1.37 at high Reynolds numbers where
   heat losses and regenerative heat flow are mini-
   mized.

The value of 1.37 is higher than the ratio of 1.076
proposed by Gamson. However, as shown in the Introduction,
Gamson's value is probably low since he assumed the surface
temperature in the evaporation of water from porous solids
to be the adiabatic saturation temperature. Therefore the
basic agreement is better than shown by a comparison of the

values. The value found for the ratio differs somewhat from unity but is within the range of 0.8 - 1.5 determined from data in literature. This range is not surprising in view of the fact that simple heat transfer in carefully controlled tube systems gives data points varying by 20 to 30%. No reason can be advanced for the difference of the present value from unity.

Heat Transfer Correlation. Figure 13 depicts the excellent correlation between the point values of j_H and the Reynolds number. The data have an average deviation of 6.4% from the best line

$$j_H = 0.922 \ (Re_r)^{-0.34} .$$ (66)

The values are also seen to compare very well with the heat transfer data of Hougen et al. (27, 79) although, as in the case of mass transfer, the present data exhibit a smaller slope than the earlier correlations. However, it would seem that either Equation (66) or the earlier correlation can be employed to predict the heat transfer characteristics of a packed bed.

Figure 15 presents a comparison of the heat transfer data with the generalized Gamson correlation. The agreement is good, the values averaging 10% above the continuation of

the turbulent line of the correlation. Here again it is
necessary to know the character of the flow before the
generalized correlation can be employed with confidence.

VI. CONCLUSIONS

General

(1) The results of the experimental work with both tubes and beds show that, under the conditions studied, the decomposition of hydrogen peroxide vapor is controlled by the rate of mass transport to the catalyst surface.

(2) The surface temperature in a diffusion-controlled, gas-solid system can be predicted from the heat and mass transfer characteristics and heat losses of the system.

(3) A simultaneous temperature gradient does not significantly affect the rate of molecular mass transfer through the film, under the conditions studied here. The influence of varying physical properties along the diffusion path may be included in correlations by the use of a film temperature.

(4) Thermal diffusion is negligible in the system studied.

Catalyst Tube

(1) The mass transfer rates are correlated with an average deviation of 9.5% by the equation

$$j_D = 0.021 \ (Re_f)^{-0.2} \ .$$

$$(62)$$

The 9.5% difference between Equation (62) and the Chilton-Colburn equation is not enough to preclude use of the latter.

(2) The heat transfer results are correlated with an average deviation of 14.8% by

$$J_H = 0.023 \ (Re_f)^{-0.2} \ .$$ (22)

This equation is identical to the Chilton-Colburn heat transfer factor equation and to the McAdams film thickness expression.

(3) The J_H/J_D ratio of 1.09 is in excellent agreement with the usual assumption of equality.

Catalyst Bed

(1) The mass transfer results are correlated with an average deviation of 5.8% by the equation

$$J_D = 0.667 \ (Re_f)^{-0.34} \ .$$ (63)

These results are somewhat lower than most of the previous work due probably to the smoothness of the spheres used as packing in the present work.

(2) Heat transfer coefficients calculated on the basis of the log mean of the entrance and exit temperature differences are in error because of the heat flow characteristics of the packed bed.

(3) An accurate determination of J_H can be made by use of the point values existing at the center sphere of the bottom catalyst layer. These values gave a 6.4% deviation

from the expression

$$J_H = 0.922 \ (Re_f)^{-0.34} \ .$$

(66)

Equation (66) agrees very well with previous data.

(4) The J_H/J_D ratio of 1.37 is in general agreement with the usually assumed value of 1.0.

(5) The data on both heat and mass transfer agree reasonably well with the extension of the turbulent lines of the generalized Gamson correlation.

VII.   RECOMMENDATIONS

(1)   In the design and analysis of gas-solid reactors, it is recommended that surface temperatures be predicted by the method described in the sections discussing Temperature Distribution.

(2)   The correlations obtained for both heat and mass transfer can be employed over the range of variables investigated.

(3)   The use of the generalized Gamson correlations for heat and mass transfer in packed beds appears advisable only if the flow conditions of the system are known.

(4)   The investigation should be continued for both lower and higher flow rates than those obtainable in the present work.   This would require a new vaporization system and different materials of construction.

VIII.   APPENDIX

A. DETAILS OF THEORETICAL ANALYSIS OF CATALYST TUBE

1. Development of Diffusion Equation (Neglecting Thermal Diffusion)

As shown in the Introduction, the basic differential equation for molecular diffusion under a concentration gradient is

$$y_A y_B \,(u_A - u_B) = - D_{AB} \frac{dy_A}{dx} \qquad (A-1)$$

This equation states quantitatively the conclusions that the resistance to diffusion is proportional to the number of molecules of each of the components, to the relative velocity of the diffusing component past interfering components and to the length of the diffusion path. The development of Equation (A-1) is discussed fully by Jeans (36), Loeb (42) and Sherwood (65).

By introducing the relationships

$$
\begin{aligned}
u &= NM/\rho & (A-2)\\
\rho &= Mp/RT & (A-3)\\
p &= yP \quad , & (A-4)
\end{aligned}
$$

Equation (A-1) may be transformed to

$$y_B N_A - y_A N_B = - \frac{D_{AB} P}{RT} \frac{dy_A}{dx} \qquad (A-5)$$

where N_A and N_B represent the transport rates of the two components in question. Equations like (A-1) and (A-5) may be developed for any number of diffusing components.

Since $y_B = 1 - y_A$, $\qquad$ (A-6)

Equation (A-5) may be modified to give

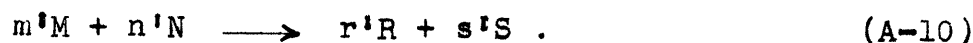$$N_A = - \frac{D_{AB}P}{RT} \frac{dy_A}{dx} + (N_A + N_B)\, y_A \quad . \qquad (A-7)$$

If the algebraic sum of the transport rates is expressed as N_t, a ratio, $\emptyset$, is defined for each component as

$$\emptyset_i = \frac{N_i}{N_t} \quad . \qquad (A-8)$$

This ratio was introduced by Wilke ($\underline{78}$) and is shown by him to be equal to

$$\emptyset_M = \frac{m'}{m'+n'-r'-s'} \qquad (A-9)$$

where m', n', r', and s' are obtained from the reaction equation

$$m'M + n'N \longrightarrow r'R + s'S \quad . \qquad (A-10)$$

The reaction is assumed to take place at the surface to and from which the reactants and products diffuse.

Equation (A-7) then becomes

$$(\emptyset_A - y_A)(N_A) = - \frac{D_{AB}P\emptyset_A}{RT} \frac{dy_A}{dx} \quad . \qquad (A-11)$$

If component A is diffusing through more than one other chemical species, it is necessary in Equation (A-11) that D_{AB} be some average value of the diffusion coefficient through the mixture of other components; in the present system, D_{AB}

represents the diffusivity of hydrogen peroxide through a mixture of water and oxygen. The various methods of obtaining this average are discussed in detail in Section A-5 of the Appendix.

For steady state conditions, Equation (A-11) can now be integrated over the diffusion path from stream to wall across the diffusion film to give

$$N_A x_D = \frac{D_{AB} P \phi_A}{RT} \ell n \frac{\phi_A - y_{AW}}{\phi_A - y_{AS}} \quad . \qquad (A-12)$$

Equation (A-12) predicts the rate of diffusion of component A countercurrent to component B along the distance x_D, the presence of the term ϕ allowing for the change in the number of mols during the reaction. The equation applies to a differential reactor in which y_{AW} and y_{AS} are fixed. For a system such as a tube through which vapor flows and reacts, Equation (A-12) must be integrated over the changing conditions along the tube. The integration is carried out with the assumption that $y_{AW} = 0$, i.e., the reaction is diffusion-controlled.

If n is the molar rate of flow of component A at any point in the tube, then

$$N_A = - \frac{dn}{dA} \qquad (A-13)$$

when − dn equals the number of mols of component A transported per unit time to a differential surface area, dA.

We may now define the fraction decomposed, f, as

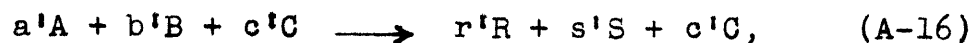$$f = \frac{n_o - n}{n_o} \qquad \text{(A-14)}$$

where the subscript zero indicates the value of n with no decomposition. Then

$$df = -\frac{dn}{n_o} . \qquad \text{(A-15)}$$

The relation between f and y is developed as follows: Assume an initial mixture of A, B, and C, C being inert, in the following proportions, mols per mol of mixture:

$$
\begin{array}{l}
\text{h' mols A} \\
\text{g' mols B} \qquad \text{h'+i'+g' = 1} \\
\text{i' mols C}
\end{array}
$$

After reaction according to the equation

$$a'A + b'B + c'C \longrightarrow r'R + s'S + c'C, \qquad \text{(A-16)}$$

there will be

$$
\begin{array}{l}
\text{h'-h'f mols A} \\
\text{g'-(b'/a')h'f mols B} \\
\text{(r'/a')h'f mols R} \\
\text{(s'/a')h'f mols S} \\
\text{i' mols C .}
\end{array}
$$

The mol fraction of A is then

$$y_A = \frac{h'(1-f)}{h'+i'+g'-\dfrac{h'}{\phi_A}f} = \frac{h'(1-f)}{1 - \dfrac{h'f}{\phi_A}} \qquad \text{(A-17)}$$

where simplification has been introduced by use of Equation
(A-9). By adding the term $(\phi_A - \phi_A)$ to the right side of
Equation (A-17), rearranging and differentiating we obtain

$$df = \frac{\phi_A(h'-\phi_A)}{h'(y_A-\phi_A)^2} \, dy_A \quad . \tag{A-18}$$

Recalling that

$$N_A = -\frac{dn}{dA} = +\frac{n_0 df}{dA} = +\frac{\phi_A(h'-\phi_A)n_0}{h'(y_A-\phi_A)^2}\frac{dy_A}{dA} \quad , \tag{A-19}$$

Equation (A-12) may now be integrated for flow through a
tube in which

$$dA = \pi \, (dia.) \, dL \quad . \tag{A-20}$$

From Equations (A-12), (A-19), and (A-20),

$$-\int_{y_{A1}}^{y_{A2}} \frac{dy_A}{(y_A-\phi_A)^2 \ln(1-\frac{y_A}{\phi_A})} = \left(\frac{D_{AB}P\pi(dia.)}{RT\,x_D n_0}\right)\left(\frac{h'}{h'-\phi_A}\right)\int_0^L dL \quad . \tag{A-21}$$

Multiplying the left integral by $(-1/\phi_A)/(-1\phi_A^2/\phi_A\phi_A^2)$ and
integrating we arrive at

$$+\frac{1}{\phi_A}\left| \ln(\ln\frac{\phi_A-y_A}{\phi_A}) - \ln(\frac{\phi_A-y_A}{\phi_A}) + \frac{\left[\ln(\frac{\phi_A-y_A}{\phi_A})\right]^2}{2\cdot 2\,!} \cdots \right|_{y_{A1}}^{y_{A2}}$$

$$= \frac{D_{AB}P\pi(dia.)}{RT\,x_D n_0} \cdot \frac{h'L}{h'-\phi_A} \quad . \tag{A-22}$$

A simplification of the above development can be made by noting that (A-12) can be written

$$N_A x_D = - \frac{D_{AB} P \phi_A}{RT} \frac{(\phi_A - y_{AS}) - (\phi_A - y_{AW})}{\frac{(\phi_A - y_{AS}) - (\phi_A - y_{AW})}{\ln(\frac{\phi_A - y_{AS}}{\phi_A - y_{AW}})}} \qquad (A-23)$$

The denominator of the extreme right term is recognized to be the logarithmic mean average of $(\phi_A - y_A)$ from stream to wall. If the term $(\phi_A - y_A)$ does not change greatly along the diffusion path, the arithmetic average may be substituted for the logarithmic average with little error, giving

$$N_A x_D = - \frac{D_{AB} P \phi_A}{RT} \frac{(\phi_A - y_{AS}) - (\phi_A - y_{AW})}{\frac{(\phi_A - y_{AS}) - (\phi_A - y_{AW})}{2}} \qquad (A-24)$$

(This assumption results in a maximum error of 0.4% for the values in the present work.)

Since $y_{AW} \doteq 0$, Equation (A-24) is simplified to

$$N_A x_D = \frac{D_{AB} P \phi_A}{RT} \cdot \frac{2 y_{AS}}{2\phi_A - y_{AS}} \qquad (A-25)$$

Combining Equations (A-25), (A-19), and (A-20),

$$\int_{y_{A1}}^{y_{A2}} \frac{(2\phi_A - y_A) dy_A}{(y_A - \phi_A)^2 \, y_A} = - \frac{D_{AB} P}{RT n_0 x_D} \frac{2h'}{h' - \phi_A} \int_0^L \pi(dia.) dL$$

$$(A-26)$$

which, on integrating, gives

$$\frac{y_{A2}-y_{A1}}{(y_{A2}-\phi_A)(y_{A1}-\phi_A)} + \frac{2}{\phi_A} \ell n \frac{y_{A2}(y_{A1}-\phi_A)}{y_{A1}(y_{A2}-\phi_A)}$$

(A-27)

$$= \frac{D_{AB}P}{RTx_D n_o} \cdot \frac{2h'}{h'-\phi_A} \cdot \pi(dia.)L \quad .$$

The development thus far has been based on the assumption that the temperature is uniform throughout the tube. In the point rate equations, the constant value can be taken as the average of the stream and wall temperature, i.e., the film temperature, while the overall Equation (A-27) may employ the average of the film temperatures entering and leaving the tube. However, the equation can be made more rigorous by considering the variation of the film temperature along the tube.

In an adiabatic system where the heat capacities of the various components are reasonably constant with temperature, the temperature of the stream may be represented as a linear function of the fraction decomposed,

$$T_s = c'f + d' \quad .$$

(A-28)

The film temperature is taken as the average of the stream and average wall temperature and can therefore be expressed as

$$T_f = cf + d \quad .$$

(A-29)

The diffusivity is also a function of temperature and, as shown in a later section, may be expressed as

$$D_{AB} = aT^{3/2} \quad .$$
(A-30)

Substitution of Equations (A-29) and (A-30) into Equation (A-12) gives

$$N_A x_D = \frac{aP\phi_A(cf+d)^{1/2}}{R} \; \ell n \; \frac{\phi_A - y_{AW}}{\phi_A - y_{AS}} \quad .$$
(A-31)

From this, using Equations (A-19 and (A-20) we get

$$\frac{dy_A}{(y_A - \phi_A)^{3/2} \left[y_A (d - \frac{c\phi_A}{h'}) - (c+d)\phi_A \right]^{1/2} \ell n (\frac{\phi_A - y_A}{\phi_A})}$$

$$= \frac{h' a P \pi (dia.) dL}{R x_D n_o (h' - \phi_A)} \quad .$$
(A-32)

Analytical integration of Equation (A-32) is not possible except by numerical methods. However, Equation (A-31) may be put in integratable form by substituting an arithmetic mean to give

$$N_A x_D = \frac{aP\phi_A(cf+d)^{1/2}}{R} \cdot \frac{2y_{AS}}{2\phi_A - y_{AS}} \quad .$$
(A-33)

By expressing f and y_A in terms of n, we now obtain

$$-\frac{dn}{dA} = \frac{aP\phi_A \left[c(\frac{n_o - n}{n_o}) + d \right]^{1/2}}{R x_D} \cdot \frac{2h'(\frac{n}{n_o})}{2(\phi_A - h') + h'(\frac{n}{n_o})}$$
(A-34)

On integration and conversion into terms of f we have the
final diffusion equation (neglecting thermal diffusion),

$$2n_0(\phi_A - h') \left| -\frac{2}{\sqrt{c+d}} \tanh^{-1} \sqrt{1-(\frac{c}{c+d})(1-f)} \right|_{f_1}^{f_2}$$

$$+ h' \left| -\frac{2n_0\sqrt{c+d}}{c} \sqrt{1-(\frac{c}{c+d})(1-f)} \right|_{f_1}^{f_2} = -\frac{2aP\phi_A h'}{Rx_D} \pi \text{ dia. L}$$

$$(A-35)$$

2. Determination of Temperature Gradient Through Film

In order to determine the possible effect of thermal
diffusion on the total transport, it is first necessary to
obtain an expression for the temperature gradient through
the film. It is assumed that the axial heat transfer is
negligible, i.e., that a negligible amount of heat is trans-
ferred along the wall. In this analysis, the system is also
assumed adiabatic, although a term allowing for heat loss to
the surroundings can be included.

The three possible mechanisms for heat transfer from
wall to stream are radiation, conduction, and that transfer
due to the sensible heat carried by the diffusing materials.
Consideration of the system showed that heat transfer from
the wall to the stream by radiation is negligible. Therefore
at steady state, we may set up a balance between the heat
transferred by conduction and that carried as sensible heat

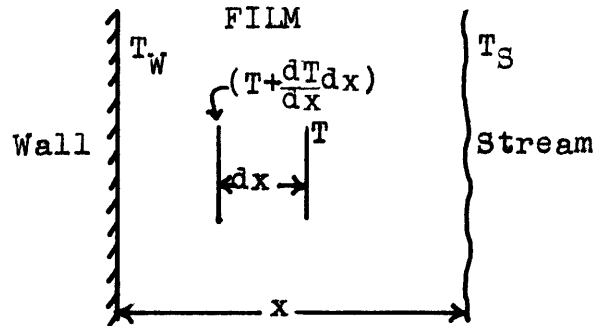by the reactants and products. Figure 1-A presents a sketch
of the system.

Figure A-1. Sketch of Film. Study of Temperature Gradient

Let
N_R = Transport rate of reactants
N_P = Transport rate of products
C_{P_R} = Heat capacity of reactants
C_{P_P} = Heat capacity of products
H_R = Enthalpy of reactants at some base temperature
H_P = Enthalpy of products at some base temperature

Conduction:

$$\text{Input} = -k \left(\frac{dT}{dx}\right)$$

$$\text{Output} = -k \left(\frac{dT}{dx} + \frac{d^2T}{dx^2}\,dx\right)$$

$$\text{Net Input} = k \frac{d^2T}{dx^2}\,dx$$

Reactants:

$$\text{Input} = N_R\left[H_R + C_{P_R}T\right]$$

$$\text{Output} = N_R\left[H_R + C_{P_R}\left(T + \frac{dT}{dx}dx\right)\right]$$

$$\text{Net Input} = -N_R C_{P_R}\frac{dT}{dx}\,dx$$

Products:

$$\text{Input} = N_P\left[H_P + C_{P_P}\left(T + \frac{dT}{dx}\,dx\right)\right]$$

$$\text{Output} = N_P\left[H_P + C_{P_P}T\right]$$

$$\text{Net Input} = N_P C_{P_P}\frac{dT}{dx}\,dx \ .$$

Summing up:

$$k \frac{d^2T}{dx^2} dx + (N_P C_{P_P} - N_R C_{P_R}) \frac{dT}{dx} dx = 0 \qquad (A-36)$$

Solving for T at a distance x within the film we get

$$T = \beta_1 + \beta_2 \, e^{-(\frac{N_P C_{P_P} - N_R C_{P_R}}{k})x} \qquad (A-37)$$

The constants of Equation (A-37) can now be determined from the boundary conditions

$$At \; x = 0, \quad T = T_S$$

$$At \; x = x_W, \quad T = T_W$$

giving as a final result

$$T = T_S + (\frac{(T_W - T_S)}{e^{-Kx_W} - 1})(e^{-Kx} - 1) \qquad (A-38)$$

$$where \; K = \frac{N_P C_{P_P} - N_R C_{P_R}}{k} \; . \qquad (A-39)$$

The value of K can be calculated for various operating temperatures from the heat capacities of steam (38), oxygen (9), and hydrogen peroxide vapor (9). It is found that the value of the exponent ($-Kx_W$) varies from -0.018 to $+0.01$ over the range of operating temperatures and flow rates, becoming 0 at a film temperature of approximately 600°F. With the use of the value 0, Equation (A-38) becomes, in the limit,

$$T = T_S + \frac{x}{x_W} (T_W - T_S) \qquad (A-40)$$

which states that the temperature is a linear function of the distance through the film. Therefore heat transfer by conduction alone need be considered. Calculations using the extreme positive and negative values of the exponent show that the gradient still remains linear and that heat transfer by the motion of the diffusing particles is negligible for the entire range of operating variables.

In a detailed analysis of the effect of mass transfer on the heat transfer coefficient, Squyres (70) determined that the ratio of the actual coefficient of heat transfer to that without mass transfer was dependent on a parameter which is equal to Kx_w. For the range of values of Kx_w in the present work, the above ratio of heat transfer coefficients ranged from 0.99^+ to 1.01^-, therefore agreeing with the above-drawn conclusion that the mass transfer in this thesis is not of sufficient magnitude to affect the heat transfer characteristics.

If we now make a heat balance on the film, we have

$$\text{Input} = - N_A (\Delta H)$$

$$\text{Output} = - k \frac{dT}{dx}$$

and
$$N_A (\Delta H) = k \frac{dT}{dx} \tag{A-41}$$

where (ΔH) is the heat of the reaction at wall temperature. Equation (A-41) is a temperature gradient expression which may be used in determining the effect of thermal diffusion.

3. Effect of Thermal Diffusion

The development given thus far has neglected the effects of temperature differences between wall and stream upon the basic diffusional relations. To allow for thermal diffusion, i.e., the separation of components under the influence of a temperature gradient, another term is added to Equation (A-1) giving

$$y_A y_B (u_A - u_B) = - D_{AB}\left(\frac{dy}{dx}\right) - \frac{D_T}{T}\left(\frac{dT}{dx}\right) . \qquad (A-42)$$

As shown in the main body of the thesis, D_T is defined by the expression

$$D_T = D_{AB} y_A y_B \alpha \qquad (A-43)$$

where α can be considered to range in this system from 0.0 to 0.3. The algebraic signs used in Equations (A-42) and (A-43) depend on the conventions employed. Component A is considered of higher molecular weight than component B, therefore giving rise to the negative sign for the thermal diffusion term in Equation (A-42).

By the use of Equations (A-2), (A-3), (A-4), (A-8), (A-9), and (A-43), Equation (A-42) can be modified to give

$$N_A = \frac{-D_{AB}\phi_A P}{RT\ (\phi_A - y_A)}\frac{dy_A}{dx} - \frac{D_{AB}\phi_A P}{RT^2} \cdot \frac{y_A(1-y_A)\alpha}{(\phi_A - y_A)}\frac{dT}{dx} . \qquad (A-44)$$

Further development of this last equation requires knowledge of (dT/dx). By introducing the previously derived temperature

gradient expression

$$N_A \Delta H = k \frac{dT}{dx} \quad , \qquad\qquad (A-41)$$

Equation (A-44) becomes

$$N_A = - \frac{D_{AB}\phi_A P}{RT(\phi_A - y_A)} \frac{dy_A}{dx} - \frac{D_{AB}\phi_A P}{RT^2} \cdot \frac{y_A(1-y_A)\alpha}{(\phi_A - y_A)} \cdot \frac{N_A(\Delta H)}{k} \cdot$$

$$(A-45)$$

Assuming an average film temperature, Equation (A-45) is rearranged to give

$$N_A dx = - \frac{\phi_A D_{AB} PTk\, dy_A}{\phi_A D_{AB} P\alpha(\Delta H) y_A(1-y_A) + RT^2 k(\phi_A - y_A)} \quad . \qquad (A-46)$$

It is now convenient to let

$$l' = \phi_A D_{AB} PTk \qquad\qquad (A-47)$$

$$m' = \phi_A D_{AB} P\alpha(\Delta H) \qquad\qquad (A-48)$$

$$n' = RT^2 k \qquad\qquad (A-49)$$

making Equation (A-46)

$$N_A dx = \frac{l'\, dy_A}{m' y_A^2 + (n'-m') y_A - n'\phi_A} \qquad\qquad (A-50)$$

which can be integrated to

$$N_A x_D = l' \left| \frac{-2}{\sqrt{4n'\phi_A m' + (n'-m')^2}} \tanh^{-1} \frac{2m' y_A + (n'-m')}{\sqrt{4n'\phi_A m' + (n'-m')^2}} \right|_{y_{AS}}^{y_{AW}}$$

$$(A-51)$$

Further integration of Equation (A-51) does not seem possible except by numerical approximation methods. However,

this procedure is not necessary since the effect of thermal diffusion in the system can be obtained by comparing Equation (A-51) with Equation (A-12). Both are point rate equations developed for the same conditions, the only difference being the consideration of thermal diffusion. Computations covering the conditions of the experimental work have been made for values of α ranging from 0.0 to 0.3, the range of values considered possible from a search through the literature. The calculations show a maximum decrease in the calculated effective film thickness of 1.5% at the highest average temperature gradients found in the present work (300°F.). The present analysis, however, has been carried out on the assumption that the polar, hydrogen peroxide-water-oxygen system behaves similarly to the non-polar systems from which the values of α employed here have been derived. It is entirely possible that the actual effect may be in the opposite direction (5)— increasing the effective film thickness—but, in any case, the effect can be considered slight.

4. Axial Heat Transfer Along the Catalyst Tube

Analysis of the heat transfer characteristics and temperature gradients in the catalyst tube system has been carried out on the basis that no heat is transferred axially along the catalyst tube wall. In this section it is shown that the amount of axial heat transfer is indeed negligible

in comparison with the amounts of heat transferred from wall to stream. This is accomplished by consideration of Run 101 in which the gradient from the 10-inch to the 22-inch thermocouple is one of the largest obtained in any run.

Data:

Temperature gradient along wall	43°F./12 inches
Thermal Conductivity of metal (approximate)	125 Btu/(hr.)(ft.)(°F.)
Inside diameter of tube	0.25 inches
Wall Thickness	0.010 inches

Area of heat flow $= \pi/4(dia._o)^2 - \pi/4(dia._i)^2$

$$= \pi/4(0.27/12)^2 - \pi/4(0.25/12)^2 = 0.000056 \text{ ft.}^2$$

Transfer along tube $= kA(\Delta T/\Delta x) = (125)(.000056)(43) = 0.3$ Btu/hr.

The increase in heat content of the gas stream between the two positions is calculated from the enthalpies of the components to be 89 Btu./lb. At the flow rate of 30.2 gms./min., the amount of heat transferred is therefore

$$(30.2)(60/454)(89) = 356 \text{ Btu./hr.}$$

The ratio of heat conduction along the tube to heat transfer is

$$0.3/356 = 0.00084 = 0.084\%$$

5. Determination of the Diffusion Coefficient

The use of the derived equations for mass transfer requires knowledge of D_{AB}, the diffusion coefficient of hydrogen peroxide through a mixture of water and oxygen. This coefficient can be obtained from the empirical equation of

Gilliland (24) which is based on the kinetic theory and on the correlation of data for diffusion of component A through a second component i,

$$D_{Ai} = \frac{0.0069\, T^{3/2}}{P(V_A^{1/3} + V_i^{1/3})^2} \sqrt{\frac{1}{M_A} + \frac{1}{M_i}} \qquad (A-52)$$

T = Absolute temperature, °R.
M = Molecular weight
V = "Molecular volume" .

For convenience in use at a constant total pressure, this equation is simplified to

$$D_{Ai} = K_{Ai}\, T^{3/2} \qquad (A-53)$$

There are three methods for combining the diffusivities of binary systems to give a mean diffusivity for component A which is diffusing through two or more other components. These are:

(1) The weighted average of the binary diffusivities — recommended by Hougen and Watson (30).

$$(1-y_A)D_{AM} = \sum y_i D_{Ai} \qquad (A-54)$$

D_{AM} = Diffusivity of A in the complex system
D_{Ai} = Diffusivity of A in binary system of A and the i-th component
y_i = Average mol fraction of component i.

(2) The harmonic mean of Wilke (78).

$$D_{AM} = \frac{1 - y_A}{\sum \dfrac{y_i}{D_{Ai}}} \qquad (A-55)$$

(3) The diffusivity of component A through an effective

second component whose properties are obtained

from a weighted average of the properties of the

other components in the system.

It is found that all three methods give virtually identical

values for D_{AB} in the hydrogen peroxide-water-oxygen system.

The atomic volumes of 7.4 for oxygen and 3.7 for

hydrogen (65) give the following values for the components

in the present system:

Component	Atomic Volume	Molecular Weight
H_2O_2	22.2	34
H_2O	14.8	18
O_2	14.8	32

These values are then used in the three methods described

above to obtain the diffusivity of hydrogen peroxide through

mixtures of water and oxygen. All three methods result in

the expression

$$D_{AB} = 1.73 \times 10^{-4} \ T^{3/2} \ ft.^2/hr. \quad (T = °K.)$$
$$(A-56)$$

There is a maximum deviation of $\pm$ 3% from this equation in

systems ranging from 0-40 wt. % H_2O_2 in the feed and 0-100%

decomposed. The error, however, is less than 2% for all but

two of the runs in this thesis (Runs 56 and 69).

As a means of checking the application of Equation (A-52)

to a hydrogen peroxide system, the diffusion coefficient of

hydrogen peroxide in air was calculated using an atomic

volume of 29.9. The resultant value of 0.189 cm.^{2}/sec. is in excellent agreement with the experimental value of 0.188 cm.^{2}/sec. reported by McMurtrie and Keyes (48). It must be admitted that, although the agreement of the experimental diffusivity with that predicted by the correlation of Gilliland is good at this temperature, there remains some uncertainty in the proper temperature dependence of the diffusion coefficient.

6. Effect of Counterdiffusion

As the last step in this analysis, it is interesting to consider the effect of counterdiffusion on the total rate of diffusion in the present system. This is accomplished by developing equations which assume that component A diffuses through a stagnant layer of the other components and comparing these equations with the counterdiffusion equations developed earlier.

Since, with the assumption of a stagnant layer, the rate of transport of component B is now zero, Equation (A-5) becomes

$$y_B N_A = - \frac{D_{AB} P}{RT} \frac{dy_A}{dx} \quad . \tag{A-57}$$

Using the equality

$$y_B = 1 - y_A \quad , \tag{A-6}$$

we obtain

$$N_A = - \frac{D_{AB} P}{RT} \cdot \frac{1}{1-y_A} \cdot \frac{dy_A}{dx} \quad . \tag{A-58}$$

Equation (A-58) can now be integrated over the diffusion path for the steady state case to give

$$N_A x_D = \frac{D_{AB} P}{RT} \ln \frac{1-y_{AW}}{1-y_{AS}} \qquad (A-59)$$

This equation can be integrated along the tube for either of the two film temperature assumptions discussed earlier to give equations comparable to (A-27) and (A-35). However, this procedure is unnecessary for the present purpose since the effect of counterdiffusion can be determined by comparing Equation (A-59) with Equation (A-12), an equation developed for the same conditions except for the consideration of counterdiffusion. Calculations over the range of variables explored in the present work show a maximum decrease in effective film thickness of 6%, indicating the relatively small effect of the counterdiffusion.

B.   DETAILS OF PROCEDURE

1.   Stainless Steel Coupling

The coupling used between the glass and catalyst tubes is shown in detail in Figure A-2. It consisted basically of a Teflon gasket and packing gland which securely butted the glass and catalyst tubes against each other. The connection between the catalyst tube and packing gland was a light push fit, a slight bit of silver solder being used to secure the tube in place. The glass tube fitted into a shoulder of the packing gland, butting against the catalyst tube. A Teflon gasket was then compressed onto the glass by a packing nut, holding the glass securely in place. The outer surface of the glass tube was accurately machined and fitted tightly into the shoulder of the packing gland and the hole in the packing nut.

When assembled and operating correctly, the coupling gave a very smooth connection between the glass and catalyst tubes. No discontinuity could be felt when a sharp-pointed probe was passed perpendicular to the surface across the joint. Any difficulty with the coupling was due to the expansion of the Teflon gasket on heating, the Teflon either breaking the glass or extruding into the joint. Either eventuality was immediately evident due to the resulting

TEFLON GASKET

SILVER SOLDER

GLASS TUBE

CATALYST TUBE

(LIGHT PUSH FIT TO PACKING GLAND)

PACKING NUT

DIA. 0.475" + 0.001
          − 0.000

DIA. 0.670" + 0.000
          − 0.001

PACKING GLAND

DIA. 0.475" + 0.001
          − 0.000

$\frac{17"}{32}$

1"

$\frac{5"}{16}$ $\frac{5"}{8}$ $\frac{1"}{4}$

$1\frac{3"}{16}$

SCALE: FULL SIZE
STOCK: 1" HEX 303 STAINLESS

$\frac{1"}{2}$ $\frac{15"}{32}$ $\frac{1"}{4}$ $\frac{13"}{32}$

$1\frac{11"}{16}$

DIA. 0.670"
+0.001
−0.000

DIA. 0.270"
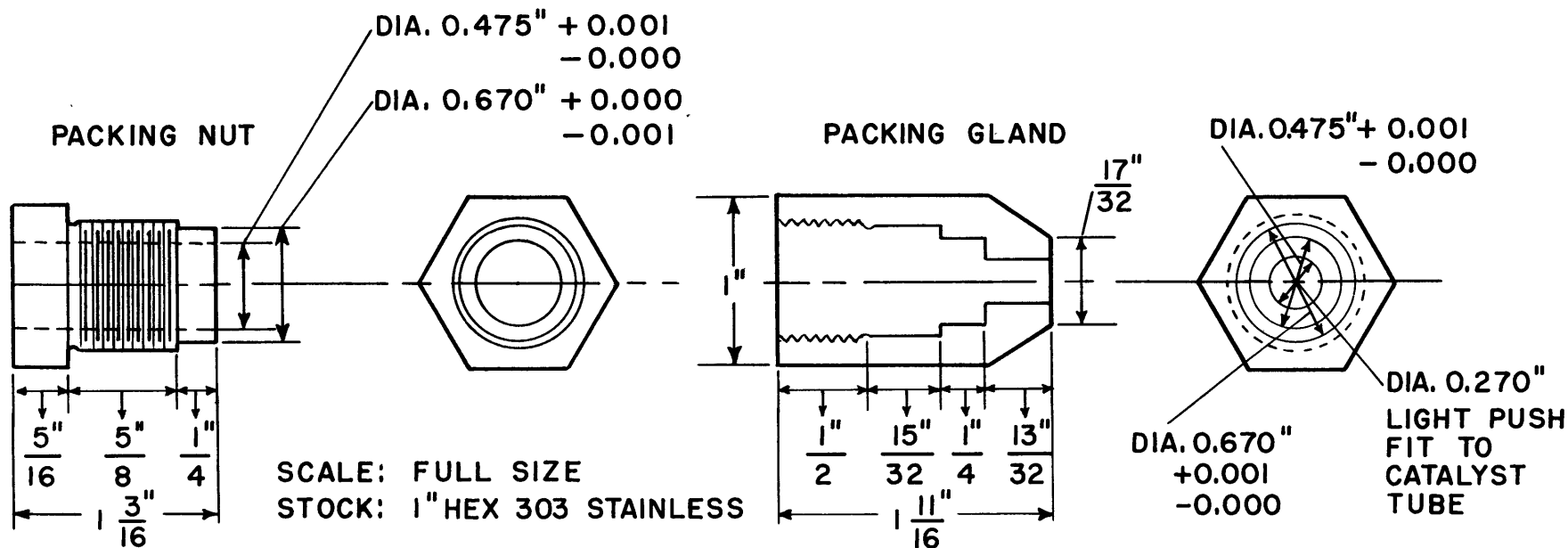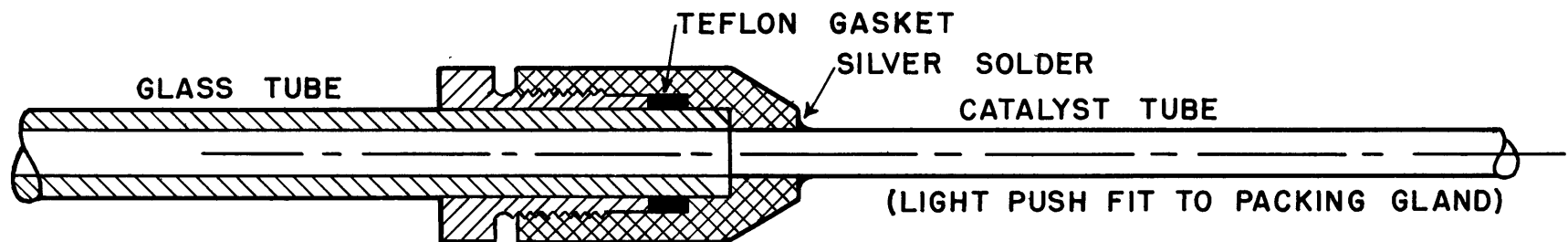LIGHT PUSH
FIT TO
CATALYST
TUBE

FIGURE A-2 DETAILS OF STAINLESS STEEL COUPLING BETWEEN
GLASS AND CATALYST TUBES

abnormally low flow rate at the boiler pressure being employed. It was found that putting shredded asbestos at the end of the gasket minimized its extrusion.

2. Analytical Procedure

Determination of Hydrogen Peroxide (31, 59). The quantity of hydrogen peroxide contained in the liquid samples was found by titration with standard potassium permanganate. A large enough portion of the sample to use 20-50 ml. of permanganate was added to 20 ml. of hot 1/20 N sulfuric acid. The hot mixture was titrated to the pink endpoint with ca. 0.2 N potassium permanganate. A blank test with 20 ml. of acid required less than 0.01-ml. of potassium permanganate to become colored.

Standardization of Potassium Permanganate. (18). About 0.3 grams of sodium oxalate (dried at 105°C.) was added to 250 ml. of diluted sulfuric acid (5 ml. acid to 95 ml. water) which had been previously boiled for 10 to 15 minutes and cooled. Potassium permanganate was added at a rate of 25 ml./ min. while stirring slowly. After the initial pink color had disappeared, the solution was heated to 55 to 60°C. and the titration completed. The excess of permanganate required to impart color to the solution was determined by adding permanganate to the same volume of diluted sulfuric acid at 55 to 60°C. This correction amounted to 0.03-0.05 ml.

3. Cleaning Procedure

Although several procedures are available, the following series of steps was employed for cleaning glass surfaces which were in contact with hydrogen peroxide vapors and solutions:

1. Wash thoroughly with soap and water
2. Soak in hot concentrated nitric acid for 24 hours
3. Rinse with distilled water
4. Soak in concentrated hydrogen peroxide for 24 hours
5. Rinse with conductivity water.

C.   SAMPLE CALCULATIONS

1. Catalyst Tube

The run to be considered in these sample calculations is Run No. 85. The following tabulation presents all the data for this run.

Tube Dimensions

Length	24 inches
Diameter	0.250 inches

General Data

Normality of $KMnO_4$ solution	0.1995 N.
Barometric pressure	30.42 in. Hg.
Titration of feed sample	65.6 ml. $KMnO_4$/ml.
Wet-test meter temperature	25.0°C.

Experimental Data. (Volumes are average values for ten samples taken during the run for a period of one minute each. Temperatures are average values for three sets of readings.)

Upstream Sample

Volume of liquid collected	7.18 ml.
Volume titrated	0.5 ml.
Volume of $KMnO_4$ used	26.65 ml.

Downstream Sample

Volume of liquid collected	33.7 ml.
Volume titrated	2.0 ml.
Volume of $KMnO_4$ used	21.56 ml.

Wet-test meter

Time per liter	26.16 sec.

Temperatures

Entering gas stream	335°F.
Exit gas stream	653°F.
First catalyst thermocouple	678°F.
Second catalyst thermocouple	728°F.
Third catalyst thermocouple	733°F.
Fourth catalyst thermocouple	728°F.
Fifth catalyst thermocouple	712°F.

a. Preliminary Calculations

The hydrogen peroxide concentration was found by titration with a standardized potassium permanganate solution in dilute sulfuric acid according to the equation:

$$2KMnO_4 + 5H_2O_2 + 3H_2SO_4 \longrightarrow 2MnSO_4 + K_2SO_4 + 8H_2O + 5O_2 \tag{A-60}$$
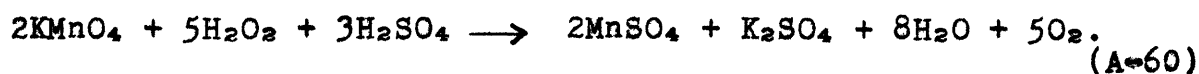
The following equations may be written for this titration:

$$\frac{g.H_2O_2}{ml.sample} = (meq.KmnO_4)(\frac{1}{ml.titrated})(\frac{mols\ H_2O_2}{meq.\ H_2O_2})(\frac{g.H_2O_2}{mol\ H_2O_2})$$

$$= (\frac{ml.KMnO_4}{ml.titrated})(N.\ KMnO_4)(\frac{1}{2000})(34) \tag{A-61}$$

$$g.H_2O_2 = 0.0170(\frac{ml.KMnO_4}{ml.titrated})(N.\ KMnO_4)(ml.sample) \tag{A-62}$$

$$wt.\%\ H_2O_2 = \frac{g.\ H_2O_2}{total\ wt.} \cdot 100 = (\frac{1.70}{Density})(N.\ KMnO_4)(\frac{ml.\ KMnO_4}{ml.titrated})$$

$$\tag{A-63}$$

The weight of hydrogen peroxide in the sample was found from Equation (A-62). Using density-concentration data (9), the weight per cent peroxide was calculated from Equation (A-63). The total weight of sample was found by dividing the grams of peroxide by the weight fraction peroxide and the weight of water was found by difference. The calculations were checked by comparing the total weight and volume of sample with the density. The results of the determinations for this run are shown in the following table:

Sample	Volume of Sample	$\dfrac{ml.KMnO_4}{ml.sample}$	Wt.% H_2O_2	Wt. H_2O_2	Wt. Sample	Wt. H_2O
Feed	--	65.6	20.73%	--	--	--
Inlet	7.18 ml.	53.1	17.02%	1.295g.	7.60 g.	6.30g.
Exit	33.7 ml.	10.78	3.62%	1.230g.	34.0 g.	32.8 g.

To find the weight of peroxide equivalent to the oxygen measured by the wet-test meter, the volume measured is corrected for (1) the vapor pressure of water at the temperature of the meter and (2) for the volume of liquid collected in the downstream separator since this volume displaced an equivalent volume in the meter.

$$\text{g./min.of } H_2O_2 \text{ equivalent to } O_2 \text{ evolved} = \left(\frac{\text{liters of } O_2 \text{ measured-liters liquid sample}}{\text{minute}}\right)$$

$$\times \left(\frac{273}{273+\text{meter temp.}}\right)\left(\frac{\text{total pressure-vapor pres.of } H_2O}{29.92}\right)$$

$$\times \left(\frac{\text{mols } O_2}{\text{standard liter}}\right)\left(\frac{\text{g. } H_2O_2}{\text{mol } O_2}\right) \qquad (A\text{-}64)$$

$$= (2.295 - 0.0337\left(\frac{273}{298}\right)\left(\frac{30.42-0.94}{29.92}\right)\left(\frac{1}{22.4}\right)\left(\frac{68}{1}\right)$$

$$= 6.19 \text{ g./min.}$$

$$\text{g./min.of } H_2O \text{ equivalent to } O_2 \text{ evolved} = (6.19)(18/34) = 3.28 \text{ g./min.}$$

A peroxide-oxygen balance may be calculated to check the data. From the known feed concentration, the amount of peroxide-oxygen that should be in the exit oxygen and downstream liquid sample can be calculated and compared with that found.

Total peroxide-O_2 = peroxide-O_2 in liquid sample + O_2
present in stream
leaving tube

$$= (1.230)(\tfrac{32}{68}) + (6.19)(\tfrac{32}{68}) = 0.58 + 2.91$$

$$= 3.49 \text{ g./min.}$$

Total weight of
stream leaving
tube

$$= 34.0 + (6.19)(\tfrac{32}{68}) = 34.0 + 2.91$$

$$= 36.9 \text{ g./min.}$$

Total peroxide-O_2
that should be
present

$$= (36.9 - 3.49)(\frac{(32/68)(0.2073)}{0.7927+(36/68)(0.2073)})$$

$$= 3.60 \text{ g./min.}$$

The error in the peroxide-oxygen balance is therefore

$$\text{Error} = \frac{3.60 - 3.49}{3.60} \cdot 100 = 3.0\% \text{ loss of peroxide-}O_2.$$

As discussed in the Procedure, this loss, which usually ranges from 1-10%, is probably due to the peculiar construction of the vaporization system which allows escape of oxygen but not of water or hydrogen peroxide. Because of this loss of peroxide-oxygen, it was convenient to define an "adjusted" feed concentration, C^*, which is the concentration of a water-hydrogen peroxide solution which, on vaporization and partial decomposition, would give the vapors which actually entered the decomposition system. It is defined as

$$C^* = \frac{\text{Wt.}H_2O_2 \text{ in sample} + \text{wt.}H_2O_2 \text{ equivalent to } O_2}{\text{Total wt. of stream leaving tube}} \cdot 100$$

(A-65)

$$= \frac{1.23 + 6.19}{36.9} = 20.1\% .$$

The ratio C^*/C represents the fraction of peroxide-oxygen in the reservoir feed that enters the decomposition system. In this case

$$\frac{C^*}{C} = \frac{20.1}{20.73} = 0.970.$$

The fraction of the hydrogen peroxide not decomposed, F, at any point is given by the ratio

$$F = \frac{\text{wt. } H_2O_2 \text{ in stream}}{\text{wt. } H_2O_2 \text{ in adjusted feed}} \qquad (A-66)$$

Calculations are to be based on the downstream data since no measurements of the upstream oxygen rate were made. As shown in Equation (A-66), the fraction not decomposed at the upstream end of the tube is given by the ratio $(H_2O_2)_1/(H_2O_2)_0$ where the quantities in parentheses are weights in grams per minute and the subscripts 0 and 1 refer to the adjusted feed and upstream conditions. Since the reaction of one mol of peroxide forms one mol of water, the sum of the mols of water and peroxide must be fixed throughout the system and one may multiply the above fraction by the ratio of the sum of the mols of water and peroxide in the adjusted feed and in the upstream sample (this ratio being unity), obtaining

$$F_1 = \frac{(H_2O_2)_1}{(H_2O_2)_0} \cdot \frac{1/18 \ (H_2O_2)_0 + 1/34 \ (H_2O_2)_0}{1/18 \ (H_2O_2)_1 + 1/34 \ (H_2O_2)_1} \qquad (A-67)$$

By rearrangement,

$$F_1 = \frac{(H_2O/H_2O_2)_0 + 0.53}{(H_2O/H_2O_2)_1 + 0.53} \ . \qquad \text{(A-68)}$$

Applying Equation (A-68) to the data,

$$(H_2O/H_2O_2)_0 = (100 - 20.73)/20.73 = 3.97$$

$$(H_2O/H_2O_2)_1 = 6.30/1.295 = 4.86$$

$$F_1 = \frac{3.97 + 0.53}{4.86 + 0.53} = 0.835.$$

The fraction decomposed at the downstream sampling point can be obtained similarly but is more easily calculated from the expression

$$F_2 = \frac{\text{wt.}H_2O_2 \text{ in sample}}{\text{wt.}H_2O_2 \text{ in sample} + \text{wt.}H_2O_2 \text{ equivalent to } O_2}$$

$$= \frac{1.23}{1.23 + 6.19} = 0.166 \qquad \text{(A-69)}$$

The mol fraction hydrogen peroxide in the vapor is obtained from the expression developed above

$$y = \frac{h'(1 - f)}{1 - (h'/\phi_A)f} = \frac{h'(1 - f)}{1 + (h'/2)f} \qquad \text{(A-17)}$$

where h' is the mol fraction H_2O_2 in the adjusted feed, f is the fraction decomposed $(f = 1 - F)$, and ϕ_A for the decomposition of H_2O_2 to H_2O and oxygen equals $2/(2 - 2 - 1) = -2$. On the basis of one hundred pounds of adjusted feed, the mol fraction hydrogen peroxide is

$$h' = \frac{\text{mols } H_2O_2}{\text{mols } H_2O_2 + \text{mols } H_2O} = \frac{C*/34}{C*/34 + (1-C*)/18} \qquad (A\text{-}70)$$

$$= \frac{20.1/34}{20.1/34 + 79.9/18} = 0.1178 \quad .$$

From Equation (A-17),

$$y_1 = \frac{(0.1178)(0.835)}{1 + (0.1178/2)(.165)} = 0.0975$$

$$y_2 = \frac{(0.1178)(0.166)}{1 + (0.1178/2)(.834)} = 0.01862$$

The log mean value of y is given by

$$y_{l.m.} = \frac{y_1 - y_2}{\ln(y_1/y_2)} \qquad (A\text{-}71)$$

$$= \frac{.0975 - 0.01862}{\ln 0.0975/0.01862} = 0.0476$$

b. Calculation of x_D, Film Thickness for Mass Transfer

The values of the film thickness are calculated from Equations (A-12), (A-27) and (A-35), which are based, respectively, on point conditions, constant film temperature along the tube, and varying film temperature along the tube. As discussed in the main body of the thesis, the equations agree within 2% but the value given by (A-35) is employed since it most accurately represents conditions in the tube.

The value of n_0, the molal rate of flow of H_2O_2 with no decomposition, is obtained from

$$n_0 = \frac{(W)(C^*)}{(34)(100)} \qquad (A-72)$$

where W is total rate of flow through the tube in pounds per hour and is obtained from the basic data by the expression

$$W = \frac{(\text{total wt. of stream leaving tube/min.})(60)}{454} \qquad (A-73)$$

$$= \frac{(36.9)(60)}{454} = 4.88 \text{ lb./hr.}$$

Therefore

$$n_0 = \frac{(4.88)(20.1)}{3400} = 0.0289 \text{ lb.mol/hr.}$$

The total rate of decomposition, w, is obtained by multiplying n_0 by the difference of the fraction decomposed:

$$w = n_0 (F_1 - F_2) \qquad (A-74)$$

$$= (0.0289)(0.835 - 0.166) = 0.0193 \text{ lb.mol/hr.}$$

As shown in an earlier section, the diffusion coefficient of hydrogen peroxide through the gas stream is obtained by the expression

$$D_{AB} = aT^{3/2} = 1.73 \times 10^{-4}T^{3/2} \text{ ft.}^2/\text{hr.} \qquad (A-30)$$

where T is temperature in $^\circ$K. The temperature functions necessary both to calculate the diffusivity and to substitute in the equations are obtained as follows:

The average wall temperature is the average of the five wall readings,

$$T_{W_A} = \frac{T_{W_1} + T_{W_2} + T_{W_3} + T_{W_4} + T_{W_5}}{5} \qquad (A-75)$$

$$= \frac{678 + 728 + 733 + 728 + 712}{5} = 716°F.$$

The film temperature used as an average value over the entire length of the tube is

$$T_a = \frac{(T_{W_A} + T_2)/2 + (T_{W_A} + T_2)_2}{2} \qquad (A-76)$$

$$= \frac{(716 + 335)/2 + (716 + 653)/2}{2} = 605°F. = 591°K.$$

The varying film temperature is obtained, as discussed in the Theoretical Analysis, from the expressions

$$T_s = (c'f + d') \qquad (A-28)$$

$$T_f = (c'f + d' + T_{W_{ave}})/2 = (cf + d) \qquad . \qquad (A-29)$$

In the present case,

$$T_{s_1} = 335°F. \qquad f_1 = 0.165$$

$$T_{s_2} = 653°F. \qquad f_2 = 0.834$$

Therefore,

$$335 = 0.165 \, c' + d'$$

$$653 = 0.834 \, c' + d',$$

$$c' = 476$$

$$d' = 257 \ ,$$

and

$$T_f = \frac{476f + 257 + 716}{2} = (238f + 486)°F.$$

$$= (132f + 526)°K.$$

The above values can now be substituted in the equations to obtain x_D. The point-rate Equation (A-12) employs the average film temperature T_a, the log mean average y, average rate of decomposition obtained by dividing the total rate of decomposition by the inside area of the tube, and a total pressure of one atmosphere. The other two equations employ direct substitution of values given above. The results are given in the following table:

Equation	x_D
(A-12)	10.29×10^{-4} ft.
(A-27)	10.19×10^{-4} ft.
(A-35)	10.11×10^{-4} ft.

It is seen that the difference between the two integrated equations is less than 1% and the difference between the point-rate equation and the integrated equations is less than 2%. The direction of the differences is not typical since in some runs Equation (A-12) gives the lowest values and in still other runs all three agree exactly. However, the difference found in the present run does represent the

highest found in any of the runs. The value given by Equation (A-35) is chosen for further work since that equation, as stated above, most accurately represents conditions in the system.

c. Calculation of Mass Transfer Factor, j_D

The mass transfer factor is calculated by converting the effective film thickness, x_D, to a mass transfer coefficient and combining this value with the physical properties and flow conditions of the system. As discussed in the Procedure, the physical properties are taken at the film temperature at the point in the tube at which the log mean driving force occurs. Therefore, it is now necessary to calculate these properties and then obtain j_D.

The fraction decomposed at this point, f_p, is obtained by rearrangement of Equation (A-17) to

$$f_p = \frac{2}{h'} \frac{(h' - y_p)}{(y_p + 2)} , \qquad (A-77)$$

where y_p is the log mean mol fraction, $y_{l.m.}$.
For Run 85,

$$f_p = \frac{2}{0.1178} \cdot \frac{(0.1178 - 0.0476)}{2 + 0.0476} = 0.584.$$

The per cent O_2 in the stream at this point is obtained from

$$(\%O_2)_p = \frac{f_p(h'/2)(100)}{1 + f_p(h'/2)} = \frac{(0.584)(.0589)(100)}{1 + (0.584)(.0589)} = 3.32$$

$$(A\text{-}78)$$

The mean molecular weight of the gases at the point is

$$(M_M)_p = 34(\text{mol frac.H}_2\text{O}_2) + 32(\text{mol frac.O}_2) + 18(\text{mol.frac.H}_2\text{O})$$

$$(A\text{-}79)$$

$$= 34\,(.0476) + 32\,(.0332) + 18\,(.9192)$$

$$= 19.2$$

The film temperature is obtained from

$$(T_f)_p = cf_p + d \qquad\qquad (A\text{-}29)$$

$$= (132)(.584) + 526 = 603°K.$$

The diffusivity at this temperature is obtained from Equation (A-30) as

$$(D_{AB})_p = (1.73 \times 10^{-4})(603)^{3/2}(1/3600) = 7.16 \times 10^{-4} ft^2/sec.$$

The gas density at the point, $(\rho_f)_p$ is obtained from the equation

$$(\rho_f)_p = \frac{(M_M)_p}{359} \cdot \frac{273}{(T_f)_p} \qquad\qquad (A\text{-}80)$$

$$= \frac{19.2}{359} \cdot \frac{273}{603} = 0.0242 \text{ lb./ft.}^3$$

The viscosity of the gas stream is obtained as the viscosity of steam at the film temperature. Unpublished work (16) indicates that the viscosity of steam-oxygen-hydrogen peroxide vapor mixtures is very close to that of steam at the concen-

trations employed. The viscosity is obtained from the
equation

$$\mu_f = \left[(0.00244)(T \ ^\circ K.) - 0.06\right] \times 10^{-5} \ \text{lb.}/(\text{sec.})(\text{ft.})$$

<div align="right">(A-81)</div>

which represents the best published values for this
property (39).

$$\mu_{f_p} = (0.00244)(603) - 0.06 = 1.41 \times 10^{-5} \ \text{lb.}/(\text{sec.})(\text{ft.}).$$

Therefore the Schmidt number can be obtained from its
definition

$$(Sc)_f = (\frac{\mu}{\rho D})_f$$

<div align="right">(A-82)</div>

$$= \frac{1.41 \times 10^{-5}}{0.0242 \times 7.16 \times 10^{-4}} = 0.814.$$

The flow properties in the system are obtained from the
basic equation for G, the mass flow rate,

$$G = \frac{(W)(4)}{3600(\pi)(d)^2} \ (\text{lb.})/(\text{ft.})^2(\text{sec.})$$

<div align="right">(A-83)</div>

$$= \frac{4.88 \ (4)}{(3600)(3.14)(0.02083)^2} = 3.98 \ \text{lb.}/(\text{ft.}^2)(\text{sec.})$$

The basic equation for j_D,

$$j_D = (\frac{k_G P_{BM} M_M}{G})(Sc)_f^{2/3} = (\frac{k_c P_{BM} \rho_f}{G \ P})(Sc)_f^{2/3}$$

<div align="right">(A-84)</div>

can be rearranged by introducing the definition

$$x_D = \frac{D_{AB}P}{RTk_G P_{BM}} = \frac{D_{AB}P}{k_c P_{BM}} \qquad \text{(A-85)}$$

to give

$$J_D = \left(\frac{D_{AB}\rho_f}{x_D G}\right)(Sc)_f^{2/3} \ . \qquad \text{(A-86)}$$

For the run being considered,

$$J_D = \frac{(7.16 \times 10^{-4})(.0242)}{(10.11 \times 10^{-4})(3.98)} (.814)^{2/3}$$

$$= 3.75 \times 10^{-3}$$

d. Calculation of Film Reynolds Number, $(dG/\mu)_f$

The film Reynolds number, Re_f, is calculated from the basic definition

$$Re_f = (dG/\mu)_f \qquad \text{(A-87)}$$

$$= (0.02083)(3.98)/(1.41 \times 10^{-5})$$

$$= 5890$$

e. Calculation of Heat Losses

The per cent of the heat released by the reaction escaping to the surroundings is calculated by comparing the heat released by the reaction with the increase in sensible enthalpy of the stream as it flows through the tube. On the basis of a pound mol of adjusted feed, the following equations may be written (all values in Btu):

Heat of reaction $= 43,660(F_1 - F_2)h'$ (A-88)

$$\text{Sensible enthalpy gain} = F_2 h'(i_{T_2} - i_{T_1})_{H_2O_2} + \frac{f_2 h'}{2}(i_{T_2} - i_{T_1})_{O_2}$$

$$+ (i' + f_2 h')(i_{T_2} - i_{T_1})_{H_2O} \qquad (A-89)$$

Heat loss = Heat of reaction - Sensible enthalpy gain (A-90)

$$\% \text{ Heat loss} = L = \frac{\text{Heat loss}}{\text{Heat of Reaction}} \cdot 100 \qquad (A-91)$$

The symbols h' and i' represent the mol fraction of hydrogen peroxide and water in the adjusted feed while i represents the enthalpy per pound mol of the designated component and at the indicated temperature. The values of the enthalpy and the molal heat of decomposition are obtained from the Buffalo Electrochemical Company's handbook of physical properties of hydrogen peroxide and its decomposition products (9) and from the steam tables (38). Substitution of the values for the present run into the above equations gives

Heat of reaction $= (43,660)(0.1178)(0.835-0.166) = 3441$ Btu.

$$\text{Sensible enthalpy gain} = (0.166)(0.1178)(6150-2560)$$

$$+ \frac{(0.834)(0.1178)}{2}(4270-1890)$$

$$+ \Big[(0.8822 + (0.834)(0.1178)\Big](1360.4-1209.3)(18)$$

$$= 2907 \text{ Btu}$$

Heat loss = 3441 - 2907 = 534 Btu.

% Heat loss = L = $\frac{534}{3441}$ · 100 = 15.5%

f. Calculation of j_H on basis of log mean ΔT

The first method of calculating j_H is on the basis of the overall heat transfer rate and the log mean of the entrance and exit temperature differences, gas temperature to average wall temperature. The overall heat transfer rate is obtained by multiplying the rate of decomposition by the heat of decomposition and correcting for heat losses,

$$Q_o = (w)(\Delta H)(1 - L/100) \tag{A-92}$$

$$= (0.0193)(43660)(.845) = 712 \text{ Btu./hr.}$$

The log mean temperature difference is calculated by

$$\Delta T_{lm} = \frac{\Delta T_1 - \Delta T_2}{\ln (\Delta T_1/\Delta T_2)} \tag{A-93}$$

$$= \frac{(716-335) - (716-653)}{\ln (381/63)} = 177°F.$$

The heat transfer coefficient, h, is now obtained from the basic equation.

$$h_{lm} = \frac{Q}{A\Delta T} = \frac{712}{(\pi)(2)(.02083)(177)} = 30.8 \text{ Btu./(hr)(ft)}^2(°F.)$$
$$\tag{A-94}$$

The value of $J_{H_{lm}}$ is now calculated from the definition of J_H,

$$J_H = (\frac{h}{C_p G})(Pr)_f^{2/3} \qquad\qquad (A-95)$$

The specific heat, C_p, is taken as that of steam and obtained from the steam tables (38) while the value of the Prandtl number has been shown to be 1.0 for the range of temperatures and pressures encountered (62). Therefore,

$$J_{H_{lm}} = \frac{(30.8)}{(0.481)(3600)(3.98)} (1.0)^{2/3} = 0.00445$$

g. Calculation of J_H on Basis of ΔT_p

The second method of determining J_H is on the basis of the point values of the heat transfer rate and the temperature difference at the point in the tube at which the log mean driving force occurs. The rate of mass transfer at this point is calculated from Equation (A-12) as

$$N_{A_p} = \frac{(7.16 \times 10^{-4})(1)(-2)}{(1.3145)(603)(10.11 \times 10^{-4})} \ln \frac{-2}{-2-0.0476}$$

$$= 0.000042 \text{ lb.mols/(sec.)(ft.)}^2 .$$

From the relationship

$$Q_p/A = (N_{A_p})(\Delta H)(\frac{100-L}{100}) \qquad , \qquad\qquad (A-96)$$

the point rate of heat transfer is

$$Q_p/A = (0.000042)(43,660)(0.845) = 1.55 \text{ Btu./(sec.)(ft.)}^2$$

The value of ΔT_p, the point temperature difference, is obtained by subtracting the value of the stream temperature, given by Equation (A-28), from the actual measured wall temperature at the point. The latter temperature is found by use of the integrated Equation (A-35) which allows the determination of the position along the tube at which the log mean driving force occurs. The application of the equation is simpler than might first appear since it was found that Equation (A-35) gives a straight line on a plot of log (1 - f) vs. tube length. Therefore, to find the distance along the tube at which the log mean driving force occurs, one plots (1 - f) vs. tube length on semi-log paper and finds the point in the tube corresponding to the value f_p. In the present run, this occurs at 9.8 inches from the tube entrance. The wall temperature measurements give the value of the wall temperature at that point as 733°F. It is noted that the temperature desired is on the flattest portion of the wall temperature profile and that a change in the distance of as much as 1 inch would not change the value of the wall temperature. The stream temperature obtained from Equation (A-28) is

$$T_{sp} = (476)(0.584) + 257 = 536°F.$$

Therefore,

$$h_p = \frac{Q_p}{A(\Delta T)_p} = \frac{(1.55)(3600)}{(733-536)} = 28.3 \text{ Btu./(hr.)(ft.)}^2(^\circ F.)$$

$$(A-97)$$

and

$$J_{H_p} = \frac{28.3}{(0.481)(3600)(3.98)} (1.0)^{2/3} = 0.00410$$

2. Catalyst Bed

The run to be considered in these sample calculations is Run No. 11. The following tabulation presents all the data for this run.

Reactor Dimensions

Bed diameter	4.80 cm.
Bed depth	2.35 cm.
Number of catalyst spheres	355
Diameter of catalyst spheres	0.508 cm.

General Data

Normality of $KMnO_4$ solution	0.1997 N.
Barometric pressure	29.58 in. Hg.
Titration of feed sample	27.5 ml.$KMnO_4$/ml.
Wet-test meter temperature	27.0°C.

Experimental Data (Volumes are average values for ten samples taken during the run for a period of one minute each. Temperatures are average values for six sets of readings.)

Upstream Sample

Volume of liquid collected	11.0 ml.
Volume titrated	1.0 ml.
Volume of $KMnO_4$ used	24.8 ml.

Downstream Sample

Volume of liquid collected	44.1 ml.
Volume titrated	10.0 ml.
Volume of $KMnO_4$ used	20.4 ml.

Wet-test meter

Time per liter	41.47 sec.

Temperatures

Entering gas stream	302°F.
Exit gas stream	493°F.
First catalyst layer	500°F.
Third catalyst layer	508°F.
Fifth catalyst layer	509°F.

a. Preliminary Calculations

The preliminary calculations for the bed are identical to those described for the tube. Therefore, only the following tabulation of the results of these calculations will be given for Run 11.

$C*$ – 8.92%
$C*/C-$ 0.984
F_1 – 0.915
F_2 – 0.0753
y_1 – 0.0450
y_2 – 0.00363
y_{lm} – 0.01648

total rate of flow through bed – 48.47 g./min. = 6.39 lbs./hr.

b. Calculation of Mass Transfer Factor, j_D

The mass transfer factor is calculated from its definition

$$j_D = \frac{k_G P_{BM} M_M}{G} (Sc)_f^{2/3} \qquad (A-84)$$

The necessary physical characteristics are determined at the mean film conditions in the bed. The calculations are carried out entirely empirically and are on the basis of a unit superficial area of the bed.

The superficial area of flow through the bed is

$$A = (\frac{\pi}{4})(\frac{4.8}{30.48})^2 = 0.01945 \text{ ft.}^2$$

The peroxide deeomposed per unit superficial area is given by the expression

$$\frac{W}{A} = \frac{(W)(C^*)(F_1-F_2)}{(34)(100)(A)} \qquad \text{(A-98)}$$

$$= \frac{(6.39)(8.92)(0.915-0.0753)}{(34)(100)(0.01945)}$$

$$= 0.725 \text{ lb.mols}/(\text{ft.})^2(\text{hr.})$$

The packed-volume fraction of the bed is

$$(1-\epsilon) = \frac{(\text{no. of catalyst spheres})(\text{volume per sphere})}{\text{total packed volume}}$$

$$\text{(A-99)}$$

$$= \frac{(355)(4/3)(\pi)(0.508/2)^3}{(\pi/4)(4.80)^2(2.35)} = 0.573$$

The catalyst surface per unit volume of packing is

$$a = \frac{\text{total surface area of spheres}}{\text{volume of packing}}$$

$$= \frac{\text{surface area per sphere}}{\text{volume per sphere}} \text{ x } \frac{\text{total volume of spheres}}{\text{volume of bed}}$$

$$= \frac{\pi(D_p)^2}{(1/6)(\pi)(D_p)^3}(1-\epsilon) = \frac{6(1-\epsilon)}{D_p} \qquad \text{(A-100)}$$

where D_p is the diameter of a sphere. Therefore,

$$a = \frac{6(0.573)}{(0.508/30.5)} = 206.6 \text{ ft.}^2/\text{ft.}^3$$

The basic equation for k_G is obtained from its definition as

$$k_G = \frac{w}{A(aH)(\Delta p)_M}$$ (A-101)

The product (AaH) is the total surface area of the catalyst in the bed while the mean partial pressure driving force is taken as the log mean mol fraction driving force since the total pressure was always essentially atmospheric. Therefore,

$$k_G = \frac{0.725}{(206.6)(2.35/30.48)(0.01648)} = 2.76 \text{ lb.mols/(atm)(ft)}^2\text{(hr)}$$

The mean partial pressure of inerts across the film, p_{BM}, is taken as the mean of the values in the bulk stream and at the wall. Since the total pressure is one atmosphere and the concentration of the hydrogen peroxide is zero at the wall, the film partial pressure of inerts at any point is given by

$$p_B = \frac{1+1-y}{2} = \frac{2-y}{2}$$ (A-102)

Therefore,

$$p_{B_1} = \frac{2-0.0450}{2} = 0.9775 \text{ atm.}$$

$$p_{B_2} = \frac{2-0.00363}{2} = 0.9982 \text{ atm.}$$

and

$$p_{BM} = \frac{0.9775+0.9982}{2} = 0.988 \text{ atm.}$$

The mean molecular weight, M_M, of the gas stream is calculated from the values of F_1 and F_2 using a basis of 100 lbs. of the adjusted feed, 8.92% hydrogen peroxide.

Component	Feed	Upstream	Downstream
	$F_o = 1$	$F_1 = 0.915$	$F_2 = 0.0753$
H_2O_2	0.262 mols	0.240 mols	0.020 mols
H_2O	5.06 mols	5.082 mols	5.302 mols
O_2	0 mols	0.011 mols	0.121 mols
Total	5.322	5.333	5.443

$$\text{Upstream molecular weight} = \frac{100}{5.333} = 18.75$$

$$\text{Downstream molecular weight} = \frac{100}{5.443} = 18.38$$

The mean molecular weight is taken as the arithmetic average of the two values

$$M_M = \frac{18.75 + 18.38}{2} = 18.53 \text{ lbs./mol}$$

The value of the Schmidt number to be used is the logarithmic mean of the values determined at the film temperatures at the entrance and exit of the bed. From Equations (A-30), (A-80) and (A-81) for diffusivity, density and viscosity respectively, the following equation for the Schmidt number is determined:

$$Sc_f = \frac{0.672\ T_f - 16}{M_M(T_f)^{1/2}} \qquad\qquad (A\text{-}103)$$

where T is in degrees Kelvin.

From the data given for Run 11,

$$T_{f_1} = \frac{302 + 500}{2} = 401^\circ F. = 479^\circ K.$$

$$M_{M_1} = 18.75$$

$$(Sc)_{f_1} = \frac{(0.672)(479)-16}{(18.75)(479)^{1/2}} = 0.745$$

$$T_{f_2} = \frac{493 + 509}{2} = 501^\circ F. = 534^\circ K.$$

$$M_{M_2} = 18.38$$

$$(Sc)_{f_2} = \frac{(0.672)(534)-16}{(18.38)(479)^{1/2}} = 0.808$$

$$(Sc)_f = \frac{0.808-0.745}{\ln \dfrac{0.808}{0.745}} = 0.772$$

The mass flow rate, G, is obtained from its definition as

$$G = \frac{W}{A} = \frac{6.39}{(0.01945)(3600)} = 0.0914\ \text{lb.}/(\text{sec.})(\text{ft.}^2) \qquad (A\text{-}104)$$

Applying Equation (A-84) for J_D,

$$J_D = \frac{(2.76)(0.988)(18.53)}{(0.0914)(3600)}(0.772)^{2/3} = 0.129$$

c. Calculation of Reynolds Number, $(D_p G/\mu)_f$

The film Reynolds number is calculated on the basis of particle diameter from the equation

$$Re_f = (\frac{D_p G}{\mu})_f \qquad\qquad (A-105)$$

D_p = sphere diameter = 0.508 cm.

G = 0.0914 lb./(sec.)(ft.)^2

From Equation (A-81),

$$\mu_{f_1} \text{ at } T_{f_1} = \Big[(0.00244)(479) - 0.06\Big] \times 10^{-5}$$

$$= 1.11 \times 10^{-5} \text{ lb./(sec.)(ft.)}$$

$$\mu_{f_2} \text{ at } T_{f_2} = \Big[(0.00244)(534) - 0.06\Big] \times 10^{-5}$$

$$= 1.24 \times 10^{-5} \text{ lb./(sec.)(ft.)}$$

$$\mu_{f_M} = \frac{1.11 + 1.24}{2} \times 10^{-5} = 1.175 \times 10^{-5} \text{ lb./(sec.)(ft.)}$$

$$Re_f = (\frac{0.508}{30.48})(\frac{0.0914}{1.175 \times 10^{-5}}) = 129$$

d. Calculation of Heat Transfer Factor, j_H

It is assumed that no heat is transferred by conduction from sphere to sphere or sphere to wall due to the small area offered by point contact of the spheres. Therefore, all the heat released by the reaction must be transferred from

the catalyst surface to the gas. Radiation and heat transfer due to the heat capacities of the diffusing gases have both been shown to be negligible and thus all the heat is transferred by conduction and convection. The rate of heat release is obtained by multiplying the rate of decomposition by the heat of decomposition,

$$\frac{Q}{A} = \frac{W}{A} \Delta H = (0.725)(43,209) \qquad \text{(A-106)}$$

$$= 31,300 \text{ Btu./(hr.)(ft.)}^2$$

The log mean temperature difference is obtained from Equation (A-93) as

$$\Delta T_{lm} = \frac{(500-302)-(509-493)}{\ln(198/16)} = 73.0°F.$$

The heat transfer coefficient is now obtained from the expression

$$h = \frac{Q}{A(aH)(\Delta T)_{lm}} = \frac{31,300}{(206.6)(2.35/30.48)(73.0)} \qquad \text{(A-107)}$$

$$= 27.0 \text{ Btu./(hr.)(°F.)(ft.)}^2$$

The value of the specific heat, C_p, is taken as that of steam.

$$C_{P_1} \text{ at } T_{f_1} = 0.465 \text{ Btu./(lb.)(°F.)}$$

$$C_{P_2} \text{ at } T_{f_2} = 0.475 \text{ Btu./(lb.)(°F.)}$$

$$C_{P_M} = 0.470 \text{ Btu./(lb.)(°F.)}$$

The value of the Prandtl number is again taken as 1.0. Substitution of the above values in the expression

$$J_H = (\frac{h}{C_p G})(Pr)_f^{2/3} \qquad\qquad (A-95)$$

leads to

$$J_H = \frac{27.0}{(0.470)(0.0914)(3600)}(1.0)^{2/3} = 0.176 \;.$$

e. Estimation of Heat Losses

The amount of heat generated by the reaction and lost from the system can be estimated from the difference between the measured exit temperature and the exit temperature that would have resulted in an adiabatic system. The adiabatic temperature for the amount of decomposition in the present run is 509°F. The temperature difference between the adiabatic temperature and the actual temperature is 509-493 = 16°F. Since C_p is 0.470 Btu./(lb.)(°F.),

$$\text{Heat loss} = (\frac{6.39}{.01945})(0.470)(16) = 2490 \text{ Btu./(hr.)(ft.)}^2$$

$$\% \text{ Heat loss} = L = \frac{2490}{31,300} \times 100 = 8.0\%.$$

f. Calculation of Point Values

As discussed fully in the Discussion of Results, the values of J_H on an overall basis were in error because of

the heat flow characteristics in the bed. To counteract this effect, calculations were carried out on the basis of point conditions at the center sphere of the first catalyst layer. It is assumed that the temperature measured by the inlet gas thermocouple gives an accurate measurement of the gas temperature actually entering the bed since the errors due to heat losses and regenerative heat flow tend to cancel. In addition, the large temperature differences at the bottom of the bed tend to make negligible any deviation from the assumption. The method of calculation of the point values is almost identical to that given thus far, the only difference being in the determination of the average conditions at the sphere being considered.

F_p is defined as the fraction of hydrogen peroxide undecomposed at the center of the sphere. As shown in the Discussion of Results, consideration of the general theory of diffusional processes as well as application of the integrated tube equations lead to the conclusion that the logarithm of F is linear with distance through the bed, i.e.,

$$\ln F = KH \qquad\qquad (A\text{-}108)$$

In Run 11 with five layers of spheres, the center of the first layer of spheres is considered to be one-tenth of the distance through the bed. Therefore, on a semi-log plot of

F vs. fraction of distance through the bed, the value of F_p
will be found at the fraction of depth equal to 0.1. In
Run 11, this value is 0.713.

From Equations (A-17) and (A-102), the values of the
mol fraction hydrogen peroxide in the stream and the inert
partial pressure are determined as y_p = 0.0349 and
p_{B_p} = 0.983. The mean molecular weight of the gas stream is
given by the method described above as 18.6. The bulk stream
temperature is obtained by assuming the stream temperature
to be linear in fraction decomposed. Therefore

$$T_{s_p} = T_1 + (T_2-T_1)(\frac{f_p-f_1}{f_2-f_1}) = T_1 + (T_2-T_1)(\frac{F_1-F_p}{F_1-F_2}) \qquad (A-109)$$

$$= (302) + (493-302)(\frac{0.915-0.713}{0.915-0.0753}) = 349°F.$$

The film temperature is calculated as

$$T_{f_p} = \frac{500+349}{2} = 424°F. = 491°K.$$

The Schmidt number is now determined from Equation (A-103)
as 0.761 and the viscosity from Equation (A-81) as
1.14 x 10^{-5} lb./(sec.)(ft.). Using the same value of k_G as
in the overall calculations, the point value of the mass
transfer factor is now given by Equation (A-84) as 0.128.
The point value of the Reynolds number is calculated as 133.
Comparing these values to the overall values of 0.129 and 129

respectively shows the slight effect of the assumptions involved in the point analysis. On Figure 11, the point values give the same agreement with the j_D correlation as do the overall values, the point as plotted being moved slightly downward and to the right, essentially parallel to the correlation.

The point value of the temperature difference is

$$\Delta T_p = 500 - 349 = 151°F.$$

leading to the heat transfer coefficient

$$h_p = \frac{(2.76)(.0349)(43,360)}{151} = 27.6 \text{ Btu./(hr.)(°F.)(ft.)}^2$$

The heat transfer factor is now obtained as

$$j_{H_p} = \frac{(27.6)(1.0)^{2/3}}{(0.472)(0.0914)(3600)} = 0.177$$

This point value agrees very well with the overall value of 0.176, since this run is an instance of low heat loss and high Reynolds number. However, in some runs with high heat loss and low Reynolds numbers, the the point value was as much as two-and-a-half times the overall value. The choice of the distance through the bed at which point calculations are made is not important since both the concentration and temperature gradients decrease simultaneously. Calculations carried out at distance fractions of 0.0 and 0.2 give less than 1% deviation from the values at 0.1.

D.   ERROR ANALYSIS

There are two types of error in the final calculated values of the transfer factors and Reynolds numbers. The first type is those errors due to the assumptions made in the calculations and derivations. From the discussions in the main body of the thesis and in the Sample Calculations, it is seen that the assumptions are well founded and in no case lead to substantial errors. The second type of error results from inaccuracies in making the experimental measurements. It is this type of error which is to be considered in this section.

The method of evaluating the effect of experimental errors is, first, to determine the maximum possible errors in the measurements. Then, the calculations are repeated using values which differ from those measured by the maximum possible percentage, thus determining directly the effect of these errors. The evaluation of the experimental errors will be demonstrated with the data of Run 11.

a. Wt. per cent hydrogen peroxide. From Equation (A-63)

$$\text{wt. } \% \ H_2O_2 = (\frac{1.70}{\text{Density}})(N.KMnO_4)(\frac{ml.KMnO_4}{ml.titrated})$$

By differentiating the function, dividing by the function, and approximating differentials by a finite error, the error

expression becomes

$$\frac{\Delta(wt.\%)}{wt.\%} = \frac{\Delta(1/\rho)}{(1/\rho)} + \frac{\Delta(N.KMnO_4)}{N.KMnO_4} + \frac{\Delta(ml.KMnO_4)}{ml.KMnO_4} + \frac{\Delta(ml.titrated)}{ml.titrated}$$

Substituting the downstream values of Run 11,

$$\frac{\Delta(wt.\%)}{wt.\%} = \frac{0.001}{0.998} + \frac{0.0002}{0.1997} + \frac{0.2}{20.4} + \frac{0.02}{10.0}$$

$$= 0.001 + 0.001 + 0.01 + 0.002$$

$$= 0.014$$

b. Wt. of H_2O_2 collected per minute. From Equation (A-62)

$$\frac{\Delta(g.H_2O_2)}{g.H_2O_2} = \frac{\Delta(ml.KMnO_4)}{ml.KMnO_4} + \frac{\Delta(N.KMnO_4)}{N.KMnO_4}$$

$$+ \frac{\Delta(ml.titrated)}{ml.titrated} + \frac{\Delta(ml.sample)}{ml.sample}$$

$$= \frac{0.2}{20.4} + \frac{0.0002}{0.1997} + \frac{0.02}{10.00} + \frac{0.3}{44.1}$$

$$= 0.020$$

c. Total weight of sample

Total weight = (ml.sample) x (density)

$$\frac{\Delta(total\ weight)}{total\ weight} = \frac{\Delta(ml.sample)}{ml.sample} \times \frac{\Delta\rho}{\rho}$$

$$= \frac{0.3}{44.1} + \frac{0.001}{1.003} = 0.008$$

d. Oxygen flow rate. The error in the wet-test meter readings is approximately

$$\frac{\Delta(\text{liters/sec.})}{(\text{liters/sec.})} = \frac{\Delta \text{ liters}}{\text{liters}} + \frac{\Delta \text{ seconds}}{\text{seconds}}$$

$$= \frac{0.01}{1.0} + \frac{0.4}{41.47} = 0.020$$

Thus the errors found in Run 11 are:

Wt. % H_2O_2	1.4%
Wt. of H_2O_2	2.0%
Total wt. sample	0.8%
Oxygen flow rate	2.0%

These magnitudes of maximum possible errors are quite typical, although in some runs with low oxygen flow rates, the error reached 4.0%. The calculations were then carried out using values reflecting the maximum possible errors. These were found to result in a maximum possible error in J_D of less than 2%. For example, if one assumes that the measured upstream concentration of Run 11 was 5% too high, a recalculation using a new value, 5% lower, gave a J_D of 0.128 as compared to the original 0.129. The reason for this small effect of a 5% error is that lowering the upstream concentration lowers the calculated values of both the total decomposition rate and the driving force, resulting in very nearly the same value of k_G.

The maximum possible error in J_H was principally a function of the accuracy with which the temperature difference could be measured. Since the temperature measurements were considered accurate to within $\pm$ 3°F., the temperature differences were accurate to $\pm$ 6°F. Comparison of this figure with the temperature differences used in calculating a value of J_H gives the maximum possible error in that value of J_H, since other errors are small in comparison. The maximum possible error was usually about 5%, but, in some runs with small ΔT's, it did range up to 15-20%.

E.   SUMMARY OF EXPERIMENTAL DATA

Table A-I presents a summary of the experimental data obtained with the catalyst tube. The volumes and percentages are averaged values for ten one-minute runs while the temperatures are averaged values for three sets of readings.

Table A-II is a summary of the packed bed data. The volumes and percentages are again averaged values for ten one-minute runs. The temperature data are not given here since they are presented on Table III.

All the original data and calculations are available at the Hydrogen Peroxide Laboratories at M.I.T.

TABLE A—I
SUMMARY OF EXPERIMENTAL DATA—CATALYST TUBE

24 Inch Tube — Runs 52 - 105
18 Inch Tube — Runs 106 - 114

C — Concentration, wt.% hydrogen peroxide; C_f, feed;
C_1, upstream condensate; C_2, downstream condensate.

S — Volume of condensate, ml.; S_1, upstream, S_2; downstream.

O_2 — Rate of oxygen flow from tube exit, standard liters per minute.

T — Gas temperature, °F.; T_1, upstream; T_2, downstream.

T_W — Wall temperature, °F.; the subscripts refer respectively to positions 1, 3, 10, 16, and 22 inches from the entrance in the 24 inch tube and 1, 3, 9, 15, and 17 inches in the 18 inch tube.

RUN	C_f	S_1	C_1	S_2	C_2	O_2	T_1	T_2	T_{W_1}	T_{W_2}	T_{W_3}	T_{W_4}	T_{W_5}	RUN
52	20.52	4.7	12.13	38.2	2.66	2.32	315	570	556	593	596	600	575	52
53	20.22	10.2	15.55	35.1	2.10	2.36	313	652	638	682	681	687	657	53
54	10.30	9.7	6.75	38.6	1.39	1.142	285	417	411	429	423	433	425	54
56	3.35	10.0	1.64	40.1	0.526	0.297	272	289	294	296	297	297	288	56
57	14.47	10.2	13.11	34.8	3.44	1.40	317	548	590	630	630	623	592	57
58	25.79	2.4	21.15	25.5	4.16	2.02	329	746	829	852	828	817	760	58
59	20.72	14.6	19.20	25.5	3.51	1.57	325	686	770	786	764	754	710	59
60	17.74	6.8	14.23	27.0	1.495	1.461	243	530	584	601	592	582	544	60
61	18.52	6.7	15.89	31.7	2.10	1.776	327	638	665	707	693	668	638	61
62	20.00	4.8	17.57	37.2	2.49	2.29	306	568	610	675	683	668	665	62
63	20.80	4.7	17.42	35.4	2.34	2.259	323	666	703	750	755	741	712	63
64	10.85	8.6	8.90	38.5	1.34	1.279	288	444	474	495	493	487	470	64
65	5.42	8.7	3.44	41.1	0.735	0.544	287	346	357	367	364	359	347	65
66	14.95	8.9	11.98	37.8	1.49	1.703	312	566	575	606	610	598	576	66
67	6.47	8.7	3.62	41.2	0.655	0.702	288	349	335	365	362	345	331	67
68	8.31	8.7	5.41	40.3	0.829	0.955	297	408	410	423	423	417	408	68
69	2.92	8.6	1.75	41.4	0.371	0.351	285	314	319	322	319	316	310	69
70	19.00	5.0	15.45	35.6	1.960	2.255	326	608	646	690	691	679	648	70
71	20.72	4.4	16.70	36.4	1.98	2.44	328	664	666	705	710	699	674	71
72	20.62	4.3	15.90	36.7	1.74	2.445	332	655	645	687	690	677	653	72
73	20.42	6.2	15.65	36.4	2.79	2.25	336	607	628	678	688	684	672	73
74	20.63	8.1	14.53	34.3	2.21	2.21	332	637	612	655	663	660	646	74
75	20.13	14.1	13.30	33.2	1.84	2.10	320	592	579	617	623	620	608	75
76	20.13	7.5	11.93	36.2	2.18	1.962	331	584	566	599	605	603	590	76
77	20.28	6.3	18.00	35.3	3.94	2.15	338	704	688	739	749	749	734	77
78	14.62	8.8	10.62	36.8	2.46	1.356	311	494	533	546	550	550	542	78
79	14.87	5.9	12.10	39.5	3.16	1.432	324	541	556	595	598	596	588	79
80	14.76	9.5	12.30	37.6	3.11	1.50	318	544	570	605	607	604	591	80
81	20.28	6.4	17.20	32.2	3.66	1.88	346	660	681	733	739	734	718	81
82	10.05	11.2	8.37	35.1	2.23	0.920	304	454	457	481	485	484	478	82
83	10.35	8.2	8.20	40.5	2.17	1.055	310	448	469	491	491	491	485	83
84	10.40	11.2	8.33	39.4	2.075	1.08	301	450	463	484	485	486	478	84
85	20.73	7.2	17.02	33.7	3.62	2.04	335	653	678	728	733	728	712	85
86	23.37	7.2	18.83	32.5	3.79	2.24	339	714	714	773	780	774	756	86
87	23.20	5.5	20.27	31.6	4.26	2.11	334	699	726	787	796	790	771	87
88	23.25	7.3	19.95	30.6	4.36	2.05	351	707	741	801	807	803	784	88
89	23.25	8.3	18.80	23.9	3.997	1.57	342	664	695	747	755	748	728	89
90	25.96	3.9	19.98	23.9	4.38	1.84	394	744	779	842	848	838	810	90
91	26.08	5.0	21.62	25.5	4.42	1.98	372	754	792	858	864	857	830	91
92	26.08	3.6	21.55	26.2	4.32	2.015	383	762	801	867	873	864	836	92
93	26.08	8.7	21.61	22.6	4.495	1.71	343	718	760	822	827	817	792	93
94	29.50	5.1	22.06	21.6	4.76	1.97	399	787	831	899	903	892	856	94
95	20.45	6.3	16.92	23.1	3.48	1.29	363	639	667	717	721	714	691	95
96	10.07	10.2	8.33	39.5	2.22	1.006	305	440	459	482	485	487	480	96
97	10.07	23.4	7.89	21.5	1.716	0.566	298	416	441	456	455	451	435	97
98	10.45	14.0	9.10	31.0	2.08	0.880	306	452	475	499	497	495	486	98
99	26.65	1.8	23.65	32.8	5.24	2.51	357	771	820	895	901	896	876	99
100	26.65	9.9	22.80	21.7	4.88	1.64	354	729	775	843	849	837	806	100
101	30.84	4.0	25.99	26.5	5.59	2.39	398	875	903	987	993	983	950	101
102	29.43	3.3	25.50	25.3	5.58	2.22	376	838	868	949	956	947	914	102
103	29.43	8.8	25.35	21.6	4.73	1.935	352	812	832	908	912	905	866	103
104	32.05	5.0	27.14	22.5	6.75	2.07	404	876	910	997	999	989	948	104
105	31.58	13.0	27.62	20.2	6.49	1.835	355	823	865	948	946	935	900	105
106	5.45	6.8	4.14	45.8	1.45	0.519	313	365	374	392	399	394	379	106
107	5.23	9.1	3.64	24.3	1.08	0.314	330	368	374	384	387	378	363	107
108	10.27	6.5	7.12	44.0	2.37	1.11	320	422	450	474	482	476	456	108
109	10.31	9.1	5.58	24.8	1.66	0.646	326	396	414	428	432	423	404	109
110	14.87	6.7	10.33	32.9	3.07	1.32	345	502	530	565	575	565	538	110
111	14.87	6.0	8.58	20.7	2.31	0.87	351	468	485	510	515	501	476	111
112	20.54	7.8	16.66	35.0	4.59	1.93	338	612	653	711	725	713	674	112
113	20.54	7.2	14.52	22.0	3.46	1.27	345	570	592	638	650	632	596	113
114	10.32	7.8	7.40	32.7	2.49	0.803	325	427	455	478	487	478	457	114

TABLE A—II
SUMMARY OF EXPERIMENTAL DATA—PACKED BED

4.7 cm. Bed - Runs 1 - 10
4.8 cm. Bed - Runs 11 - 24
7.5 cm. Bed - Runs 25 - 33

C - Concentration, wt.% hydrogen peroxide; C_f, feed;
C_1, upstream condensate; C_2, downstream condensate.

S - Volume of condensate, ml.; S_1, upstream, S_2, downstream.

O_2 - Rate of oxygen flow from exit of bed, standard liters per minute.

RUN	C_f	S_1	C_1	S_2	C_2	O_2	RUN
1	9.95	7.6	7.59	55.0	0.740	1.66	1
2	10.46	10.0	8.75	47.1	0.649	1.58	2
3	10.06	14.4	7.92	46.1	0.764	1.42	3
4	9.93	17.1	6.42	28.6	0.378	0.834	4
5	9.62	33.5	6.96	12.9	0.114	0.411	5
6	10.84	20.0	8.02	37.8	0.439	1.273	6
7	5.21	17.7	3.61	47.9	0.338	0.731	7
8	5.31	20.0	3.01	31.9	0.174	0.521	8
9	14.87	7.6	10.26	46.1	0.645	2.16	9
10	15.11	8.6	10.98	33.9	0.380	1.591	10
11	9.08	11.0	8.21	44.1	0.695	1.233	11
12	8.95	16.8	7.58	25.1	0.328	0.702	12
13	15.18	5.7	13.47	41.7	0.642	2.150	13
14	15.60	14.6	11.87	17.5	0.185	0.895	14
15	15.22	9.1	13.82	30.6	0.308	1.608	15
16	8.97	8.4	8.00	45.1	0.609	1.219	16
17	15.35	12.2	13.40	31.5	0.722	1.542	17
18	15.35	8.7	10.20	10.3	0.153	0.477	18
19	20.70	3.9	18.25	32.5	1.260	2.200	19
20	22.77	4.9	21.30	31.3	1.625	2.43	20
21	22.77	13.7	20.55	18.5	0.708	1.518	21
22	21.08	3.9	18.60	36.2	2.060	2.325	22
23	20.60	11.1	16.37	11.6	0.441	0.788	23
24	15.20	4.1	8.16	8.0	0.086	0.327	24
25	5.38	11.1	4.20	48.1	0.470	0.718	25
26	10.22	9.5	8.15	45.2	0.760	1.402	26
27	10.58	8.5	7.36	24.0	0.340	0.782	27
28	15.10	8.6	12.56	40.2	0.870	1.990	28
29	15.30	8.9	10.98	22.0	0.378	1.073	29
30	20.15	6.6	16.82	36.2	1.310	2.430	30
31	20.13	7.6	14.90	18.7	0.491	1.256	31
32	24.12	5.5	20.45	33.0	1.430	2.87	32
33	24.12	8.1	18.93	16.0	0.518	1.332	33

F. NOMENCLATURE[*]

a   Coefficient in equation for diffusion coefficient, $D = aT^{3/2}$

a   Catalyst surface area per unit volume in bed, $ft.^2/ft.^3$
     (In Sample Calculations, Part 2)

A   Area, $ft.^2$

c   Concentration, lb. mols/$ft.^3$

c   Constant in equation $T_f = cf + d$

c'   Constant in equation $T_s = c'f + d'$

C   Boiler feed concentration, wt. % H_2O_2

C*   Adjusted feed concentration, wt. % H_2O_2

C_p Specific heat at constant pressure, Btu./(lb.)(°F.)

d   Tube diameter, ft.

d   Constant in equation $T_f = cf + d$

d'   Constant in equation $T_s = c'f + d'$

dia. Tube diameter, ft.

D   Diffusion coefficient, $ft.^2/hr.$; D_{AB}, diffusion coefficient
     of component A through component B

D_p Particle (sphere) diameter, ft.

D_T Thermal diffusion coefficient, lb. mols/(hr.)(ft.)

E_H Eddy diffusivity for heat transfer $(ft.^2/hr.)$

E_M Eddy diffusivity for mass transfer $(ft.^2/hr.)$

f   Fanning friction factor, dimensionless (In Introduction,
     Part C)

f   Fraction H_2O_2 in adjusted feed decomposed; f_1, entering
     tube or bed; f_2, leaving tube or bed

---

[*] Where meaning or units differ from those given in this
table, the symbol is defined in the context.

F   Fraction H_2O_2 in adjusted feed <u>not</u> decomposed, $f + F = 1$

g_c Gravitational constant

G   Mass flow rate, lb./(ft.)^2(sec.)

h   Heat transfer coefficient, Btu./(hr.)(°F.)(ft.)^2

h'   Mol fraction H_2O_2 in adjusted feed

ΔH Heat of decomposition of H_2O_2, Btu./lb. mol.

H   Height of packed bed, ft.

i   Enthalpy, Btu./lb. mol

i'   Mol fraction H_2O in adjusted feed

j_D Mass transfer factor, $(k_G p_{BM} M_M/G)(Sc_f)^{2/3}$, dimensionless

j_H Heat transfer factor, $(h/C_p G)(Pr_f)^{2/3}$, dimensionless

k   Thermal conductivity, Btu./(hr.)(ft.)^2(°F./ft.)

k_c Coefficient of mass transfer, ft./hr.

k_G Coefficient of mass transfer, lb.mols/(hr.)(ft.)^2(atm.)

l'   Symbol in Equations (50) and (A-51), $l' = \phi_A D_{AB} PTk$

L   Tube length, ft.

L   % of heat released by reaction lost from system

L/D   Length-to-diameter ratio

m'   Symbol in Equations (50) and (A-51), $m' = \phi_A D_{AB} P\alpha(\Delta H)$

M   Molecular weight

n   Rate of flow of H_2O_2 in tube, lb.mols/hr.; n_o, initial rate

n'   Symbol in Equations (50) and (A-51); $n' = RT^2 k$

N   Rate of mass transfer, lb.mols/(ft.)^2(hr.); N_A, component A, N_t, algebraic sum of rates in complex system

p   Partial pressure, atm.; p_{BM}, mean partial pressure of inerts

P   Total pressure, atm.

Pr   Prandtl number, $(C_p\mu/k)$, dimensionless

q   Rate of heat transfer, Btu./(ft.)^2(hr.)

Q   Rate of heat transfer, Btu./hr.

r   Ratio of velocity at boundary of laminar film to average velocity in tube

R   Gas constant

Re   Reynolds number; (dG/μ) in tube; (D_pG/μ) in bed; dimensionless

Re_M Modified Reynolds number, $D_pG/\mu(1-\epsilon)$

Sc   Schmidt number, $(\mu/\rho D)$, dimensionless

T   Temperature, °F.; T_W, wall temperature; T_a, average film temperature; T_f, film temperature; T_s, stream temperature

U   Velocity, ft./hr.

u   Convection velocity, ft./hr.

u^+ Dimensionless velocity parameter

V   Molecular volume

w   Rate of decomposition, lb.mols/hr.

W   Total rate of flow, lbs./hr.

x   Thickness through film, ft.; x_H, effective film thickness for heat transfer; x_D, effective film thickness for mass transfer

y   Distance from pipe wall, ft. (Introduction, Part C)

y   Mol fraction H_2O_2 in vapor; y_1, entering tube or bed; y_2, leaving tube or bed; y_A, component A

y^+ Dimensionless length parameter

α Proportionality constant in Equation $D_T = y_A y_B D_{AB}{}^{\alpha}$

α_H Thermal diffusivity, ft.^{2}/hr.

$\int$ Thickness of laminar layer, ft.

Δ Finite difference

ϵ Coefficient of eddy viscosity, ft.^{2}/hr. (Introduction, Part C)

ϵ Void fraction in packed bed

μ Viscosity, lb./(sec.)(ft.)

ν Kinematic viscosity, (ft.)^2/hr.

π 3.1416

ρ Density, lbs./ft.^{3}

τ Shear stress, lb. force/ft.^{2}

ϕ Ratio of transport rates, $\phi_A = N_A/N_t$

Subscripts

a   Average

A   Component A, usually refers to H_2O_2

B   Component B, usually refers to mixture of steam and oxygen

f   Film conditions

i   Component i

L.m.   Log mean value

M   Mean value

p   Point value; in tube refers to point at which log mean driving force occurs; in bed refers to conditions at center sphere of bottom layer

P   Products

R   Reactants

s,S Stream conditions

w,W Wall conditions

o   Adjusted feed conditions

o   Stream conditions (Introduction, Part C)

1   Entrance of bed or tube

2   Exit of bed or tube

δ Conditions at boundary of laminar layer

G.   LITERATURE CITATIONS

(1) Apel'baum, I. L., and Temkin, M., J. Phys. Chem., (U.S.S.R.), $\underline{22}$, 179 (1948).

(2) Baker, B. E., and Ouellet, C., Can. J. Research, $\underline{23B}$, 167 (1945).

(3) Bakhmeteff, B. A., "The Mechanics of Turbulent Flow," Princeton University Press, Princeton, N. J., 1936.

(4) Bellinger, F. et al., Ind. Eng. Chem., $\underline{38}$, 160, 310, 629 (1946).

(5) Benedict, M., Mass. Inst. of Tech., Personal Communication, 1952.

(6) Bernard, R. A., and Wilhelm, R. H., Chem. Eng. Progress, $\underline{46}$, 233 (1950).

(7) Bloom, R., Davis, N. S., and Levine, S. D., J. Am. Rocket Society, $\underline{3}$, No. 80 (1950).

(8) Boelter, L. M. K., Martinelli, R. C., and Jonassen, F., Trans. Am. Soc. Mech. Engrs., $\underline{63}$, 447 (1941).

(9) Buffalo Electrochemical Company, "Hydrogen Peroxide-- Physical Properties," Station B, Buffalo, New York, 1949.

(10) Chapman, S., and Cowling, T. G., "Mathematical Theory of Non-Uniform Gases," University Press, Cambridge, England, 1939.

(11) Chilton, T. H., and Colburn, A. P., Ind. Eng. Chem., $\underline{26}$, 1183 (1934).

(12) Colburn, A. P., Ind. Eng. Chem., $\underline{22}$, 967 (1932).

(13) Colburn, A. P., Trans. Am. Inst. Chem. Engrs., $\underline{29}$, 174 (1933).

(14) Davis, H., and Hottel, H. C., Ind. Eng. Chem., $\underline{26}$ 889 (1934).

(15) Deissler, R. G., Trans. Am. Soc. Mech. Engrs., $\underline{73}$, 101 (1951).

(16) Demetriades, S., Mass. Inst. of Tech., Personal Communication, 1952.

(17) Dryden, C. E., Strang, D. A., and Withrow, A. E., Paper presented at the 44th Annual Meeting of the A.I.CH.E., Atlantic City, N. J., 1951.

(18) Fowler, R. M., and Bright, H. A., J. Res. Natl. Bur. Standards, 15, 493 (1935).

(19) Furry, W. H., and Jones, R. C., Rev. Mod. Phys., 18, 151 (1946).

(20) Gaffney, B. J., and Drew, T. B., Ind. Eng. Chem., 42, 1120 (1950).

(21) Gamson, B. W., Chem. Eng. Progress, 47, 19 (1951).

(22) Gamson, B. W., Thodos, G., and Hougen, O. A., Trans. Am. Inst. Chem. Engrs., 39, 1 (1943).

(23) Giguere, P. A., Can. J. Research, 25B, 135 (1947).

(24) Gilliland, E. R., Ind. Eng. Chem., 26, 681 (1934).

(25) Gilliland, E. R., and Sherwood, T. K., Ind. Eng. Chem., 26, 1183 (1934).

(26) Goldstein, S., "Modern Developments in Fluid Mechanics," Oxford University Press, London, 1938.

(27) Hobson, M., and Thodos, G., Chem. Eng. Progress, 45, 517 (1949).

(28) Hobson, M., and Thodos, G., Chem. Eng. Progress, 47, 370 (1951).

(29) Holmes, F. E., Ind. Eng. Chem., Anal. Ed., 12, 483 (1940).

(30) Hougen, O. A., and Watson, K. M., "Chemical Process Principles," Part III, John Wiley and Sons, Inc., New York, 1947.

(31) Huckaba, C. E., and Keyes, F. G., J. Am. Chem. Soc., 70, 1640 (1948).

(32) Hurt, D. M., Ind. Eng. Chem., 35, 522 (1943).

(33) Isbin, H. S., "Heterogeneous Decomposition of High Strength Hydrogen Peroxide," Sc.D. Thesis in Chem. Eng., M.I.T., 1947.

(34) Isbin, H. S., et al., "Experimental High Pressure Flow Studies of the Catalytic Decomposition of Hydrogen Peroxide Solutions," Report No. 21, O.N.R. Contract No. N5 ori-78, T.O. XIX, M.I.T., 1947.

(35) Isbin, H. S., "Theoretical Analysis of the Decomposition of High Strength Hydrogen Peroxide Solutions," Report No. 22, O.N.R. Contract No. N5 ori-78, T.O. XIX, M.I.T., 1947.

(36) Jeans, J. H., "The Dynamical Theory of Gases," 4th ed., University Press, Cambridge, England, 1925.

(37) Karman, T. von, Trans. Am. Soc. Mech. Engrs., $\underline{61}$, 705 (1939).

(38) Keenan, J. H., and Keyes, F. G., "Thermodynamic Properties of Steam," John Wiley and Sons, Inc., New York, 1947.

(39) Keyes, F. G., J. Am. Chem. Soc., $\underline{72}$, 433 (1950).

(40) Klinkenberg, A., and Mooy, H. H., Chem. Eng. Progress, $\underline{44}$, 17 (1948).

(41) Linton, W. H., Jr., and Sherwood, T. K., Chem. Eng. Progress, $\underline{46}$, 258 (1950).

(42) Loeb, L. B., "The Kinetic Theory of Gases," 2nd ed., McGraw-Hill Book Co., New York, 1934.

(43) McAdams, W. H., "Heat Transmission," 2nd ed., McGraw-Hill Book Co., New York, 1942.

(44) McAdams, W. H., ibid. For references since 1942 see, for example, Kays, W. M., Tech. Report No. 14, Navy Contract N6-ONR-251 T.O. 6, Stanford Univ., Calif., 1951; Drexal, R. E., and McAdams, W. H., N.A.C.A. Wartime Report W-108 (1945); Cholette, A., Chem. Eng. Progress, $\underline{44}$, 81 (1948).

(45) McCune, L. K., and Wilhelm, R. H., Ind. Eng. Chem., $\underline{41}$, 1124 (1949).

(46) MacKenzie, R. C., and Ritchie, M., Proc. Roy. Soc. (London), $\underline{A185}$, 207 (1946).

(47) McLane, C. K., J. Chem. Phys., 17, 379 (1949).

(48) McMurtrie, R. L., and Keyes, F. G., J. A. C. S., 70, 3755 (1948).

(49) Martin, J. J., McCabe, W. L., and Monrad, C. C., Chem. Eng. Progress, 47, 91 (1951).

(50) Martinelli, R. C., Trans. Am. Soc. Mech. Engrs., 69, 947 (1947).

(51) Meeken, S. R., "The Role of Diffusional Processes in the Heterogeneous Decomposition of Hydrogen Peroxide Vapor," S.B. Thesis in Chem. Eng., M.I.T., 1950.

(52) Miller, B., Trans. Am. Soc. Mech. Engrs., 71, 357 (1949).

(53) Murphree, E. V., Ind. Eng. Chem., 24, 726 (1932).

(54) Nikuradse, J., Forschungsheft, No. 356 (1932).

(55) Olson, R. W., Schuler, R. W., and Smith, J. M., Chem. Eng. Progress, 46, 614 (1950).

(56) Parker, A. S., "Combustion of Carbon," Sc.D. Thesis in Chem. Eng., M.I.T., 1936.

(57) Prandtl, L., Z. Physik., 11, 1072 (1910).

(58) Reichart, H., Natl. Advisory Comm. Aeronaut., Tech Mem. 1047 (1943).

(59) Reichert, J. S., McNeight, S. A., and Rudel, H., Ind. Eng. Chem., Anal. Ed., 11, 194 (1939).

(60) Resnick, W., and White, R. R., Chem. Eng. Progress, 45, 377 (1949).

(61) Reynolds, O., "Scientific Papers of Osborne Reynolds," Cambridge University Press, London, 1901.

(62) Rubin, F. L., Chem. Eng. Progress, 47, 541 (1951).

(63) Satterfield, C. N., Kavanagh, G. M., and Resnick, H., Ind. Eng. Chem., 43, 2507 (1951).

(64) Satterfield, C. N., Kavanagh, G. M., and Resnick, H., "Explosive Characteristics of Hydrogen Peroxide Vapor," Report No. 31, O.N.R. Contract No. N5 ori-07819, NR-223-008, M.I.T., 1950.

(65) Sherwood, T. K., Absorption and Extraction," McGraw-Hill Book Co., New York, 1937.

(66) Sherwood, T. K., Trans. Am. Inst. Chem. Engrs., $\underline{39}$, 583 (1943).

(67) Sherwood, T. K., Ind. Eng. Chem., $\underline{42}$, 2077 (1950).

(68) Sherwood, T. K., and Woertz, B. B., Ind. Eng. Chem., $\underline{31}$, 1034 (1939).

(69) Smith, F. W., "Influence of Gas Flow on the Heterogeneous Reactions of Carbon," Sc.D. Thesis in Chem. Eng., M.I.T., 1949.

(70) Squyres, A. L., Mass. Inst. of Tech., Personal Communication, 1952.

(71) Taecker, R. S., and Hougen, O. A., Chem. Eng. Progress, $\underline{45}$, 188 (1949).

(72) Taylor, G. I., Brit. Advisory Comm. Aeronaut., Repts. and Mem., $\underline{272}$, 423 (1916).

(73) Taylor, G. I., Proc. Roy. Soc. (London), $\underline{A159}$, 496 (1937).

(74) Tu, C. M., Davis, H., and Hottel, H. C., Ind. Eng. Chem., $\underline{26}$, 749 (1934).

(75) Wentworth, R. L., "High Temperature Decomposition of Hydrogen Peroxide," S.M. Thesis in Chem. Eng., M.I.T., 1948.

(76) Wentworth, R. L., Richey, C. F., and Ploen, E. A., "The Role of Diffusion in the High Temperature Decomposition of Hydrogen Peroxide," Report No. 26, O.N.R. Contract No. N5 ori - 07817, NR 223-008, M.I.T., 1949.

(77) Whalley, E., J. Chem. Phys., $\underline{19}$, 509 (1951).

(78) Wilke, C. R., Chem. Eng. Progress, $\underline{46}$, 95 (1950).

(79)   Wilke, C. R., and Hougen, O. A., Trans. Am. Inst. Chem. Engrs., 41, 445 (1945).

(80)   Winter, E., Trans. Far. Soc., 46, 81 (1950).

H. BIOGRAPHICAL NOTE

The author was born on December 21, 1924, in Cambridge, Massachusetts, and attended grade school and high school in Boston, Massachusetts. He entered Northeastern University in September, 1941, but in June, 1944, was called to active service in the U. S. Navy. After his discharge in June, 1946, he returned to Northeastern and received the degree of Bachelor of Science in Chemical Engineering in June, 1947. The author then entered the Graduate School of the Massachusetts Institute of Technology and received the degree of Master of Science in Chemical Engineering Practice in June, 1949. He was a member of the research staff of the Division of Industrial Cooperation, Hydrogen Peroxide Project, from graduation until he reentered the Graduate School in February, 1950. During his doctorate work, he has been a research assistant in the Chemical Engineering Department.